THE ANODIC BEHAVIOUR OF ALUMINIUM IN AQUEOUS SOLUTION

A thesis presented for the degree of
Doctor of Philosophy in Chemical Engineering
in the
University of Canterbury,
Christchurch, New Zealand

by

K. J. Kirkpatrick

1967

Acknowledgment

This work was carried out under the supervision of Dr T. Hagyard whose guidance and insight are truly appreciated. During the first stage of this work many very useful discussions were had with my associates, Drs Earl and Watson; without the results of their research to hand, a great deal less could have been achieved in the present work.

I gratefully acknowledge the contribution made by Professor Lawden in developing the mathematical relations of the model, presented in Section 6 of this thesis. Members of this and several other departments in the University have provided valuable assistance on innumerable occasions.

Thanks are due to the New Zealand Dairy Research Institute for making personal financial assistance available during part of this work.

CONTENTS

1. SUMMARY

Electrolytic dissolution of pure aluminium in aqueous halide electrolytes has been investigated and found to exhibit the behaviour conventionally termed the "difference effect". The weight loss from the aluminium anode was greater than predicted by Faraday's law for trivalency of aluminium, and hydrogen gas was simultaneously evolved from the anode. A quantitative relationship has been established between the extent of these processes and the magnitude of the applied anode current density in the range 10^{-2} to 10^{2} amp/cm^{2}. This and related information has been used to demonstrate the inadequacy for aluminium of previously advanced explanations such as the "local corrosion" hypothesis and the "monovalent aluminium cation" hypothesis.

To account for the observed phenomena, a statistical model of the anode behaviour has been developed, based on the hypothesis that aluminium metal can react non-electrochemically with water. When the experimentally determined time dependent anodic kinetic parameters of Earl[5] and Watson[6] are incorporated, a satisfactory quantitative account of the electrode behaviour is achieved. The relevance of the results to practical corrosion of aluminium, especially pitting, has been established.

2. INTRODUCTION

2.1 General

In spite of a very extensive literature on the subject many aspects of the diverse electrochemical and corrosion behaviour of aluminium are not well understood. Applied corrosion research, although invaluable, has generally gone little beyond discovering the factors relevant to a specific situation, or obtaining a solution to an immediate problem. Because of the inherent reactivity of aluminium, study of its fundamental electrochemistry presents formidable difficulties of both experimentation and interpretation. However, a novel technique devised and used by Hagyard et al[1,2,3], Earl[4,5], and Watson[6], in this department, has enabled measurement of meaningful electrode kinetic parameters for the pure metal under restricted but well-defined conditions. The present work goes some distance towards bridging the gap between knowledge of these fundamental properties, and an understanding of the long-term anodic behaviour of the metal.

2.2 Short-term Electrochemistry

An aluminium electrode, freshly cut in 1N KCl pH 3.2, exhibits the no load potential behaviour shown in Fig. 2.1 (after Watson[6]). Clear proof has been obtained from joint work[7] that this transient potential results from electrochemical processes, and is not a spurious effect

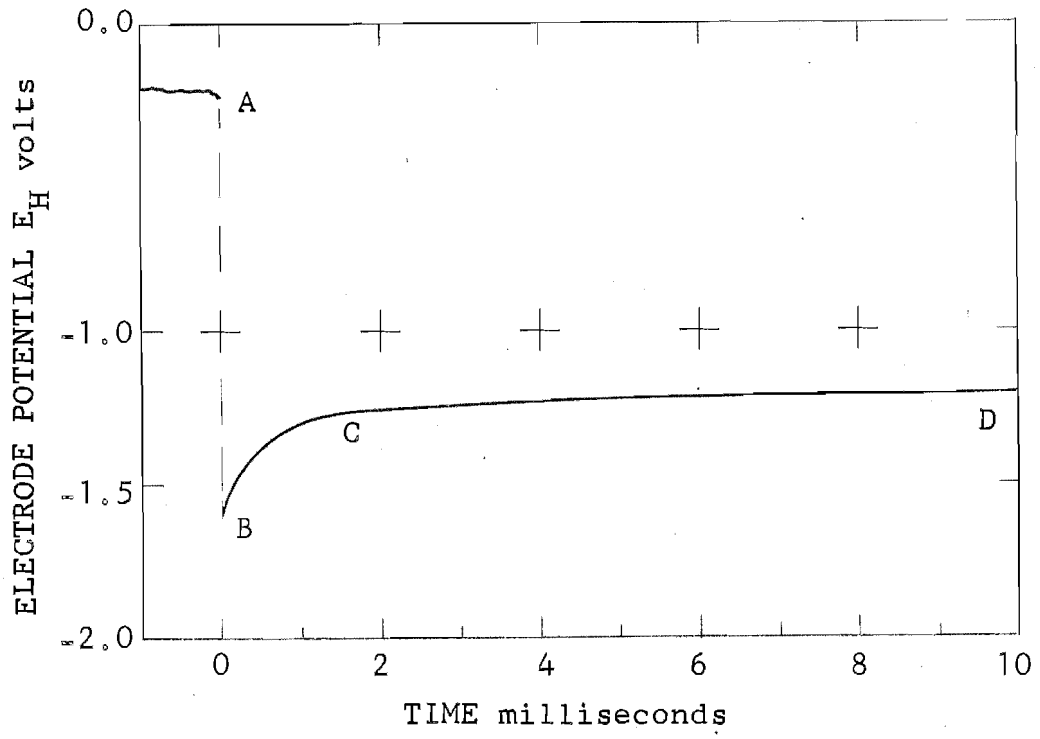

FIG 2.1 NO LOAD POTENTIAL TRACE (After Watson[6])

generated by cutting phenomena since rapid immersion of a vacuum evaporated aluminium film gives the same electrode potential response. (See APPENDIX B.)

Earl[5] established that, during the 20μ sec fall A-B to the minimum, the bare metal surface was wholly anodic and measured the kinetic parameters. He also measured independently, the cathodic hydrogen evolution parameters within 1-5 msec of cutting. The millisecond transition B-C to the mixed potential C-D, was then shown to result if there was (i) an approximately 20 micro-sec delay before onset, and subsequent exponential establishment, of the cathodic process, and (ii) a concurrent 200-fold decrease in the anodic

activity of the surface. This model is consistent with the earlier finding of Hagyard and Williams[2] that change in electrolyte aluminium ion concentration influenced the peak but apparently not the mixed potential, and conversely that the effect of pH was confined to the mixed potential region.

Watson[6] examined the steady increase of about .3v in the mixed potential that occurred over the next 10 seconds of electrode life. The principal cause of the potential increase was found to be a steady, many decade decrease in the anodic metal dissolution parameter i_{oa}, apparently resulting from film formation on the surface of the metal. Direct chemical reaction of aluminium with water appeared to be the only feasible means of forming this film in the time available.

Because of their relevance to the anodic phenomena considered later, an outline of the formation and nature of oxide films on aluminium follows; "oxide" film should not be taken as describing closely the nature of such films but rather as a convenient non-defining name.

2.3 Film Formation

2.3(i) With oxygen

Dry oxygen is rapidly taken up by aluminium at -183°C to the extent of about a monolayer[8]. At 25°C

Hart[9] found that amorphous oxide films formed on electropolished aluminium to an estimated thickness of 30Å in dry oxygen, and about 40Å in humid oxygen after several days exposure. Growth mechanism of the film was postulated to be by outward diffusion of cations under the influence of the potential estimated from energy data[10] to be

$$2Al^{+++} + 3O^{--} = Al_2O_3 \qquad E = \frac{\Delta G}{6F} \qquad 2.72 \text{ volts.}$$

A clear demonstration of the protectiveness of these films is afforded by the fact that film formation effectively stops even when the growth promoting field across the film is still greater than 10^7 volts/cm. Strong evidence of the presence of oxygen ion vacancies in the lattice of freshly formed atmospheric oxide film on aluminium and other metals has been obtained from electron emission studies by Grunberg et al[11]. The film is recognised as having a metal excess compared with stoichiometric composition.

Natural films formed on aluminium in the atmosphere at room temperature were found by Hunter and Fowle[12] to have a total thickness of about 30Å with an inner "barrier" layer only 10 ± 2Å thick. In dry atmospheres barrier film alone was formed and in thickness proportional to temperature. When exposed to humid air of lower temperature, barrier layer thickness was decreased by the action of water vapour

over a period ranging from hours to several days.

The surface changes on vacuum-deposited metal films when exposed to various atmospheres were examined by Andreeva et al.[13,14] using the very sensitive elliptical polarised light technique. In 50% humid air at 25°C, a film 21Å thick was formed "instantaneously" on aluminium but application of a 10^{-6} mm Hg vacuum reduced this thickness to 9Å in a few hours. Re-exposure to the atmosphere brought the thickness back to 18Å. A slow increase in thickness to 30-70Å after 70 days was observed but there was no further change in 3 years. It may be noted that under the same treatment complete vacuum removal of films formed on chromium and gold occurred.

These researches point to a two-layer model for the structure of atmospherically formed film on aluminium; an inner permanent and coherent barrier layer and an outer porous layer formed by the action of water vapour leading to continued but very slow growth in total film thickness although probably with no increase in protectiveness. In part at least and in the short term, the effect of water vapour on the film at room temperature appears to be reversible.

2.3(ii) With water

From the foregoing it is clear that between aluminium and molecular oxygen there is a rapid film forming chemical reaction of self limited extent. There arises the question of whether molecular oxygen either gaseous or dissolved is essential for film formation, or are aluminium and water alone able to react with similar outcome? While it is not common experience for aluminium to dissolve rapidly in pure water with concurrent hydrogen evolution in the well-known manner of, for example, sodium or potassium, this inertness may be attributed to the protective natural oxide film already present. Spontaneous water aluminium reaction is thermodynamically feasible and although kinetic considerations might limit the rate, reaction of significant extent has been shown to occur. Thus amalgamated aluminium dissolves in water with evolution of hydrogen[15]. Aluminium was found to evolve hydrogen when, and only so long as, it was abraded under water[16]. Similarly, when vacuum evaporated films of aluminium were first exposed to aqueous solution, a brief gas evolution was observed[7].

Evidently the reaction between water and aluminium also, is self limiting, presumably by formation of a protective film. This matter was investigated by Watson[6] in work where aluminium electrodes were cut in and exposed to various atmospheres for measured times

before rapid immersion and measurement of open circuit potential behaviour in 1N KCl pH 3.2 The atmospheres used were:

Dry hydrogen : 10 msec exposure

Humid hydrogen: 10 msec, 15sec exposure

Dry oxygen : 10 msec, 10sec, 15 min exposure.

When the observed potential response after each type of pretreatment was compared with that of an electrode cut under solution, it was clear that all atmospheres except dry hydrogen had interacted significantly with the metal in the available time. From other tests it seems certain that 10 msec exposure to liquid water produces an oxide film comparable in properties with that formed in the same time in oxygen. It appears that in water vapour, formation of a similar film might take place in about 10 sec exposure.

In further work, Watson[6] used pure aluminium carrying an atmospheric oxide film before its immersion in 1N KCl pH 3.2 and showed that the values measured for electrode kinetic parameters were dependent on time of immersion. After a few minutes in solution the values were not significantly different from those measured on electrodes cut under and immersed in 1N KCl for the same period. This result suggests that much the same film properties result from either formation path.

2.4 Electrolytic Behaviour

2.4(i) General

Whether or not spontaneous corrosion of an immersed specimen of aluminium occurs depends on the balance of tendencies to film damage and film repair. Relevant factors such as solution pH[17], anion type and concentration, presence of cupric ion, dissolved molecular oxygen concentration[18], aluminium oxide saturation of electrolyte[19], temperature[20], diffusion and general mass transport phenomena[21] have been extensively investigated and a comprehensive review is available[16].

When aluminium is made anode in an electrolytic cell, any of three processes other than oxygen evolution may occur, depending on current density and the nature of the electrolyte. These processes are:

(1) Anodic dissolution, with etching or pitting.

(2) Anodic growth of the oxide film - anodization.

(3) Anodic dissolution with brightening - electro-polishing.

A coherent picture of anodic behaviour in general and the differing conditions which lead to each of these processes is presented in a detailed review by Hoar[22].

Anodic dissolution of aluminium with etching or pitting occurs only under certain circumstances;

this process, the study of which forms the substance of the present research, is in effect forced corrosion. As such the process is influenced by some of the factors listed above as important in spontaneous corrosion, but most of these are overshadowed by the effect of applied current and the greatly increased aggressiveness of the electrolytes used. In particular the influence of the nature and concentration of the anion become paramount. A detailed review of reported work is presented in the next section. On aluminium, anodization and electropolishing are two processes related to one another but, both being of a high voltage film-forming nature, they are entirely different from dissolution.

When a tartrate, citrate or borate electrolyte is used, anodization produces an essentially pore free barrier type film[23]. However, a two-layer film is formed when a sulphuric, phosphoric, or chromic acid medium is used. In the latter electrolytes simultaneous chemical solution of the oxide film at the film-liquid interface causes the formation of a porous outer layer[23]. Anodic dissolution with brightening or polishing takes place when the rate of solution of the solid film by the electrolyte equals its rate of electroformation. Metal dissolution is said[22] to be controlled then by the random arrival of cation

vacancies in the film lattice thereby leading to smoothing of the metal surface.

2.4(ii) Anodic dissolution of aluminium

During the course of studying the electrode potential behaviour of freshly cut aluminium electrodes under static anodic load in 1N KCl electrolyte (see Sec.7), two unexpected observations were made by the author.

(a) Over the range of applied current density from 10^{-3} to 5×10^{-1} amp/cm^2, the electrode potential varied only a little from a value of about -0.5 volts NHE.

(b) The aluminium anodes evolved gas, evidently hydrogen, quite vigorously, the quantity increasing notably with increase in applied anodic current even up to very high current density.

Since hydrogen evolution whether from H_2O or H^+ is a cathodic reduction involving a gain of electrons by the hydrogen, it is clear that anodic current cannot of itself result in hydrogen evolution. A search of the literature revealed that neither were the observations new nor the phenomena unique to aluminium, but it was found that conflicting hypotheses had been advanced by different workers in

explanation of these and other closely related effects observed during anodic dissolution of aluminium and other metals such as magnesium and beryllium.[64,71]

Straumanis and Wang[24] measured the volume of hydrogen gas evolved from aluminium anodes during electrolysis in aqueous hydrofluoric and hydrochloric acids, and described the results in terms of the positive and negative "difference effects". In the hydrofluoric acid solutions increase in applied anodic current density resulted in decreased hydrogen evolution as might be expected from the polarisation of the electrode to more positive potentials; this was the positive difference effect. However, in hydrochloric acid solutions it was found that hydrogen evolution rate increased with increasing anodic current; this was the negative difference effect. This negative difference effect was explained on the basis of the hypothesis of the "impact of emerging cations" causing damage to the passivating oxide film, proportional in extent to the applied current, thereby exposing new cathodic sites for hydrogen evolution. In a later paper, Straumanis[25] suggested that the metal surface exposed by this mechanism was able to react with the electrolyte by "acid coming into direct contact with the bare metal" thus increasing the rate of "self-dissolution".

When electrolyses were carried out with aluminium in a number of aqueous electrolytes (Cl^-, Br^-, I^-, NO_3^-, ClO_3^-, BrO_3^-, ClO_4^-), Davidson & Raijola[26] found the weight lost by the anodes was always greater than calculated from the electrochemical equivalent of aluminium. The proportion of excess was about 15% - 50% of the expected weight loss and dependent on the anion in the electrolyte. Hydrogen was found to evolve from the anode in Cl^-, Br^- and I^- solutions and a white or greyish turbidity appeared in the anolyte in all cases. The anolyte was observed qualitatively to possess reducing properties during and after electrolysis. In non-aqueous electrolytes such as liquid ammonia, anhydrous acetic acid, and pyridine, Davidson et al[27,28,29] had found reasonable evidence for the formation of monovalent cations in anodic dissolution of aluminium and other metals. These ions if formed would be unstable, hence short-lived and highly reducing and were thought therefore to react swiftly with any reducible species in the electrolyte. Such reduction was observed and compared quantitatively with electrode weight loss; the results were consistent with hypothesis. By analogy these workers postulated the formation of Al^+ in aqueous solution and explained thus the excess weight loss (Al^+ equivalent weight 3 x Al^{+++} equivalent weight) and the greyish particles by

$$3Al^+ = Al^{+++} + 2Al \qquad \text{(disproportionation)},$$

the hydrogen evolution by

$$Al^{+} + 2H_2O = Al^{+++} + H_2 + 2OH^{-}$$

and similarly the other reducing effects.

The Russian workers, Tomashov and Modestova[30] published in 1956 the results of an investigation into the anodic behaviour of aluminium. However, a photo-copy and subsequent translation of their paper was not obtained by the author until the present work was well under way. These workers used super-pure aluminium anodes in electrolytes of 0.5n H_2SO_4 with from 0.005n - 2.5n NaCl, or 0.05n - 2.5n NaBr, or .1n - 2.5n NaI, in hydrogen atmosphere. During dissolution the aluminium electrode potential and hydrogen gas evolution from the anode were measured as functions of time, anion type and concentration, and applied anodic current density in the range 1-100 ma/cm^2.

Steady-state conditions were attained within seconds and thereafter both anode potential and gas evolution were independent of time. During anodic dissolution in any one of the solutions the steady-state potential of the electrode was almost constant over the range of current density 1-100 ma/cm^2. For each halide at each concentration this was a characteristic and reproducible voltage which was most negative -.57v NHE for 2.5n NaCl and least negative -.12v NHE for .1N NaI. The rate of gas evolution from the anode was equivalent to 10.5% on

the applied anodic current in iodide, independent of its concentration and about 13% in chloride independent of its concentration, with bromide results intermediate. In fluoride the electrode was oxidised by the anodic current.

The potential response to step change in current was observed in several of the electrolytes. When switching to a different current density a brief (seconds) potential excursion was observed; duration and magnitude of the transient was least in concentrated chloride and greatest in dilute iodide. Visual observation of the aluminium anodes showed that pitting had occurred at low current density and more general attack at higher current density; pits were few and deep in iodide, shallow and wider in chloride.

These results were explained on the basis of disruption of the protective oxide, by and in proportion to, the applied current; by implication current flowed only through bare areas leading to constant real current density and hence independence of electrode potential on current density in the steady state. From the bare areas self-dissolution by direct reaction of water and aluminium was postulated to give hydrogen and a film, leading to excess weight loss when the oxide film so formed was continuously disrupted by the halide ions. No weight loss measurements were made however. Their qualitative

conclusions and the independent quantitative model proposed in this thesis are strikingly similar.

Numerous other investigations have touched on some aspects of the subject. Thus, pitting of aluminium and related potential behaviour have been investigated by Masing et al[31,32,33]. Japanese research[34,35,36] into the use of aluminium for dry cell battery anodes, involving measurements of the current efficiency and electrode potential, has encountered these phenomena but no new information has resulted. Each author subscribed to which ever already published hypothesis he preferred.

The very similar but even more marked pecularities in the anodic dissolution of magnesium have been subjected to at least as much scrutiny as those of aluminium and analogous hypotheses have been advanced in explanation[37,38,39,40,41]. Related observations from research into pitting have been reviewed by Kolotyrkin [42,43].

2.5 Scope of the Present Work

From a careful examination of published work on the phenomena attending the anodic dissolution of aluminium in aqueous chloride, it was clear that more information was needed before sure answers could be given to questions such as the following.

(i) What is the nature of the steady electrode potential

under a wide range of current density?

(ii) What is the origin of the gas evolved from the anode?

(iii) What is the origin and mechanism of excess weight loss from the anode?

While the published work summarised above suggested possible mechanisms for the processes, there was a lack of explanation of these fundamental issues. For example, why should the amount of excess be, say, 13% in chloride? Why should the electrode potential be -.57 volts NHE in 2.5N chloride? None of the explanations was entirely satisfactory; limitations in extent and thoroughness of experimental work had led to unsupported assertions. Those suggesting that anode hydrogen evolution arose from local cathodes on the aluminium did not have even order of magnitude values of cathodic parameters to support their hypothesis. Proponents of the monovalent ion hypothesis overlooked the need to explain the steady potential behaviour, and the fact that the proportion of excess was constant for the entire range of applied current density in a given medium. The proportionality of active area to applied current was no more than implied by results; no direct experimental proof had been obtained.

The scope of the present work was to answer these questions and as far as possible account quantitatively

for the observed behaviour. It was hoped to establish a connection with the previously reported behaviour in aluminium pits[21] and on micro-electrodes[44,45,46] of the metal and to incorporate the kinetic data already determined by Earl[5] and Watson[6].

Extension of work to higher current densities held promise of providing a decisive test especially of the hypothesis that active area keeps pace with the applied current since a limit is clearly reached when the total area is involved in dissolution.

3. EXPERIMENTAL

3.1 Outline of Experimental Programme

It was taken as established that steady dissolution occurs in only some electrolytes and it is this type of process which has been investigated. The specific object of the experimental work was to determine the origin and mechanism of the excess metal dissolution, the anode gas evolution, the nature of the steady electrode potential, and the limits of these phenomena especially with respect to current density, since indications were that high local current densities occur in pits and at pores in surface film. No reported studies of these phenomena had involved concurrent observation of all the effects nor had they available to them the kinetic data[5,6] available to the author.

Electrolyses were therefore carried out first to find the effect of variation in:

(1) Current density,

(2) Duration of electrolysis,

(3) Nature and concentration of the anion, and

(4) Solution pH,

on the observed dependent variables which were:

(1) Anode gas evolution rate, the so-called difference effect,

(2) Anode weight loss, the current efficiency,

(3) Anode working potential, and

(4) The appearance of the electrode after dissolution.

Complete mass balances were produced but when the results were assessed it was found that the origin of the effects could not be determined unequivocally. Thus the rate of hydrogen evolution from the anode was found to be much too great for spontaneous cathodic reaction to be responsible, but the possibility of some abnormal cathodic process could not be excluded on the grounds of electrode potential. Similarly, qualitative evidence of a strong reducing effect was found which supported the monovalent ion proposal. From these indications further tests were undertaken with the aim of obtaining diagnostic criteria for the purpose of differentiating amongst the alternative hypotheses. These were:

(1) An attempt at detection and quantitative assessment of any short-lived reducing effect in the anolyte during electrolysis.

(2) Analysis of the gas evolved from the anode at high current densities as a possible indication of electrode potential if oxygen were detected.

Neither set of experiments produced the expected information. From the reducing effect experiments, it became clear that hydrogen evolution by reduction of water was occurring so close to the electrode surface

as to preclude the possibility of detection of a reducing species in solution at a distance from the electrode, and the attempt was abandoned. Since it was found impossible to sustain steady high-current density dissolution under the conditions in the gas evolution apparatus, results were inconclusive and gave no definite indication of electrode potential. It was then decided to extend the earlier electrolyses to even higher current densities in the reasonable expectation (Sec.2.5) that behaviour near limiting conditions would produce decisive information. A more elaborate apparatus was designed and constructed to overcome the substantial experimental difficulties already encountered. This work produced the necessary information.

A brief investigation with electrodes cut under solution using steady anodic loads from the instant of cutting had earlier been undertaken, and results gave some indication of the early potential behaviour.

3.2 General Experimental

3.2(i) Materials

Two types of aluminium were used in the present work, pure and super-pure designated 4N and 5N respectively. Analyses provided by the suppliers, British Aluminium Association for the 4N and

Koch-Light Laboratories Ltd, England, for the 5N, are:

4N		5N	
Al	99.99%	Al	99.999%
Si max	.0004	Ca	0.1 ppm
Fe max	.0003	Cu	0.1 ppm
Cu max	.0025	Mg	0.2 ppm
		Mn	0.2 ppm
		C	< 1 ppm

To avoid contamination, electrodes used in electrolysis experiments were machined to size using a special ruby lathe tool.

Apart from a few cases noted later, all electrolytes used were prepared from A.R. grade chemical dissolved in either distilled or deionised water. Impurities in solution were not considered to be likely to influence the course of anodic dissolution processes except possibly at very low current density, where their accumulation might result from restricted diffusion within pits.

When desired, bulk pH was measured with a glass electrode pH meter and adjusted to the required level by addition of A.R. acid or alkali. Solution concentrations were standardised by the normal methods until it was found that precise concentration was not a critical factor.

In most experiments the electrolyte was purged with

hydrogen gas. For early runs the gas was purified by passage over heated platinised asbestos and later by using a palladium-silver diffusion apparatus. Purification was discontinued when it was shown to be unnecessary; the gas was then taken straight from the cylinder.

3.2(ii) Equipment

Current supplies

In work with anodically loaded electrodes cut under solution, a simple transistor circuit, described by Earl[5], was used to supply the constant current.

Two different sources of direct current were used for the electrolyses. In the first series of experiments a Heathkit type IP-20, transistorised regulated DC power supply was used for currents in the range 1 ma - 1.5 amps at 0-50 volts DC. Ripple voltage was extremely small. Total coulombs passed during a run was calculated from the volume of cathode hydrogen gas evolved, and compared with the approximate figure from average current and run duration.

For later work where higher currents up to 15 amps were needed, power was drawn from a 3-phase input, full-wave rectified 260v DC power source. Use of an additional capacitor-choke network reduced ripple to less than 1%. Voltage dropping rheostats were used to

adjust the current, and acting as large external resistances, they provided a fair measure of stabilisation to the working current load.

Accurate measurement of the total coulombs passed during a run was achieved by the following means. Circuit is shown in Fig. 3.1. Electrolysis current passed through a very large capacity current shunt, R_s, of suitable low, but stable resistance, and the millivolt output signal was monitored by a Honeywell type 153x 18 high-speed single point recorder. The relation between voltage signal $V_o = IR_s$ and current I was fixed by the use of a dummy load resistance and a calibrated precision ammeter. Immediately before and after each run, standard current lines were established on the recorder chart just above and just below the current being used for the particular run. By this means recorder zero error was minimised and the effect of amplifier non-linearity minimised. Frequent checks and adjustments were made to ensure optimum response of the recorder. Timing by hand stopwatch was checked from the recorder chart speed; agreement to 1/10 sec was regularly achieved. Total coulombs were therefore obtained by integrating the area on the recorder chart.

A check on the overall accuracy of the system was carried out by high current density (70 amp/cm^2) dissolution of pure cadmium. Agreement with expected

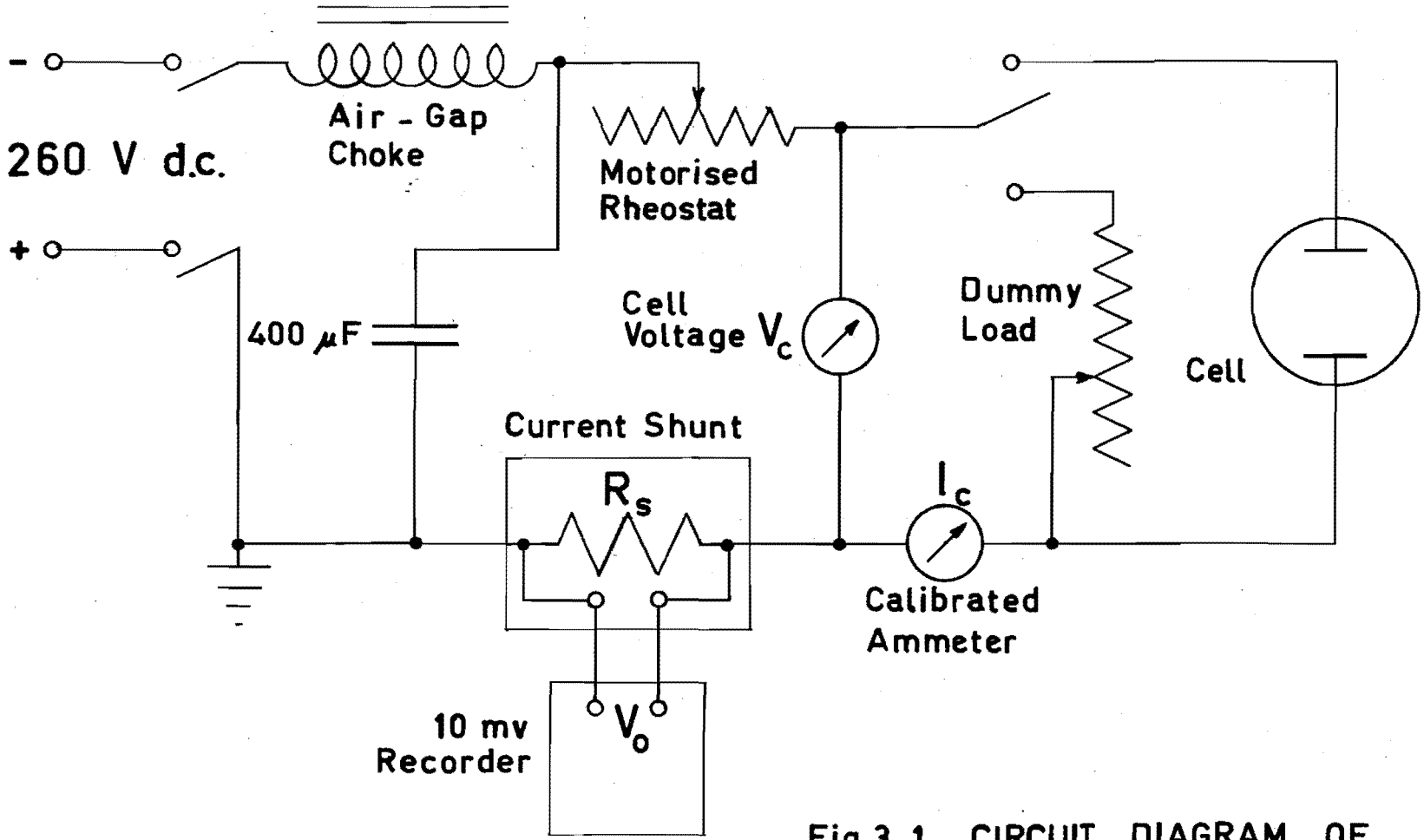

Fig 3.1 CIRCUIT DIAGRAM OF HIGH CURRENT SUPPLY.

weight loss was within 0.6% in each case. Other apparatus used for each set of experiments is described in the appropriate later sections.

4. ELECTROLYSES WITH STATIC ELECTROLYTE

The word "phenomena" will be used from now on in this thesis to indicate specifically and collectively all the effects noted earlier which have been found to occur at an aluminium anode undergoing steady-state dissolution in chloride solution, for example. A comprehensive examination of the phenomena in 1N chloride solution over a wide range of apparent current density was undertaken, and the effect of changes in pH, anion type and concentration, were obtained by comparison with the results in chloride.

4.1 Experimental

Electrolyses were carried out in a simple apparatus, Fig. 4.1, constructed largely of glass, under the conditions set out in Table 4.1. Dead-space at the top of the measuring limbs A and B, Fig. 4.1 , was calibrated by weighing contained mercury. In preparation for each run the following steps were carried out.

1. The electrode was machined from a polyethylene-coated ¼" diameter rod of 4N aluminium and the exposed area measured. It was then degreased in refluxing acetone vapour, dried, cooled and weighed to 0.1 mg before being inserted into the apparatus so that the working surface was close to the capillary connection to the N calomel half-cell, in order to minimise the effect on the measured

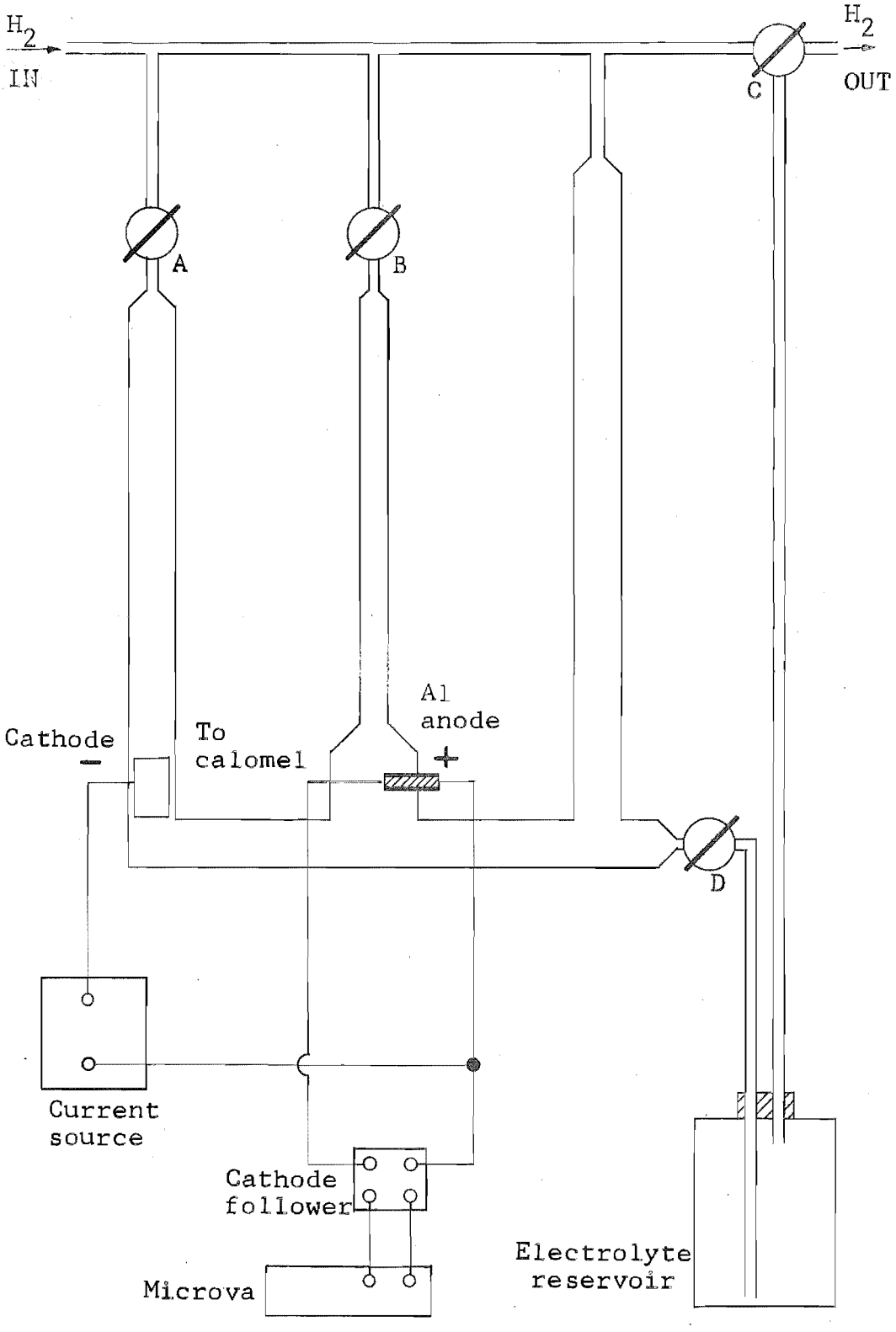

FIG 4.1 ELECTROLYSIS APPARATUS

potential of electrolyte ohmic resistance.

2. The whole apparatus and electrolyte were purged for about 1 hour with a downward flow of purified hydrogen.

3. The 10^{15} ohm input impedance cathode follower[46] was warmed up and balanced, the potential measuring circuit and Microva volt meter checked and standardised, and the Heathkit power supply (Sec.3.2(ii)) adjusted to give the desired current.

To start a run, the stopcocks C and D were set to fill the apparatus quickly with electrolyte, stopcocks A and B were then closed and the hydrogen turned off. Current and stopwatch were started simultaneously and the electrode potential measured periodically during the electrolysis. Displaced electrolyte was run back into the reservoir when necessary. After the run, gas bubbles adhering to the inside of the graduated tubes were dislodged by tapping, and for each limb in turn total gas pressure was adjusted to atmospheric and volume read. Electrolyte temperature was noted before and after each run to allow correction for solution vapour pressure.

The electrode was removed from the apparatus, rinsed in distilled water, dried, weighed and subjected to visual and microscopic examination. A variety of shapes of exposed electrode area including flat circular, cylindrical plus flat circular, cylindrical plus truncated cone, and hemispherical was used in an effort to obtain reasonably

uniform current distribution over the surface, and offset in part the unsymmetrical configuration of electrodes in this apparatus. The inherent non-uniformity of attack, described below, in large part negated these efforts but also made them unnecessary, since it was soon apparent from the appearance of electrodes after a run that it was not very meaningful to base current density on geometric exposed area, whatever the current distribution.

4.2 Calculations and Errors

By use of Faraday's Law the total coulombs passed was obtained with an accuracy of $\pm$ 1%, from the cathode gas volume corrected to dry NTP conditions. From the number of coulombs passed, the expected weight loss of aluminium was calculated and compared with the actual weight loss, which was itself subject to 1%-2% error depending on the magnitude of total weight loss. The difference between actual and expected weight loss gave the excess weight loss of the aluminium electrode; this quantity was subject to as much as 20% error. The ratio of cathode to anode gas volume was obtained, and was subject to $\pm$ 2% error. Precision and accuracy are low because the results involved the calculation of small differences between large quantities. The best reproducibility was obtained in the relative gas volume calculation since gas conditions were similar in each

limb and no other factors enter. Examination of the results presented in Figs 4.2, 4.3, 4.4 bears this out, although the reproducibility is generally rather better than might be expected from the large error estimates.

Table 4.1

Conditions under which static electrolyses were carried out.

Anion Type	Concentration Range N	pH Range	Anode Current Density amp/cm^2
Cl^-	.1 - 1	0,3.2,11,13	10^{-2} - 10
$Cl^- + SO_4^=$	.1 + 1	1	.1 - 1
Br^-	1	3.1	10^{-2} - 8
I^-	1	Neutral	.14
F^-	1	Neutral	-
* CN^-	1	Neutral	-
* $SO_4^=$	1	3	-
* ClO_4^- ≠	1	0, 3	.1 - 8

* Commercially pure material used.

≠ Discussed in Appendix A.

4.3 Results

4.3(i) Effect of Electrolyte on Type of Anode Reaction

In order to determine whether excess dissolution could be obtained with any electrolytes other than halide, a number of different salt solutions was tried; conditions are listed in Table 4.1. In fluoride, cyanide and sulphate at 1N concentration, no steady dissolution was obtained.

A passivating reaction occurred in both sulphate and fluoride, while in cyanide the high pH allowed a small amount of unsteady attack. However, rather surprisingly in 1N perchlorate solutions, behaviour resembling quite closely that in chloride was observed. A detailed examination of these and later runs in perchlorate is presented separately (Appendix A).

4.3(ii) Visual Observation

During electrolysis a stream of dense electrolyte flowed down from the electrode, cf. Hagyard and Santhiapillai[21]. When examined under strong light a multitude of very small shiny particles was visible in this stream, and also in the bulk electrolyte after the run.

All electrodes initially carried an oxide film formed in air during the several hours between machining and start of dissolution. There was a very non-uniform pattern of attack; at low current density and low pH in chloride numerous discrete but shallow pits were formed with some areas quite unattacked. Increase in current density led to spread of attack over the entire surface so that at .5 amp/cm^2 the electrode under stereo-microscopic examination revealed an almost spongelike appearance over the exposed area. Further increase in current density to 5-10 amp/cm^2 produced a much smoother etched surface although grain boundaries were not revealed. Change to

alkaline conditions caused a greater localisation of attack leading to fewer and deeper pits; a similar trend to more localised attack was observed in the transition from 1N chloride to 1N bromide to 1N iodide at similar current densities. Comprehensive photographic records of these effects were not made because of the near impossibility of obtaining an other than misleading representation of the three-dimensional structure. At best, only qualitative indications were obtained from the visual examination of the electrodes.

4.3(iii) Steady State

Several of the runs were carried out in three or four consecutive short stages in order to determine if any long-term trends were occurring. Current was switched off after a short period, gas volumes read and the current restarted for the next section of the run. Results are shown in Table 4.2.

It is clear that steady-state gas evolution, and by implication metal weight loss, was established in times short when compared with the 2 to 15 minutes of each section of these runs. Upon closing the switch, near full current flow was established immediately, although in .1N Cl^- attainment of the full final value took place over a period of a few tens of seconds. A corresponding anode potential transient was observed qualitatively. In the

1N electrolytes the transient was appreciably briefer.

Table 4.2

Results of Steady State Runs

Electro-lyte	Current Density amp/cm^2	Time min' and sec" % Anode gas*				Totals
1N$HClO_4$	.455	2'21" 13.7%	2'13" 14.6%	2'23" 16.4%	2'41.5" 13.9%	9'38.5" 14.6%
.1NHCl	.097	7'30.8" 14.5	7'16.5" 14.2	7'31.5" 14.2	12'18.2" 14.5	34'37" 14.35
1NKI	.138	13'40" 10.3%	14'24" 9.8%	12'38" 9.85%		40'42" 10.0%

*Volume of hydrogen evolved from the anode is expressed as a percentage of cathode gas volume.

4.3(iv) Electrolyte Analysis

Electrolyte from a number of runs, after being filtered, was subjected to quantitative analysis for dissolved aluminium. The figures obtained were compared with total electrode weight loss, in order to estimate whether a significant proportion of the weight loss from the anode was due to detachment of some solid metal fragments, such as the shiny particles observed in the electrolyte after most runs.

Filtration was carried out with Buchner funnel using a double thickness of Whatman 542 filter paper, which has a nominal mean pore size of 0.5 micron.

After filtration, the solution was nearly, but not quite, completely clear and the filter paper showed that material had been retained. Analyses were made either gravimetrically, by weighing as ignited Al_2O_3, or volumetrically by E.D.T.A. titration, both methods being carried out according to standard procedures[47,48]. Results of some analyses are presented in Table 4.3.

As might be expected from the small differences involved, the general accuracy of figures in the last column is only moderate, but sufficient nevertheless to prove the effect real and indicate its order of magnitude. Its significance is examined in the discussion, Sec. 4.4.

Table 4.3

Results of quantitative analysis of filtered electrolyte for dissolved aluminium content.

Electrolyte	Expected Wt Loss A gm	Actual Wt Loss B gm	Dissolved Al C gm	Total $\frac{B-A}{A}$ % excess	Nett $\frac{C-A}{A}$ % excess
1NHCl	.0488	.0578	.0565	18.4	15.8
1NHCl	.0185	.0214	.0210	15.7	13.5
1NHCl	.0163	.0189	.0182	16.0	11.6

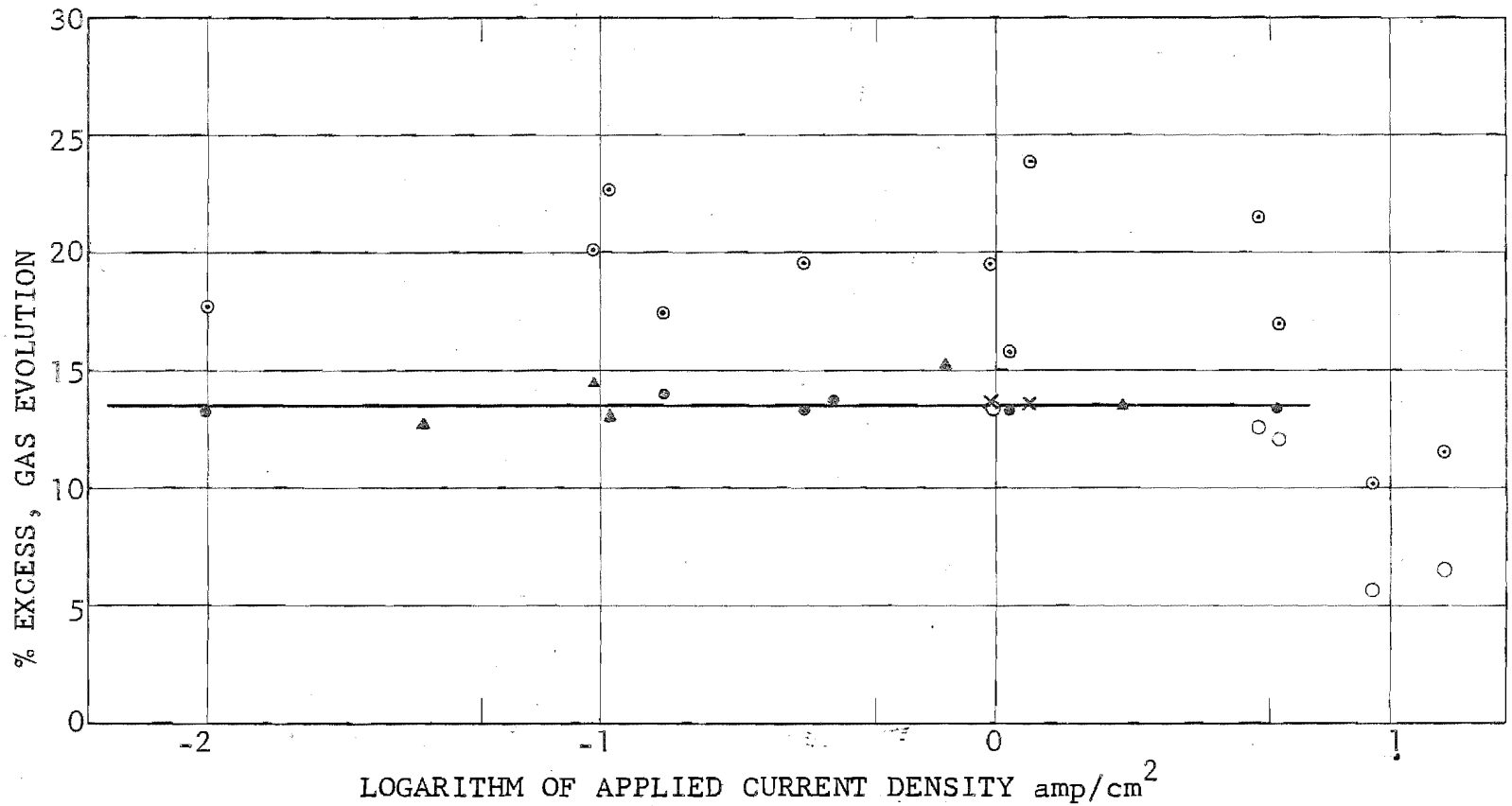

FIG 4.2 % EXCESS WEIGHT LOSS, % GAS EVOLUTION vs ANODE CURRENT DENSITY

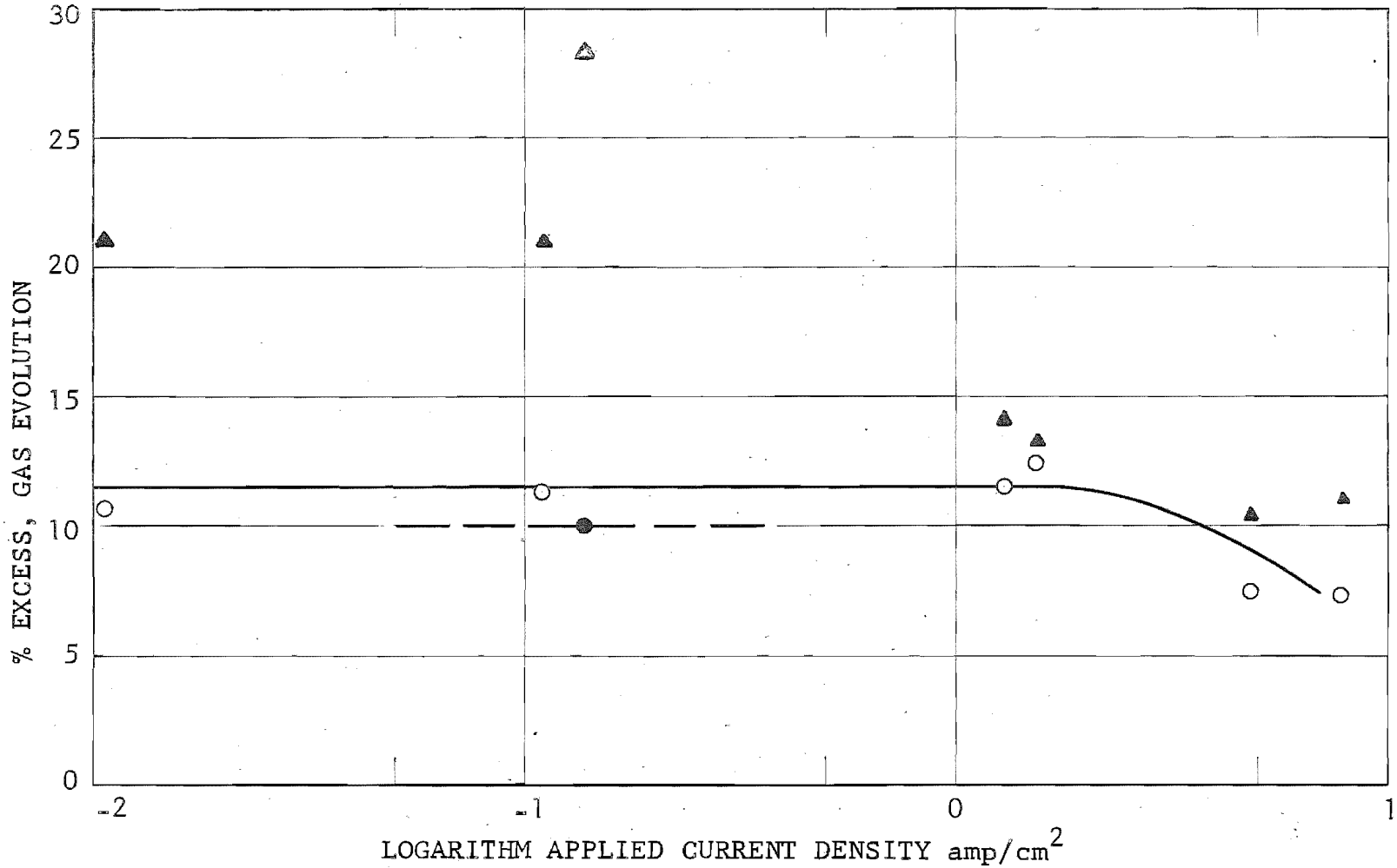

FIG 4.3 % EXCESS WEIGHT, % GAS EVOLUTION vs CURRENT DENSITY

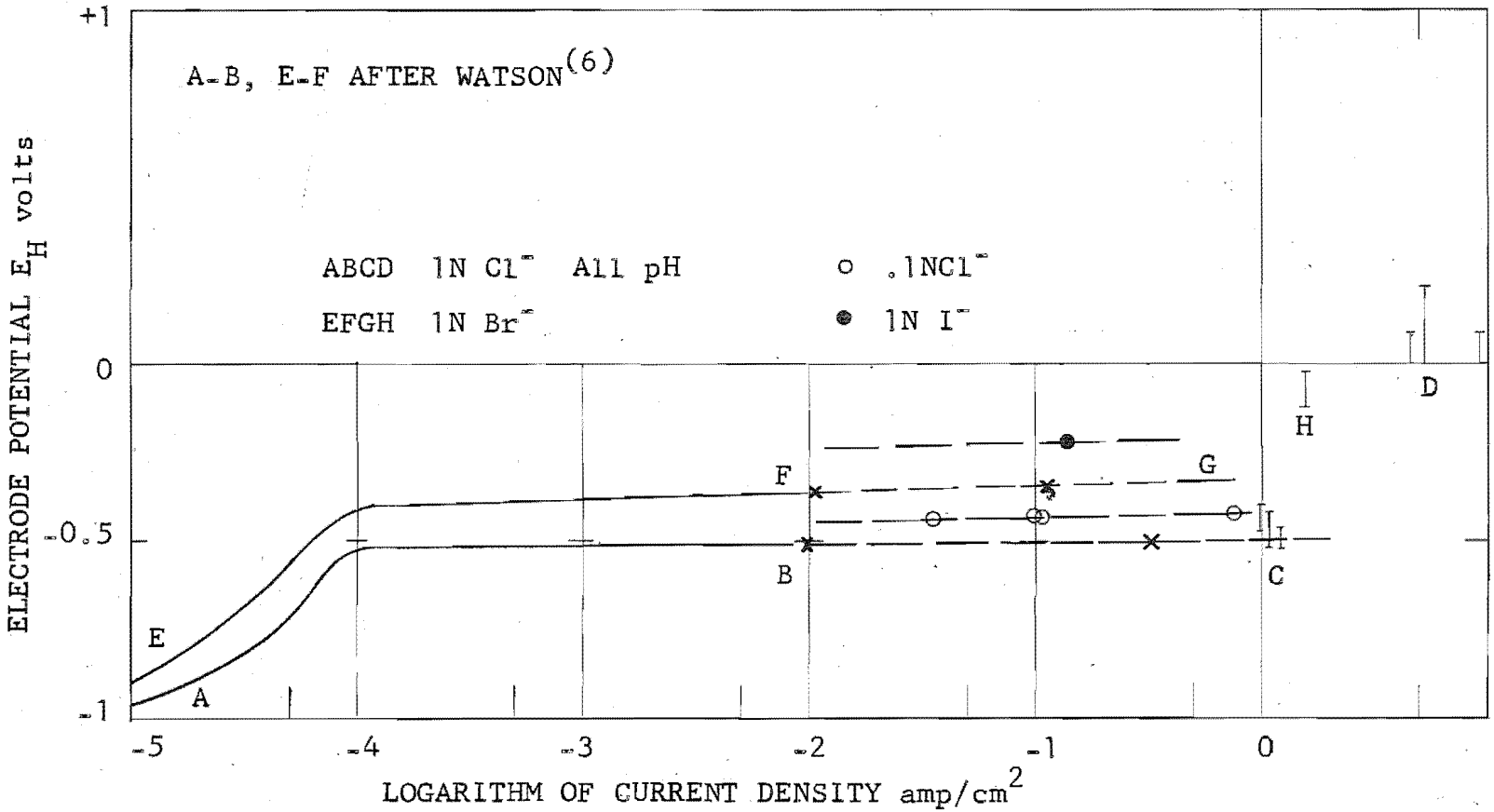

FIG 4.4 ELECTRODE POTENTIAL vs CURRENT DENSITY

4.3(v) Anode Gas Evolution, Excess Weight Loss, Electrode Potential

For easy comparison, representative values from the general results plotted in Figs 4.2, 4.3, 4.4 are presented in Table 4.4.

Excess weight loss has been expressed as a percentage of the weight loss expected from the applied anodic coulombs. Similarly, the coulomb equivalent of the evolved hydrogen has been calculated, and expressed as a percentage of the applied coulombs. Electrode potential has been converted from 1N calomel to the normal hydrogen scale by subtraction of 0.283 volt from the observed potentials.

Table 4.4

Summary of Results from Figs 4.2, 4.3 and 4.4.

Anion Type and Concentration	Potential at .1 amp/cm^2 volts E_H	Av.% Excess Wt Loss	Av. Anode Gas Evolution %
1N Cl^-	-.51	17.3	13.5
.1N Cl^-	-.44	21.3	13.5
1N Br^-	-.34	19.1	11.5
1N I^-	-.22	28.3	10.0

In the lower current density range of the present work, where the conditions are comparable with those used by Tomashov and Modestova[30], values obtained for electrode potential and gas evolution rate are in excellent agreement with their results. In the range of variables covered by these runs, the following effects were observed.

(1) Electrode working potential was not influenced by pH but was affected by both type and concentration of anion.

(2) Gas evolution also was influenced by the type of anion but not by its concentration, nor was it affected by pH.

(3) Bearing in mind the limitation of the data, the excess weight loss appeared to depend upon the electrolyte used and increased in the order 1N Cl^-, .1N Cl^-, 1N Br^-, 1N I^-.

(4) Comparison of results in .1N HCl with those in .1N HCL + 1N K_2SO_4 showed gas evolution proportion and electrode potential to be unaffected by the excess of indifferent electrolyte. Gas evolution and excess weight loss obtained at high current density are unreliable because of the significant effect of electrolyte heating on the accuracy of measurement of gas volume and hence the coulombs passed. However, the trend to lower excess, Fig 4.2, seems real enough and visual observations confirm that since

the whole of the anode surface is involved at apparent current densities somewhat less than the maximum used here, no further increase of active area in step with current would be possible. Under this condition an increase in real current density would have taken place. Electrode potentials measured at high current density are unreliable because the conflicting requirements of closeness of the calomel capillary to the working electrode, to minimise the influence of solution voltage drop, yet adequate separation, to prevent shielding and current maldistribution, cannot be satisfied simultaneously.

4.4 Discussion

Whatever the proposed mechanism of hydrogen evolution from the anode may be, a weight of metal electrochemically equivalent to that amount of hydrogen gas must dissolve, over and above the weight expected to dissolve under the applied anodic coulombs, i.e. gas evolution and excess weight loss should be equivalent to each other.

Examination of the results in Figs 4.2, 4.3 and Table 4.4 shows that gas evolution from the anode is significantly less than equivalent to the excess weight loss. This fact has not previously been quantitatively observed, although Davidson's[26] observation of

concurrent gas evolution and aluminium particle formation, whatever the mechanism, imply the result, i.e. total weight loss is made up of weight of undissolved particles together with weight of dissolved aluminium equivalent to the hydrogen. As outlined in Sec. 2.4(ii), he attributed particle formation to disproportionation of the hypothetical Al^{+} ion, thus $3Al^{+} = 2Al + Al^{+++}$. However, before particles of visible size could be formed, nucleation and growth of metal crystals is necessary. Such a process is highly improbable in view of the following facts.

(1) Solution of "Al^{+}" would be quite dilute (Sec. 4.4 (iii)) and, in the probable lifetime of such a species, distance travelled under diffusion would be negligible. This fact becomes more apparent after examination of results in Sec. 4.5.

(2) Attempts at cathodic deposition of aluminium from aqueous solution under much more likely conditions, viz. high cathodic potential and a freshly cut 5 micro-second metal surface in a more concentrated electrolyte, have failed completely[55].

(3) Microscopic examination of particles shows their size and shape to be extremely variable and generally inconsistent with the proposed mechanism of formation.

The real origin of the discrepancy between the two rates is almost certainly a small but significant loss

of microscopic metal particles directly from the anode, concurrently with the ionic dissolution. When results of analyses for dissolved excess aluminium weight loss (13.6% average) (Table 4.3) are compared with the anode gas evolution (13.5% average)(Table 4.4) a good agreement is found; the remaining excess weight loss is therefore in the form of undissolved particles, giving a near quantitative overall mass balance. Possible mechanisms for the loss of particles are discussed in Sec. 7. Since this process need not equate with applied current, some of the variability of excess weight loss measurements (Figs 4.2, 4.3) may be attributed to effects of the disintegration of the metal.

The most difficult result to explain is the independence of excess dissolution on the concentration of any given activating anion (Fig 4.2 and Ref 30). From Table 4.4 and Fig 4.4 it may be seen that there is a characteristic dissolution potential for each anion and it might be reasoned that the dependence of amount of excess dissolution on anion type is simply a consequence of the different electrode potentials. If this were so, then noting (Table 4.4) the clear difference in dissolution potential between 1N and .1NCl^-, would lead to a prediction of different amounts of excess dissolution in these two media; paradoxically this is not so since the amounts of excess dissolution are the same for both,

Fig. 4.2. There follows an examination of the results in terms of the two main hypotheses that have been advanced in the literature (Sec. 2.4(ii)).

4.4(i) Local cathode gas evolution hypothesis

The apparent lack of influence of pH, both on potential and gas evolution, tends to discredit this hypothesis. However, Hagyard and Santhiapillai[21] showed that inside active pits on aluminium the pH quickly fell from near neutral to pH 3.2, that of stoichiometric $AlCl_3$ approximately .1N, which suggests the possibility that electrolyte at the surface of the electrode might be heavily buffered by anodic products and remain close to this value; whether pH would rise to 3 from more acid levels is another matter. Some stirring due to vigorous gas evolution would promote mixing with the bulk electrolyte. If constancy of pH at the surface is accepted for the moment, the hypothesis may be quantitatively tested by the use of Earl's[5] cathodic kinetic parameters, determined in 1N KCl pH 3.2. In chloride at 5 amp/cm^2, anodic current density, the rate of hydrogen evolution is equivalent to approximately 0.7 amp/cm^2, while from Earl's parameters the maximum rate of cathodic hydrogen evolution on the whole surface is only 10^{-5} amp/cm^2 at a potential of -.5v NHE. Alternatively the electrode potential needed to carry

.7 amp/cm^2 of cathodic process is about -2.3 volts. While the exact electrode potential is uncertain, in view of the high anodic current density and consequent increase in polarisation, -0.5v is the most negative value possible under the conditions and hence the most favourable to the cathodic process. It is pertinent, however, to examine the validity of using Earl's[5] cathodic parameters in the present situation. At 5 amp/cm^2 of uniform anodic current density, the average lifetime of atoms on the aluminium surface is only 150 micro-seconds, compared with Earl's determination of cathodic parameters 1-5 milliseconds after cutting of an electrode in solution. These considerations overall rendered most unlikely the hypothesis of hydrogen evolution being the result of the normal spontaneous process at local cathodic sites. There remained the possibility of some abnormal or specially enhanced cathodic process for hydrogen evolution.

At high anodic current densities the electrode potential appeared to be tending appreciably in the positive direction, although the precise value was uncertain (Fig 4.4). If it were possible to show definitely that the electrode potential was more positive than the hydrogen reversible potential in the solution, then any cathodic process of hydrogen evolution could be entirely discounted. An attempt to do so is described in Sec. 4.6.

4.4(ii) Monovalent aluminium hypothesis

Examination of the results in terms of the monovalent aluminium ion hypothesis proved interesting, in that an apparently plausible explanation of the observed facts could be constructed. Analogical arguments involving the properties of elements in either the same period, or the same group, of the Periodic Table as aluminium, and considerations of electron configuration and ionisation potential all point to the possibility of monovalency of aluminium. A review of such information is presented by McGeer[49]. As originally proposed, ref. (26), the monovalent aluminium ion hypothesis was merely a qualitative suggestion made on the basis of very limited experimental observation so that the present discussion goes well beyond any previously published.

In the present context and in accord with visual observations, it might be proposed that by some process the active area during dissolution increases in proportion to anodic current density. In consequence, for a wide range of apparent current density in a given electrolyte, the electrode potential would remain nearly constant, since the real steady state current density would be unchanged. At a constant potential the ratio of rates of monovalent and of normal trivalent dissolution processes would also be constant, leading to the observed invariant proportion of excess in a given electrolyte. Estimates of the

standard potential of the hypothetical process

$$Al \rightarrow Al^{+}_{aq} + e$$

have been calculated using various approximation techniques for obtaining the thermodynamic quantities involved. Two independent estimates have been published which give values of -.55v [50] and -.59v [51] NHE, a quite fair agreement in view of the possible error of such estimations. Somewhat surprisingly it appears that no published work has in any way linked the constant potential observed in anodic dissolution of aluminium, Fig. 4.4 (e.g. -.51v NHE for 1NCl^{-}) with these estimated standard potentials, although the similarity of the two values clearly favours identification of excess dissolution with the monovalent aluminium ion process. The difference between the hypothetical Al^{+} potential and the always more positive value of the observed dissolution potential (Table 4.4) could then be interpreted as overvoltage arising from concentration and activation effects; this is in accord with the fact that the smallest difference between calculated Al^{+} potential and observed dissolution potential was in concentrated chloride, and the greatest difference in dilute iodide. (Dissolution potentials are taken from the present work and closely similar values contained in reference 30.) From this suggestion, and also from the very specific nature of the excess dissolution of aluminium with respect

to the anion in the electrolyte, there is the implication that the anion would take a direct part in the basic steps of monovalent cation formation. If so, the decrease in excess dissolution at high current density, Fig 4.2, might then be explained as the result of a limiting supply of the anion.

By using the calculated standard potentials of the individual ions it has been calculated[50,51] that the redox potential of the couple Al^{+}/Al^{+++} would be -2.20v NHE, indicating that at -.5v only an extremely low concentration (approx. 10^{-57}N) of Al^{+} could exist in equilibrium with unit activity of Al^{+++}, and also showing a powerful reducing ability for the Al^{+} ion, which would consequently be very shortlived. Any aluminium dissolved as monovalent ions would therefore rapidly reduce an amount of water, equivalent to the remaining valency, causing the observed quantity of hydrogen evolution. Such a process is stoichiometrically indistinguishable from local cathodic hydrogen evolution with an equivalent amount of excess metal dissolution; observations of overall excess dissolution can therefore give no clues to mechanisms.

A most telling observation which upsets this picture comes from Earl's[4] early determination of anodic dissolution parameters by measurement of peak potentials of electrodes cut under solution and a static anodic load.

If monovalent ions were evolved by a process similar to that outlined above, a break in the anodic Tafel line would be expected at the appropriate potential. In fact, the Tafel line was straight in the region -1 volt to 0 volts, NHE.

Further inadequacy of this hypothesis is revealed on closer examination of the proposed proportionality of active area and applied anode current density as an explanation of the near invariant electrode potential in a given electrolyte. The characteristic, exactly reproducible dissolution potential, implies for the process controlling active (bare) area a mechanism involving an electrolytic reaction proportional in extent to the applied anodic current. A process of this type, namely film damage proportional to the anion transport number, was found to hold for magnesium[38] under similar circumstances. However, for aluminium this mechanism does not hold, since in the present work (Sec. 4.3) measurements in .1N HCl (t_{Cl^-}-approximately .5) and in .1NHCl + 1N K_2SO_4 (t_{Cl^-}-approximately .04) showed both anode dissolution potential and anode gas evolution to be uninfluenced by this difference between electrolytes. If it is taken for the moment that the active area does <u>not</u> remain proportional to the applied current, it is not clear how the electrode potential could then be controlled by a process contributing at most one-seventh of the total dissolution.

To account for this, it would be necessary to have at least the improbable circumstance of an exactly parallel dependence of trivalent and monovalent dissolution processes on anion type and concentration. As an alternative explanation of the near constant potential, it might be proposed that the monovalent dissolution process have a large i_{oa} and in consequence be difficult to polarise by increasing current density. A moment's consideration shows that contrary to experimental observation, this would lead to the proportion of excess dissolution increasing considerably with current density, since at constant potential the absolute rate of trivalent dissolution would not change.

Although these points put the monovalent aluminium ion hypothesis in an unfavourable light, an experimental observation was made during measurement of excess dissolution in 1N $HClO_4$ (see Appendix A for details) that seemed then not readily explained except by this hypothesis. It was the discovery that, after a run carried out in what was initially chloride free 1N A.R. grade $HClO_4$, a significant amount of chloride was present, indicating that reduction of perchlorate ion had taken place. According to Sidgwick (52) the perchlorate ion in aqueous solution of moderate strength is notably stable, being reduced only with difficulty. The implication of a powerful reducing agent being necessary, is clearly in favour of the formation of

Al^+ at a dissolving anode. Detection of these ions in solution at a distance from the electrode, seems unlikely in view of their instability and probably extremely short life-time. It seems doubtful whether the clearly longer term reducing effect observed by Davidson et al[26] (Sec. 2.4(ii)) can reasonably be attributed to such a species. However, it was decided to attempt a quantitative measurement of any reducing effect that could exist in detectable quantity for a few milliseconds. This work is described in the next section (Sec. 4.5).

4.5 Detection of Reducing Effect

Experimental:

The experiments were carried out in the simple glass apparatus shown diagrammatically in Fig 4.5. Electrolyte flowed from the reservoir to replenish that drawn from the immediate vicinity of the electrodes by vacuum applied via the collecting vessels. The solution of reducible species was drawn up through the capillary to mix with the electrolyte at the tee-junction. In operation, flow rates were such that less than three milliseconds were required for the electrolyte to travel the 2cm of capillary to the mixing zone. Reynolds number in the side arm was about 10,000, which promoted rapid mixing of the two streams. The quantity of solution of reducible species drawn up was determined from the weight change of the beaker, allowance

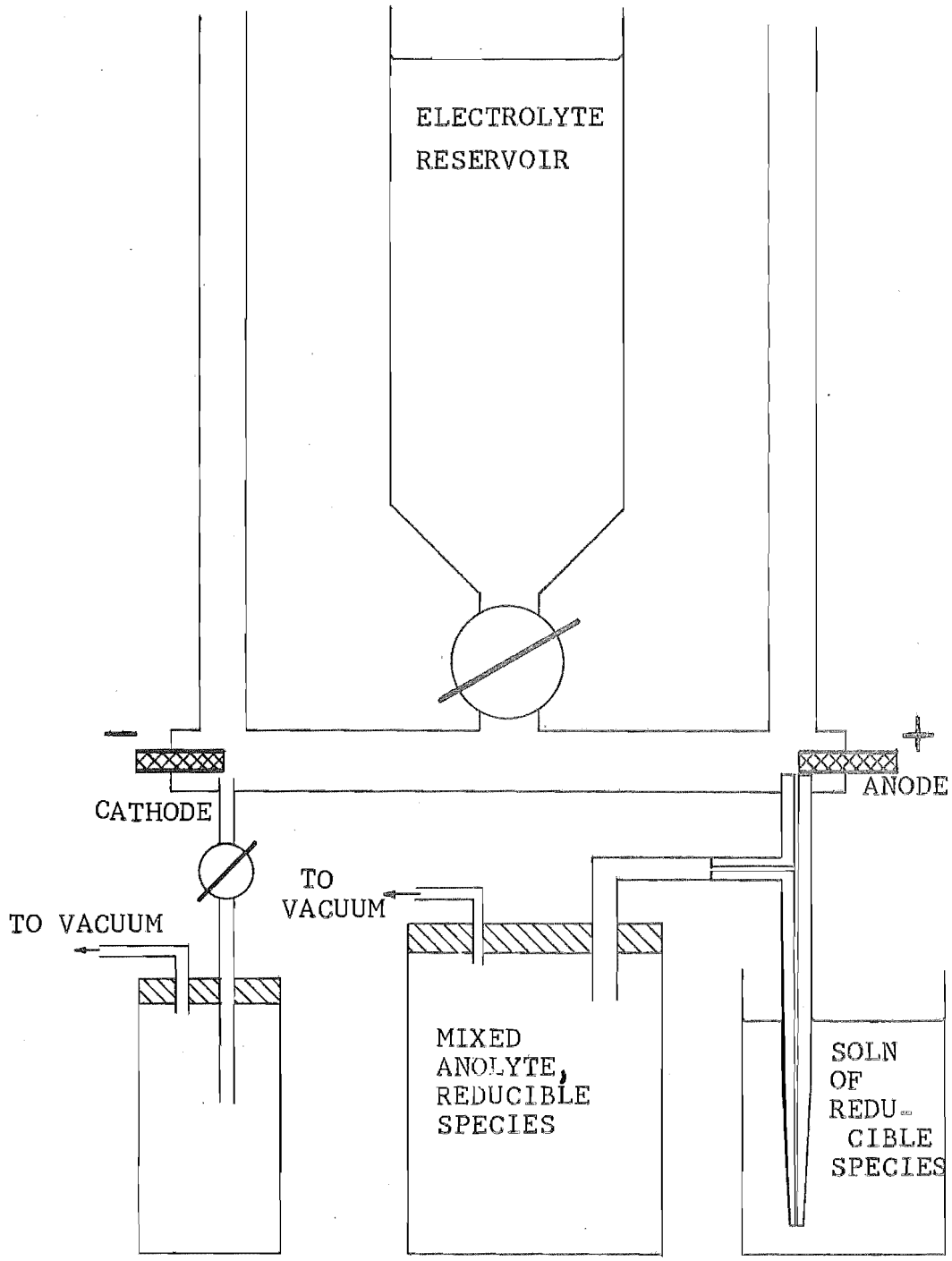

Fig. 4.5 Reducing Effect Apparatus

being made for evaporation loss. The mixed solution and electrolyte was then titrated.

Current was supplied by the Heathkit power supply (Sec. 3.2) run at 1.5 amps to give an anode current density of 5 amps/sq.cm. Both anode and cathode were 4N aluminium since it was decided to compare results in both anolyte and catholyte for reducing species, in view of the possibility of atomic hydrogen formation. The reducible species was a dilute solution of ceric sulphate standardised against ferrous ammonium sulphate solution. Blank titrations were made to determine any effect of the presence of HCl electrolyte on the standardisation of the dilute ceric sulphate solution.

Results:

Visual observation during a run showed that the apparatus successfully drew a very rapid stream of electrolyte past the anode. However it was observed that even at the highest flow rates gas bubbles were formed, indicating that reduction of water to hydrogen was occurring. Although these bubbles were entrained by the downward flow of electrolyte, their formation indicated either an extremely rapid reduction in solution or else a reaction at the electrode surface itself. In either case the present method could not be expected to detect any reducing effect due to the species sought if

it could react so close to the electrode surface. In fact, the titrimetric analysis gave no definite positive indication, the largest effect being about one per cent, approximately equal to the experimental error.

Discussion:

The reducible species chosen was not ideal for the present situation, and even at the smallest concentrations that were usable the sensitivity was inadequate. In the light of the visual observation it seemed pointless to pursue the search for a reducing species in solution, since even if a high-speed sensitive technique were to detect an effect it would probably be too small for useful interpretive work. In any case the visual observations pointed to a reaction substantially at the surface of the metal. The particular case of reduction of perchlorate to chloride is left to be examined in Section 10 in the light of further experimental evidence.

Subsequent to the above investigation, work has been published by Uhlig et al[53] demonstrating clearly the presence of small concentrations of atomic hydrogen in solution near nickel and platinum cathodes, and also in the anolyte from a magnesium anode undergoing solution. Half-life of the species in solution was about five minutes, quite sufficient to be detected by the qualitative tests of Davidson et al[26]. There had been a suggestion by

Straumanis[54] that fine metal particles in solution could be the origin of the reducing effect. The idea has little merit, since it overlooks the fact that the protective oxide film on aluminium is so thin as to be small even when compared with the size of particles, which should therefore be no more reactive than the massive metal.

4.6 Gas Analysis

The outcome of the work described in the previous section led to a re-assessment of the possible origin of the Phenomena, and emphasised that definite information on electrode potential during dissolution at high anodic current density could prove decisive. Methods, such as rapid interruption of the current, for the accurate measurement of potential of electrodes carrying a high current density were investigated, but extremely high-speed switching at the desired current level was found to be beyond the capability of contemporary electronic components. An indirect method was devised for an attempt at determining whether the electrode potential at high anodic current density was substantially more positive than the hydrogen reversible potential. At potentials near +1.5v NHE the evolution of oxygen or chlorine became theoretically possible. Earl's anodic kinetic parameters, from measurement of anodically loaded peak potentials,

indicated that such a potential might be reached by the dissolving anode at high current density. If, therefore, oxygen or chlorine were present together with hydrogen in the evolved gas, cathodic evolution of the hydrogen could be ruled out on the grounds of electrode potential. A few brief exploratory runs with small electrodes showed that dissolution and vigorous gas evolution occurred even at 80 amps/sq.cm. A chemical test for dissolved chlorine in the electrolyte after such a run, gave what was taken as a slight positive indication.

Experimental:

The technique was therefore to analyse gas evolved from the aluminium anode dissolving at highest possible current densities in chloride solutions. A small glass apparatus for collection and analysis of the gas was designed and constructed, the gas analysis section being based on the Ambler apparatus (47). A diagrammatic cross-section of the whole apparatus is shown in Fig 4.6. Operation of the apparatus was quite straightforward. Current was passed until a sufficient volume of gas, about 5 to 10 ml, had been collected and the total volume was measured approximately. The gas was transferred to the thermostatted bulb and its pressure read at constant volume. The gas was then exposed to the first absorbent for sufficient time, the change in pressure at constant volume noted, and a second absorbent then used. Analysis of 5ml

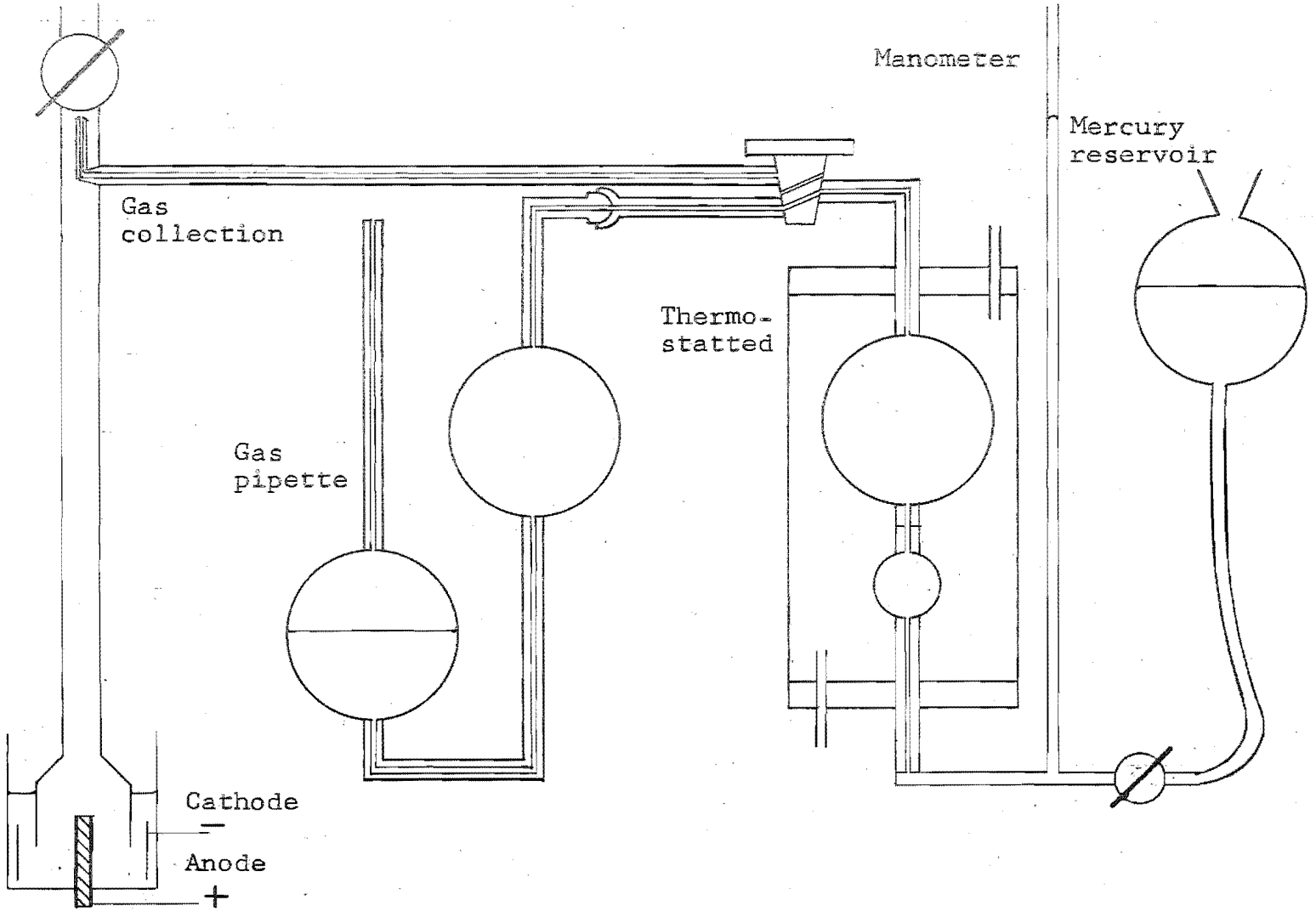

FIG 4.6 APPARATUS FOR GAS COLLECTION AND ANALYSIS

to better than .5% was readily achieved. Electrodes of 4N aluminium were dissolved in 1N HCl, chosen for its good conductivity. Absorbents were 30% KOH for chlorine and alkaline pyrogallol for oxygen.

Results and Discussion:

This work was an almost total failure, since a steady high current density dissolution could not be sustained for long enough to collect the necessary gas volume. In the small volume of near-stationary electrolyte adjacent to the anode, considerable heating took place and depletion of chloride resulted in a sudden change from dissolution to oxidation and temporary passivation, which broke down intermittently and violently under the high electric field stress. Although some oxygen was found in the gas, under these circumstances of unstable and uncharacteristic electrode process, no significance could be attached to its presence. It is of importance, however, that the bulk of the gas evolved at anodic current densities of 25 amps/sq.cm. and higher, was hydrogen.

4.7 Conclusions

Although the work described so far has served to point the weaknesses of the two hypotheses commonly advanced in the literature, even in their more developed form here presented, there is not yet sufficient evidence to enable the outright dismissal of either. However,

further investigation, described in the next section, led to information decisive in this matter.

5. HIGH CURRENT DENSITY DISSOLUTION

As the most promising means to the end of distinguishing sufficient of the nature of the anomalous dissolution to enable determination of its origin and mechanism, an apparatus was designed and constructed in which steady ultra-high current density anodic dissolution of aluminium was carried out.

5.1 Design of Apparatus

From the experience gained in the work already described, it was evident that the following characteristics were required of and for the apparatus.

(1) A source of controlled direct current of sufficient amperage and means for measuring the coulombs passed.

(2) A means for ensuring uniform anodic current distribution.

(3) A means for keeping the anodic area constant and uniformly accessible throughout the run by compensating for the considerable rate of metal removal at high current density (2mm/min at 100amp/sq.cm).

(4) A controlled and steady flow of sufficient pure electrolyte to the anode.

(5) A means of determining whether the total electrode weight loss represented the true dissolution rate.

(6) Preferably a cell designed to allow visual observation of the anode process.

The final form of the apparatus was evolved through numerous trials of different electrode geometries and simple but unsatisfactory fluid flow arrangements. Constructional detail of the cell is shown in Fig 5.1, the function and arrangement of the remaining equipment being illustrated diagrammatically in Fig 5.2. A description of the power source and method of coulomb measurement is given in Sec. 3.2 (ii).

In the following description, numbers, e.g. 10, correspond with features of Fig 5.1.

From this diagram, it is clear that electrolytic current between cathode and anode was constrained to flow via the "nozzle", 10, which had the same internal diameter as the electrode external diameter, was accurately co-linear with the electrode and placed within 0.025cm of the plane of the electrode surface. With this arrangement there was an inherent evenness of current distribution that was maintained independently of the size and shape of the cathode.

The method used to keep the dissolving surface of the anode coplaner with the PTFE seal, 12, and therefore uniformly accessible throughout a run, simply involved rotating the cell on its threaded PTFE mounting base, 15, at a predetermined rate appropriate to the current density. This caused the cell, 14, to move downwards keeping pace with the retreating electrode surface.

Rotation of the cell was accomplished by a capstan device, which steadily unwound several turns of copper wire from around the cell glass, 9; the rate of rotation, governed by the relative diameters of the capstan and cell, could be changed to suit the current density. A small interference fit of the electrode in the low friction PTFE seal, 12, effectively prevented the leakage of electrolyte past, or electrolytic current to, the cylindrical surface of the aluminium. Examination of Fig 5.1, feature 16, will show that independent rotation of the electrode at any desired speed was possible; however, after some initial tests this facility was not used.

Under the influence of positive pressure, fresh electrolyte flowed radially in through the narrow gap between the PTFE anode seal, 12, and the "nozzle", 10, past the anode up through the "nozzle" to the cathode and on. This arrangement minimised the temperature rise at the anode surface, and ensured effective sweeping away of evolved gas bubbles. The maximum liquid flow used at high current density was about two litres/min, corresponding with maximum radial velocity of 1100cm a second, calculated at electrode diameter, and a mean velocity up the nozzle of 340cm a second. The full electrolyte circuit is shown in Fig 5.2.

Uniformity of dissolution, which was dependent on all of these factors, and a test of the effectiveness of

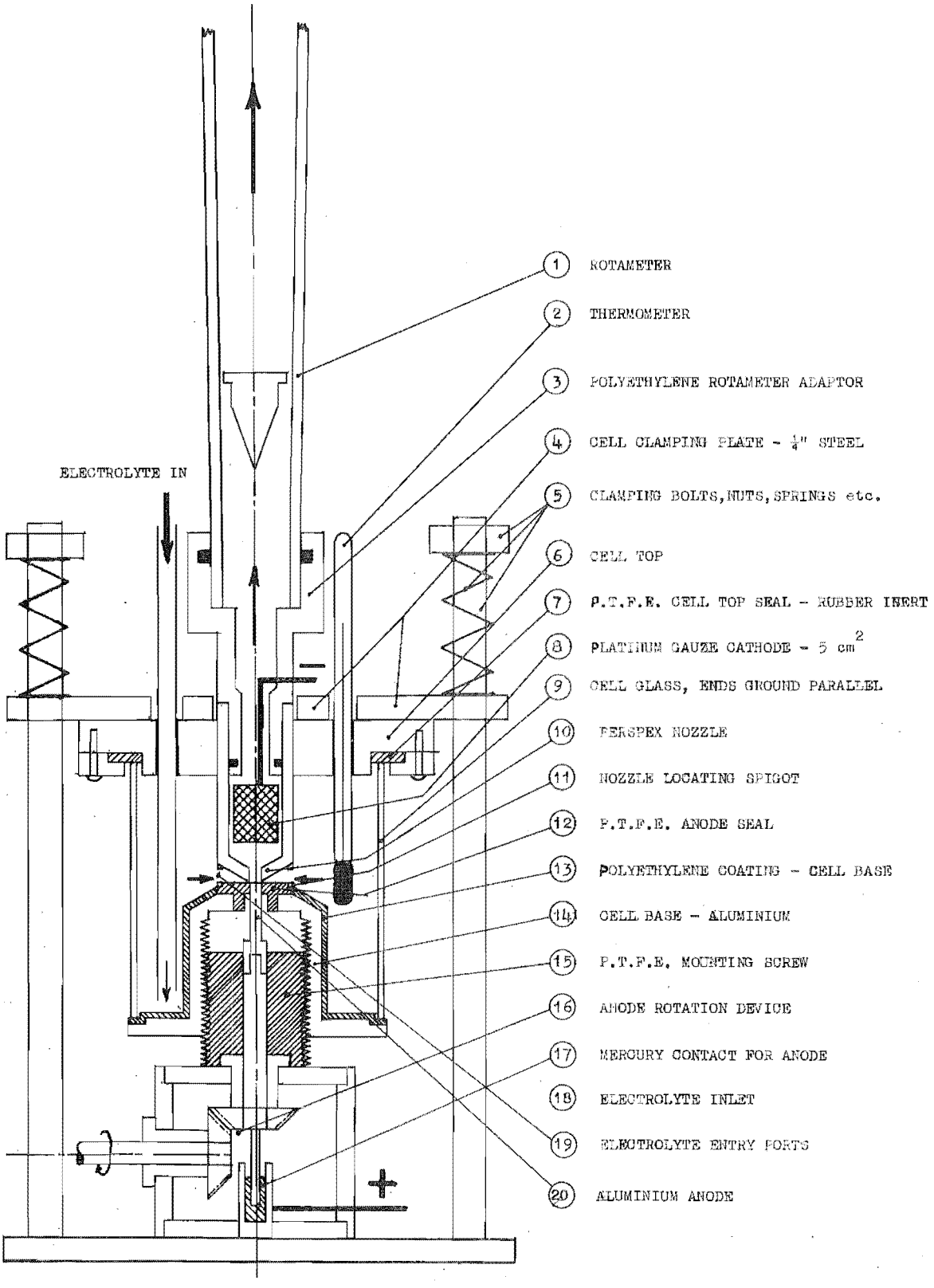

Fig. 5.1 Diagrammatic Section of Cell Assembly

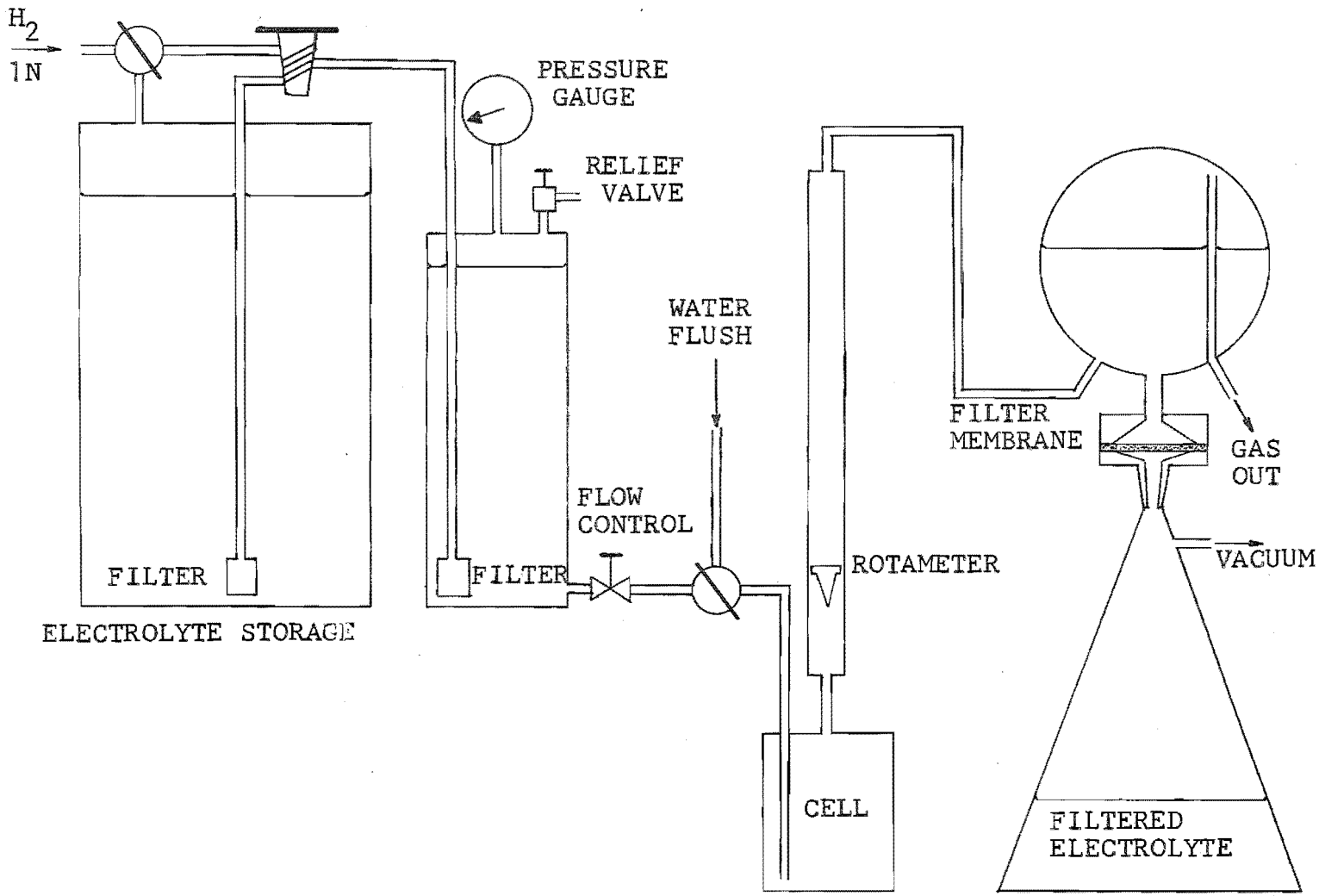

Fig. 5.2 Electrolyte Flow Circuit
High Current Density Dissolution Apparatus

the design features, was checked by comparing total "depth" of metal removed during a run with the deviation from flatness of the final electrode profile, see Fig 5.3. A range of 1% to 10% departure from ideality was found with a usual value of about 3%.

In order to determine whether a significant amount of aluminium was lost from the electrode as fine particles, a special filtration step was incorporated in the electrolyte flowpath immediately after the rotameter, Fig 5.2. A holder was made for the use of Millipore type AAWG04700 filter membranes. These membranes, with a pore size of 0.8 $\pm$ .05 microns, ensured retention of all but the very finest particles, while the free area of 82% allowed a high liquid throughput (approximately three litres/minute at 13.5 psi). Since the cellulose ester from which the filters were made was unaffected by up to 6N HCl and could be dried quantitatively at 80^{o}C, direct measurement of the weight of solid material retained was expected to be possible. Inspection by microscope of the material retained on the flat filter surface could be made with either reflected or transmitted light, since immersion oil rendered the membrane quite transparent.

5.2 Experimental

Materials:

Aluminium used for the electrodes was either 4N or 5N grade. Most runs were carried out in an electrolyte of 1N A.R. HCl chosen for its high conductivity, purity, relative freedom from insoluble matter, ease of standardisation, availability in quantity and cheapness. Other electrolytes used are listed in Table 5.1; some of these were made up with commercial grade salts because of the quantities needed and the apparent insensitivity of results to moderate impurity levels. However, in no case was electrolyte re-used for later runs. Hydrogen gas was taken straight from the cylinder.

Operation of Equipment:

In brief, the following steps were taken to carry out a run. Under hydrogen pressure enough electrolyte was transferred from bulk storage to fill the five litre aspirator, and glass cocks were then adjusted to give a hydrogen purge of this solution. The electrode was machined to shape, degreased, weighed to 0.02 mg, screwed on to its mount and the cell assembled. Several turns of wire were wound around the cell and the slack taken up on the capstan drum. A filtering membrane was weighed and fitted in its holder. All fluid flow connections were made and the electric circuit completed and adjusted

ELECTROLYTE	ELECTRODE ALUMINIUM GRADE	CURRENT DENSITY RANGE amp/cm^2	NUMBER OF RUNS
1N HCl	4N	5-120	20
1N HCl	5N	15-120	5
1N HCl+3N NaCl	5N	86	1
5N NaCl	5N	86	2
1N H_2SO_4 + .1N HCl	5N	85	1
1N KOH + 1N HCl	5N	83	1
3N NaCl + 1N NaOH	5N	50-80	3

TABLE 5.1 CONDITIONS UNDER WHICH FLOWING ELECTROLYTE DISSOLUTIONS WERE CONDUCTED

as described in Sec. 3.2(ii). After about one hour's hydrogen sweeping of the electrolyte, the relief valve on the aspirator was adjusted to give a pressure of 5-10 psi and the flow of electrolyte then started and rapidly set at the desired level. Recorder chart drive, cell rotation, polarising current and stopwatch were started and exact adjustment of current made as quickly as possible with the motorised rheostat. Close adjustment of current and fluid flow was maintained continually throughout the run and the dissolution also observed visually. After a sufficient length of time, usually two to five minutes, current and stopwatch were stopped, electrolyte flow and all switches turned off, and a two-minute flush of distilled water started. Anode weight loss was determined and the electrode surface examined visually and microscopically. The filter membrane was dried, reweighed and examined by microscope.

5.3 Results

5.3(i) Errors and Minor Effects

As described in Section 3.2, an experimental test showed that overall accuracy obtained from the balance of weight loss with energy supply was better than $\pm$ 1%, so that percentage excess weight loss figures presented later have values of, for example, 3 $\pm$ 1% or 10 $\pm$ 1%, this being a consequence of differencing relatively large

numbers.

Provided electrolyte flow was adequate for steady dissolution to take place, at a given current density the excess dissolution seemed independent of flow rate, there being no significant effect of a more than two-fold increase in flow. Electrolyte temperature was measured, but not controlled, although a fairly steady laboratory temperature ensured that most runs were carried out at 20 $\pm$ 2°C and only a very few near the extremes of the temperature range 17° to 25°C. Within this range no effect of temperature was discernible. Electrolyte static pressure at the anode surface, which might influence gas evolution processes, would have been little above atmospheric, since the restricted section of the "nozzle", 10, was short and the pressure drop over the rotameter only 1.5 mm of mercury.

5.3(ii) Particles

Collection of solid particles from the electrolyte by the filtering membranes was extremely effective, so much so in fact that not only were all aluminium fragments larger than one micron retained, but there was as well a varied assortment of other solid matter. Unfortunately the quantity of extraneous matter picked up from the electrolyte was often comparable with the weight of aluminium particles. Stability of the basic

membrane weight through wetting and drying stages seemed less consistent than was expected; for this reason and also because of the relatively high background solids level, direct weighing of membranes to obtain the mass of aluminium particles was not usually possible. Quantitative analysis of a solution of aluminium retained by the filter was carried out for a number of runs using the EDTA titration method[47]. The mass balance closed within experimental error of the analysis; particles seemed to form up to 15% of excess weight loss for some runs, while for other runs they were of negligible quantity. Runs during which a relatively greater quantity of aluminium particles was collected, were perhaps those during which the liquid flow was not well controlled. However it was found that unless the filter showed a relatively heavy load of particles, that was easily visible to the naked eye as a grey discoloration of the membrane, and could be confirmed by microscopic examination, the proportion of electrode weight lost as particles, was no more than comparable with the experimental error. Because of this, pre-filtration of the electrolyte was considered unnecessary, and in any case much of the extraneous matter seemed to have come from the inside surface of the cell assembly and could not be readily eliminated. The range of aluminium particle size was about one to thirty microns, with most about three to ten

microns. Contrary to the indication of Straumanis[25] it appears unlikely that many particles were formed in the sub-micron range, too small to be collected by a filter membrane of the pore size used here. Certainly no significant weight of such small particles would have been formed. A more detailed consideration of the origin of the aluminium particles is presented, with photographs in Section 7.

5.3(iii) Visual Observations

Vigorous gas evolution from the aluminium anode was observed during each run in chloride; no gas evolution at all was seen in exactly parallel circumstances during the high current density dissolution of cadmium in 1N HCl, (Sec. 3(ii)) showing that the veritable storm of gas bubbles from aluminium was not the result of some effect such as dissolved gas coming out of solution, vaporisation of water or cavitation. Close observation with the aid of a 40 x stereo microscope put the seat of gas evolution at the surface of the electrode. Even under the high liquid velocity (greater than 10 ft/sec) ruling outside the boundary layer, no gap was discernible between the electrode surface and the cloud of fine gas bubbles formed. So far as could be determined by visual methods, the start and finish of gas evolution was judged to be exactly co-incident with the switching of current.

When retreat of the dissolving electrode surface was over-compensated for, the final profile of the electrode was slightly convex, while under-compensation resulted in a slightly concave surface. Careful equalisation of the rates of anode surface retreat and compensating cell movement, minimised these effects, which were seemingly caused by changes in the electrolyte flow pattern induced by the different electrode positions; they would have both, affected the accuracy of apparent current density determination, and to a certain extent contributed to spread of results.

Under 600 x magnification with a metallurgical microscope, the surface appearance of an electrode after a run was not greatly different whether the current density had been ten or one hundred amp /sq.cm. There appeared in general to be two different sorts of surface structure; one rounded and somewhat amorphous and the other a block pattern showing steps and ledges consonant with the cubic aluminium metal lattice. The significance of this observation is not clear; some ideas on this subject are included in Sec. 7. Useful photographic recording of these features required much greater depth of focus than was obtainable with an optical microscope. However, an indication may be gleaned from Figs 5.3 and 5.4.

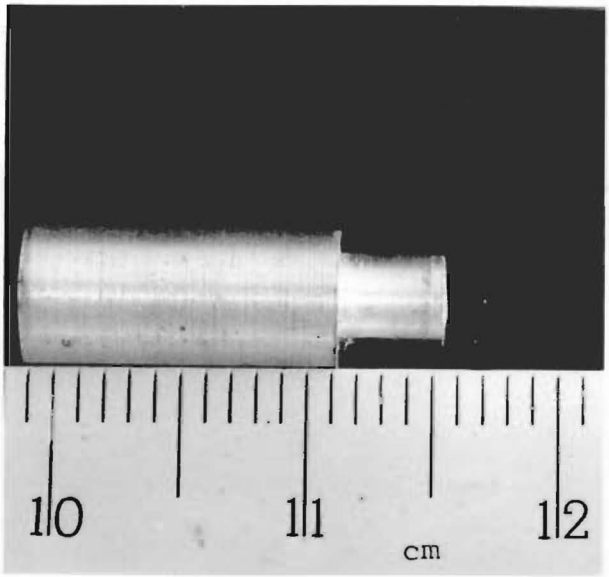

FIG. 5.3(a) Electrode Profile after Dissolution at 95 amp/cm^2. Total metal removed = 4.6 mm. Non-flatness = 2.5%.

FIG. 5.3(b) Same Electrode End On

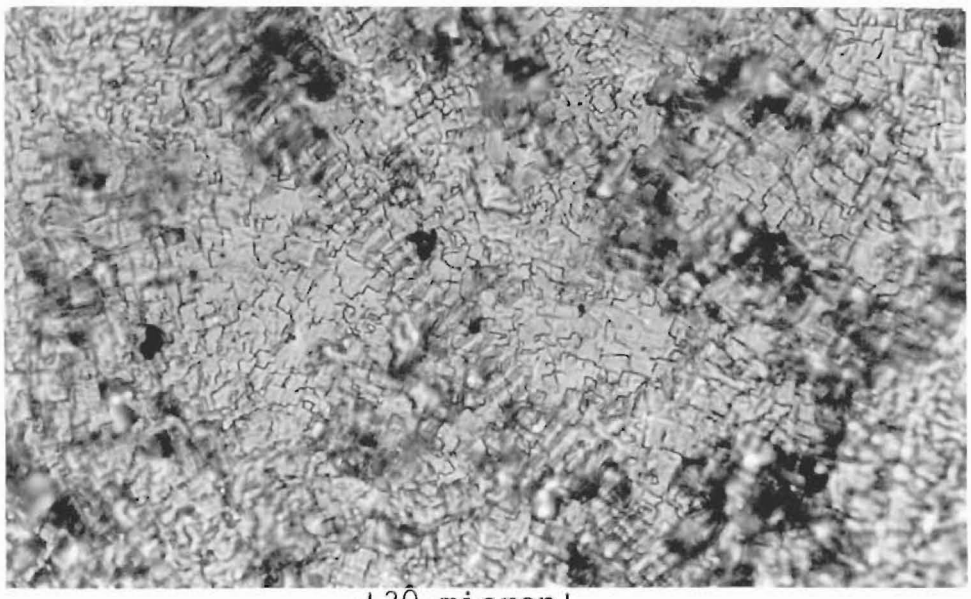

FIG. 5.4 Microphotograph of Electrode Surface after Dissolution (10 amp/cm^2)

5.3(iv) Excess Weight Loss

Experimental values for excess weight loss obtained from all the runs in chloride electrolyte listed in Table 5.1, together with some results from Sec. 4, are plotted as a function of applied current density in Fig 5.5.

5.4 Discussion

Overlap of values in the 5-10 amps/sq.cm. range of current density, (Fig 5.5) makes it clear that results obtained by both flowing and static electrolyte techniques are consistent and fall on a continuous curve representing the dependence of one and the same process on applied current density. The trend to a lower weight loss noted at currents over 5 amps/sq.cm. in static electrolyte has been confirmed and shown to continue to 80 amps/sq.cm. At still higher current densities than this, there seemed to be a levelling off at about 4% excess dissolution; spread of experimental results in this current density range makes the significance of individual values somewhat uncertain. The most that can be said is that any effect on excess dissolution of variation in pH, 0 to 14, or chloride ion concentration .1 to 5N, appears to be small. No effect of difference in purity of the two different aluminium samples was detected.

Various methods for the measurement of volume of

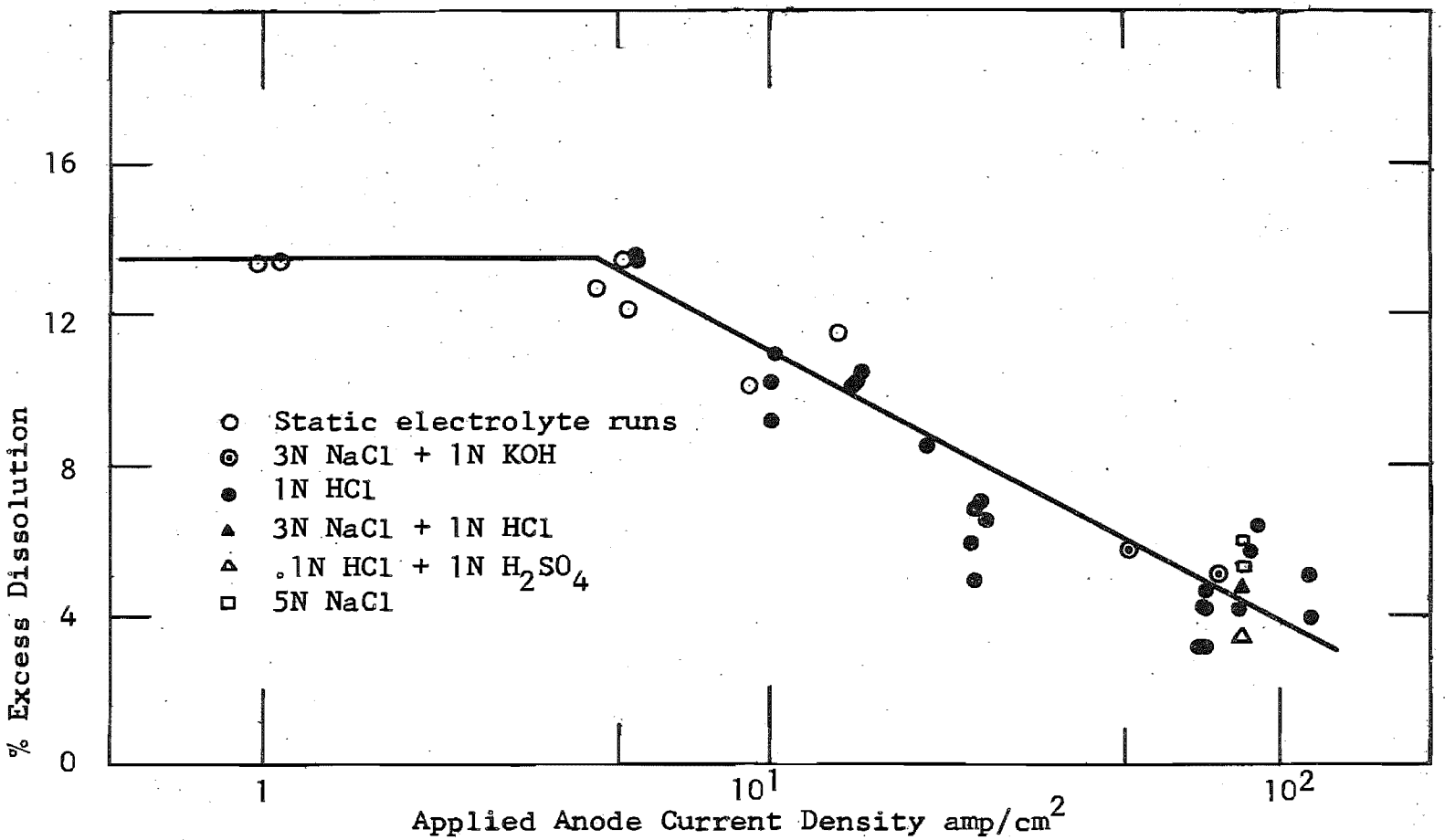

Fig. 5.5 Excess Dissolution vs Current Density

anode gas evolved during the flowing electrolyte experimentals were examined critically, but it was found that adequate accuracy would be difficult to obtain because of solution, temperature and pressure effects and mixing of the anode and cathode gases. However, since at high current density it has been shown clearly that hydrogen is in fact evolved from the anode (Sec. 4.6), and that anode weight loss as particles is too small to be significant (Sec. 5.2), it has been taken by implication that the visually observed gas evolution at applied anode current densities in the range 10 to 120 amps/sq.cm. was electrochemically equivalent in amount to the concurrent excess dissolution.

The two hypotheses already examined in some detail in Section 4 are now reviewed further in the light of these additional data, which are interpreted to show clearly that neither hypothesis satisfactorily accounts for the experimental observations.

5.4(i) Local cathodic hydrogen evolution hypothesis

On the grounds of both the rate at which the gas evolution takes place and also the working electrode potential, cathodic hydrogen evolution at local sites on the anode can be shown to be quite impossible.

The trend of excess weight loss and hence anode gas evolution with increasing applied anodic current density

is to decrease as a proportion of the total process, but to increase in absolute rate. Visual observation of electrodes that have been exposed to anodic densities of 5 amps/sq.cm. and greater, shows that the whole of the surface was involved in the dissolution process, and hence that no further increase in active area with current density was occurring. Even assuming that the electrode potential was no less favourable (negative) than at lower current densities, the cathodic hydrogen hypothesis must therefore predict no change in absolute gas evolution rate as the anode current density changes. This is contrary to observed fact. Furthermore, the electrode potential whatever the level, must become more positive with increase in real anodic current density and the rate of any cathodic process should decrease correspondingly. This is the opposite of observed fact.

Electrode potentials at any high applied anodic current density may be calculated by using Earl's[5] short-term anodic kinetic parameters; justification for their use under these conditions is given below. By this means it was calculated that at 15 amps/sq.cm. anodic current density, the electrode potential would be at least 0v NHE while at 100 amps/sq.cm. it would be at least +.5v NHE even with no allowance having been made for concentration or activation over voltages which effects would both move the working potential even further

in the positive direction. At such potentials cathodic hydrogen evolution is impossible, clearly a contradiction of the hypothesis since the rates of hydrogen evolution were about 1.5 and 4 amps/sq.cm. at applied currents of 15 and 100 amps/sq.cm. respectively. The legitimacy of using Earl's[5] anodic kinetic parameters (obtained by the no-load process outlined in Sec. 2.2) for the conditions prevailing during high current density dissolution, depends on the following considerations.

(1) Even at the high current densities used in this work the anodes were undergoing anodic dissolution as distinct from an oxide forming process. (Sec. 2.4(ii)).

(2) Earl[5] demonstrated that short-term anodic parameters were insensitive to nature of the electrolyte, e.g. Cl^- or $SO_4^=$. Nor was there any effect of pH.

(3) At 100 amps/sq.cm. the average lifetime of atoms on the surface is 7.36 microseconds, and at 15 amps/sq.cm. 49 microseconds, quite close to the 20-50 microseconds of Earl's[5] parameter determinations.

(4) Plumb[56] has investigated surface roughness and the effective surface area of metals subject to various preparation methods and found the "roughness" factors to be 1.5 for lathe turned and about 2 for chemically polished surfaces. The former figure may be taken as indicative of the "cut" electrode surface and the latter

figure the electrochemically dissolved surface; the differences are therefore relatively small.

(5) Earl[5] held that anodic parameters were not unduly sensitive to small temperature changes that might have occurred in the present work.

These considerations show the pertinence of Earl's anodic kinetic parameters and are taken as justification for their use above and also later in the development of the quantitative model, Section 6. The relevance and usefulness of the concept of electrode area, especially at high current densities, is discussed later, in Section 6.

To these objections may be added the further point that Earl[5] found an approximately 20 microsecond delay before the start of any cathodic activity on aluminium at favourable overvoltage of 1.5 volts, and approximately 1 millisecond was needed for the rate to reach about 10^{-4} amp/cm^2. At 100 amp/cm^2 the average atom lifetime is 7.36 microseconds and the electrode potential is at least 0v NHE; the observed excess dissolution under these conditions (and therefore hydrogen evolution) is about 4 amp/cm^2. Normal spontaneous evolution of hydrogen by local action is therefore quite impossible.

5.4(ii) Monovalent aluminium ion hypothesis

Of its nature the monovalent cation hypothesis outlined in Section 4.4(ii) is not easy to refute outright, since it seems possible for the characteristics of the proposed mechanism to be tailored to suit the experimental observations, although increasingly at the expense of credibility. Thus it might be expected that if the excess dissolution were due to monovalent ion formation, the formation would increase with increasing current density. Clearly, on the basis of their calculated standard potentials, any shift of electrode working potential in the positive direction gives a relatively greater change in driving force to the monovalent than the trivalent dissolution process and might therefore be parallelled by an increase in the relative rate of the monovalent process. Again, in view of the short average lifetime of atoms on the surface at high current densities (7 microseconds at 100 amps/sq.cm), the presumably stage-wise formation[57] of the trivalent aluminium cation might, at higher current densities, be expected to be more easily interrupted before completion, resulting in increased evolution of lower valent species.

However, the experimentally observed trend of decrease in excess dissolution as the current density increases, may be explained within the terms of the hypothesis by the apparently reasonable proposition of

different Tafel line slopes for the monovalent and trivalent dissolution processes. By using the change in relative rates of the processes with current density and Earl's value of $a = 0.1$ for dissolution, the value of a for the monovalent dissolution would be only 0.028, a quite improbably low value. When these arguments are combined with those of Section 4.4(ii) it can be seen that the monovalent aluminium hypothesis not only lacks experimental verification, but even with recourse to unsatisfactory assumptions cannot account for a number of the experimental observations.

5.5 Conclusion

It has been demonstrated that neither of the hypotheses examined so far has been able to account satisfactorily for the experimental facts. In view of this, an alternative explanation of the phenomena observed at a dissolving aluminium anode has been developed. Quantitative aspects of the proposed model are developed in Section 6 and a discussion of mechanism presented in Section 7.

6. DEVELOPMENT OF THE PROPOSED MODEL

The order used for presentation of the hypothesis, that is, model, in Section 6 and the mechanism in Section 7 has been chosen so that the validity of quantitative aspects can first be demonstrated with a minimum of assumptions about mechanism, thereby avoiding the complexity of simultaneous development of all aspects while providing the firm quantitative basis needed to justify later detailed discussion of mechanisms. It will become evident that the model is quite flexible in that it can stand in its own right, independently of precise details of mechanism.

6.1 Requirements

In essence it is necessary to account for the following observed facts of anodic dissolution of aluminium.

1. More aluminium goes into solution than expected from Faraday's laws.
2. Hydrogen gas is evolved concurrently from the anode in amount electrochemically equivalent to the excess aluminium dissolved.
3. In chloride electrolytes the equal amounts of (1) and (2) above have the dependence on applied anodic current density shown in Figs 5.5 and 4.2.

All other observed characteristics detailed in earlier sections are incidental to these or will be shown to arise naturally from details of mechanism considered in Section 7.

6.2 Outline of the Hypothesis

Recognition of the fact that several observed characteristics of the Phenomena pointed to a reaction at the surface of the aluminium was a starting point for this hypothesis. Basically, it is postulated that somewhat in the manner of sodium and water, bare aluminium metal and water can react together to evolve hydrogen, but with the notable difference that, for aluminium, reaction leads normally to the formation of a protective "oxide" film and is therefore usually rapidly self-stifling. However, if in the presence of certain anions a sufficiently positive electrode potential is reached and maintained by aluminium, for example when it is subjected to anodic loading, the inhibition is presumed not to occur since the required development of a protective film (i.e. coherent and at least two-dimensional) is prevented by the dissolution process as long as these conditions obtain.

In this respect it is important to differentiate between the initial reaction of an atom of aluminium with a water molecule, and the formation of a coherent

film. The former is a point or one-dimensional occurrence between a pair of reactants on the surface, whereas the latter is the sum of reaction at many points, leading eventually to a two or more dimensional film. In the present context these two outcomes are taken to be distinctly separated in time scale and possibly by several stages. Emphasis is laid on this concept since, as will become clear later, it leads simply to an exact stoichiometric reaction for the excess dissolution; an exact mechanism of this type is considered to be much more compatible with the observed nature of the Phenomena, for example the precise and characteristic potential dependence, than say the indiscriminate "blasting off" of areas of oxide proposed by Straumanis[29]. This is not to deny the occurrence of undermining of the surface and loss of some aluminium particles, especially at low currents; it means only that excess weight loss by that process is irregular and incidental to the excess dissolution process.

Between water and aluminium the reaction is envisaged as being chemical, that is, the rate essentially independent of electrode potential. It is proposed that this reaction results not only in the evolution of hydrogen but also in the formation of a dischargeable aluminium-oxygen species on the surface

of the metal; the species or intermediate so produced at any one point on the surface of the aluminium is taken to be a precursor of the protective two or three-dimensional film, but since it is also taken to be temporarily capable of electrochemical dissolution as a "modified" aluminium cation, film formation will not occur as long as dissolution of these species continues at a sufficient rate. If these species are not discharged within a relatively short time, then the remaining step/steps to film formation will occur. Since each of these entities is effectively an aluminium cation with part of its normal valency of three satisfied by chemical reaction, its dissolution would naturally involve on average less charge transfer to the anode than would dissolution of a normal trivalent ion, wherein it is asserted lies the excess dissolution equivalent in amount to the hydrogen evolved.

6.3 The Model

On the basis of this hypothesis, the following model of electrode behaviour has been drawn up; it is clearly statistical in nature, although the dependence of probability of dissolution on the history of each individual atom on the surface represents a novel and complex statistical situation. The amount of excess dissolution will depend on the following factors.

1. Clearly during steady uniform anodic dissolution, at any given current density there will be on the active surface of the metal a distribution of ages of atoms, ranging around an average value which is directly related to current density and the valency of the dissolving species. Since the chemical reaction between aluminium and water will occur at some finite rate, there will be a relation between age of an atom on the surface, since its exposure to the electrolyte, and the probability of its having reacted with water; this relation would be expected to have the general characteristics of low probability at short surface lifetimes and unit probability or certainty of reaction as the "age" of an atom on the surface tends to infinity.

An experimental indication of this relation can be deduced (see Sec. 6.5(i)) from the work of Earl[5] and is shown in Fig. 6.1.

2. On a time scale appropriate to any given current density, the dissolution process may be thought of as an essentially statistical process, involving repeated selection for evolution of ionic species from amongst those available on the surface of the electrode. On the basis of the present hypothesis there will be populations of the two types of cationic species available for selection, normal trivalent and also

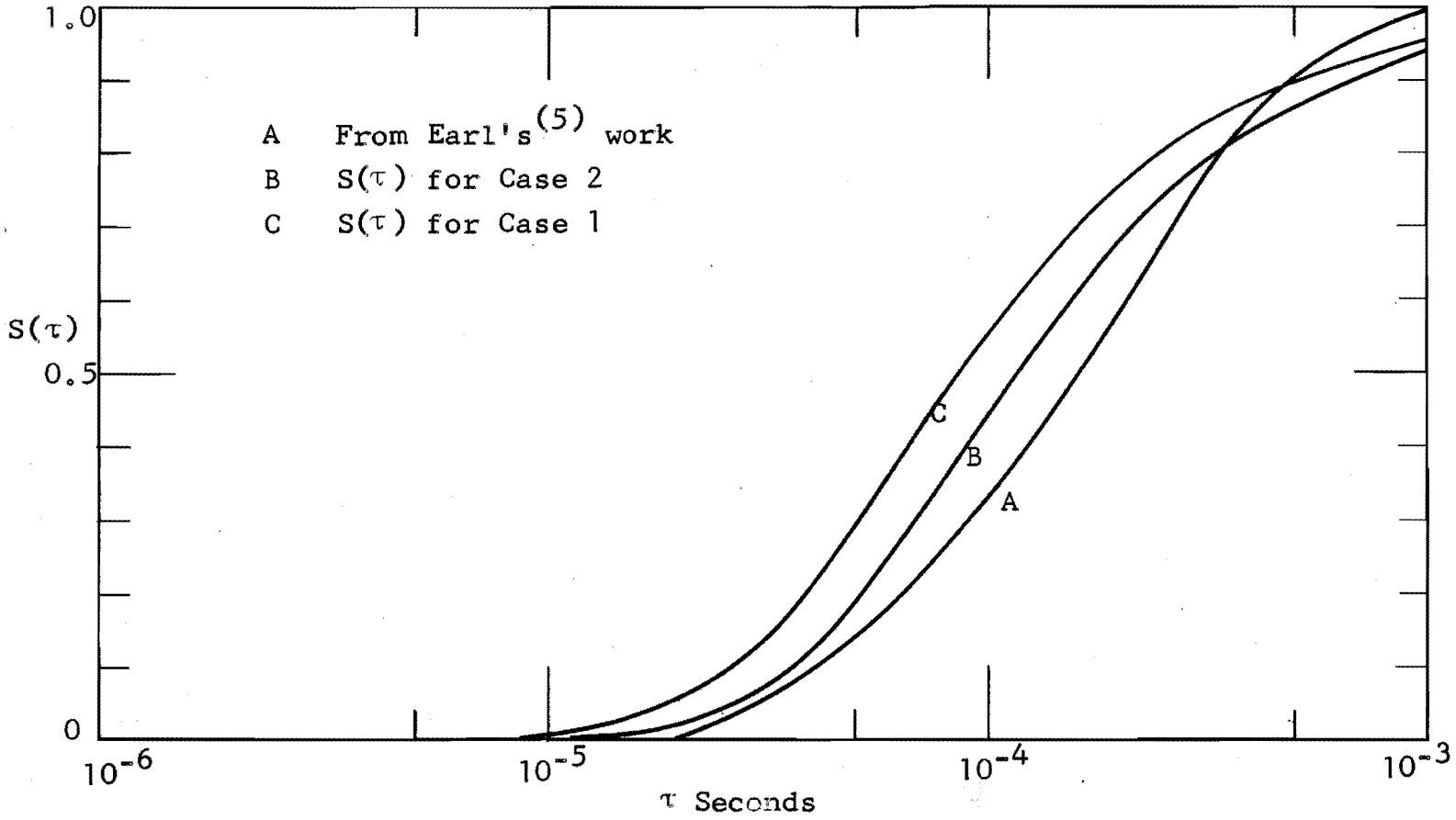

Fig. 6.1 Reaction Probability vs Atom Age

reacted atoms/ions effectively of reduced valency. Mean valency of the dissolving species, or the related quantity "excess dissolution", will then depend on the relative rates of evolution of each species. In turn this is dependent upon the following factors under steady-state conditions.

(a) The relative numbers of reacted and unreacted species available for dissolution; this will be a function of current density and the rate of reaction between aluminium and water ((1) above).

(b) The relative tendencies of each species to evolve or the relative probabilities of removal of reacted and unreacted species.

It is suggested that for a single atom on the surface its relative probability of removal might change with age on the surface in a manner qualitatively similar to that illustrated in Fig. 6.2. In this case as long as it remains unreacted the atom has an unchanged tendency to evolve in spite of its increasing age; upon reaction there is an immediate reduction in its tendency to evolve while further decrease in probability of removal with increasing age occurs in some unspecified but quite possibly stagewise manner.

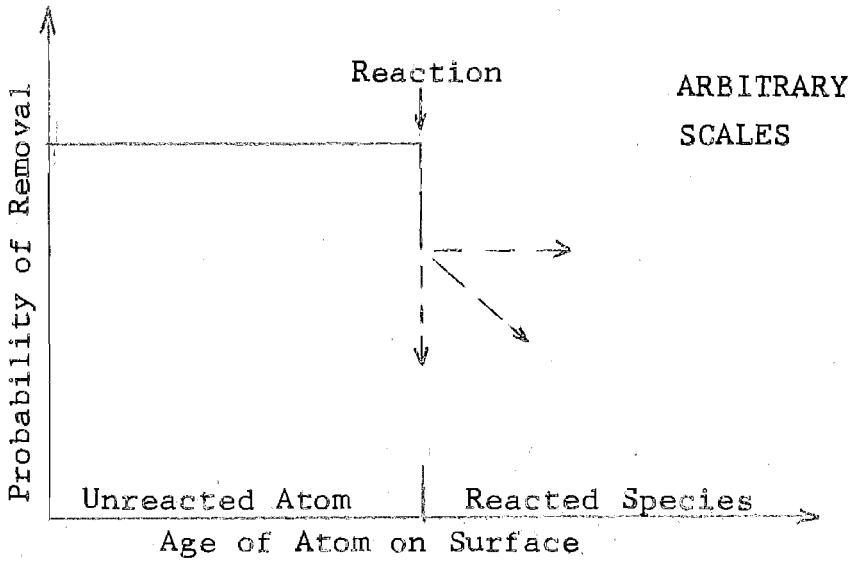

Fig. 6.2 Possible Removal Probability - Atom Age Relation for a Single Atom

For the whole electrode the averaging effect of having approximately 10^{15} atoms/cm^2 of exposed area and the influence of atom age on the probability of reaction (Fig. 6.1) both work to make the probability of removal vary as a continuous function of atom age. In the present work the relative probability of removal is equated exactly with relative exchange current density. Earl[5] and Watson[6] have determined experimentally the variation of exchange current density with electrode age; their data are plotted on Fig. 6.3.

It may be deduced on the basis of these influences

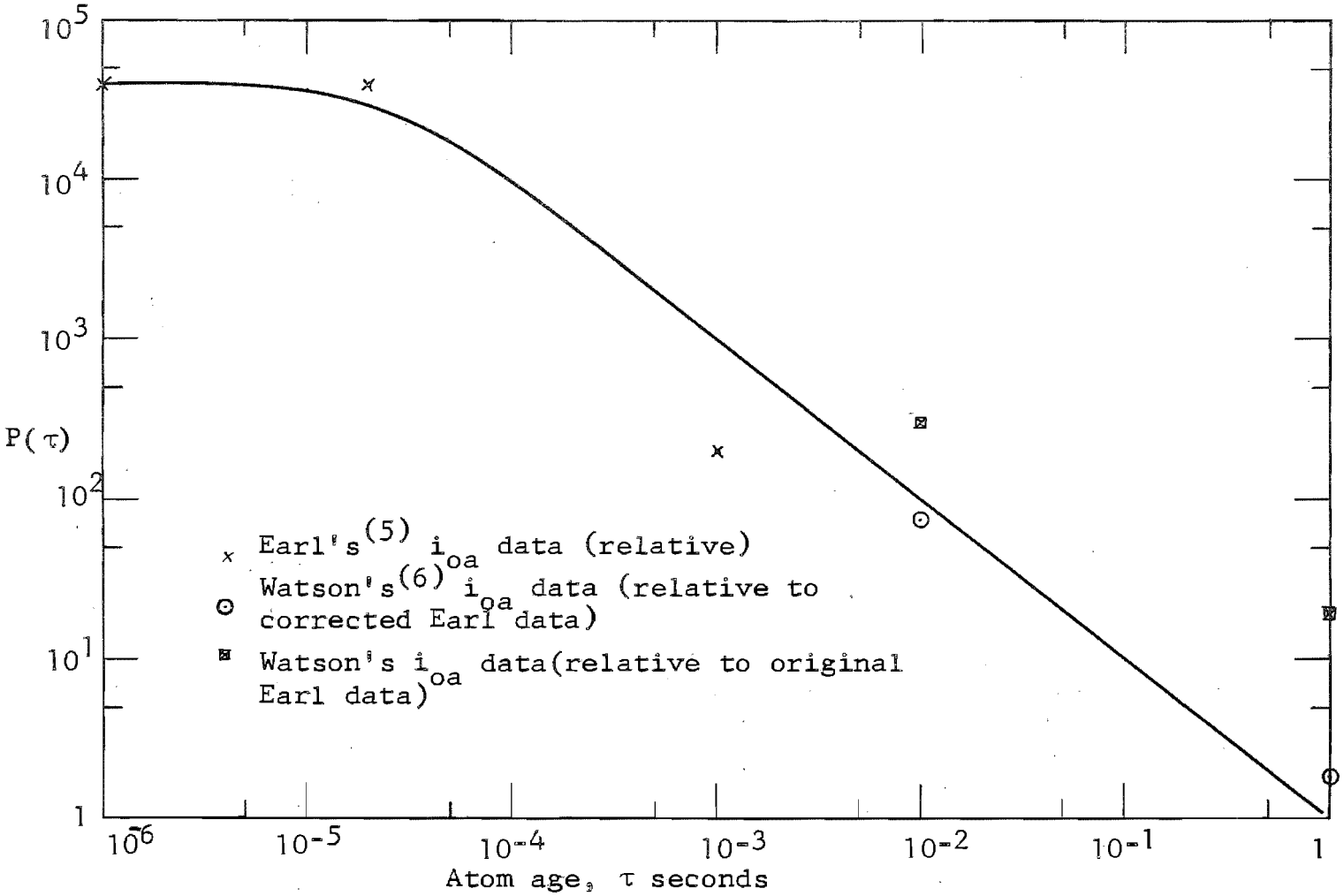

Fig. 6.3 Relative Dissolution Probability - Atom Age Relation

that the dependence of excess dissolution on current density has qualitatively the required characteristics of tendency to constant level at low current density and decrease in amount at higher current densities. A complete analysis of the mathematical relations involved in the model was necessary in order to obtain quantitative confirmation of the ability of the model to predict the experimental current density - excess dissolution relationship when using only the independently determined fundamental electrode kinetic parameters of Earl[5] and Watson[6].

Professor Lawden has completed the following mathematical analysis of the model. Some assumptions and idealizations involved are explicitly stated in the derivation while others are implicit; their electrochemical significance is examined in the subsequent discussion, Section 6.6.

6.4(i) General theory

We will let the function $S(\tau)$ be the probability that an atom of age τ has reacted (Fig. 6.1); τ is the time since the atom was first exposed to the electrolyte. Similarly we will let the function $P(\tau)$ (Fig. 6.3) be a measure of the relative probability of atoms of different ages passing into solution (Fig. 6.3). $P(\tau)$ is arbitrary to the extent of a numerical multiplier.

Let N be the number of atoms at the surface of the anode exposed to the electrolyte. We assume that N remains constant as the dissolution proceeds; that is to say, whenever any atom passes into solution it exposes just one fresh unreacted atom to the electrolyte that is identical with other unreacted atoms except for its age. At any instant in time t, let $n(\tau,t)d\tau$ be the number of surface atoms that have been exposed to the electrolyte for a period lying in the interval $(\tau, \tau+d\tau)$. In the steady state n will be independent of t. n determines the frequency distribution of the surface atoms with respect to their ages τ. Clearly it is necessary that

$$\int_0^\infty n(\tau, t)d\tau = N \qquad (1)$$

Consider the situation when an atom is about to be evolved by anodic dissolution. The probability that it will be an atom having an age lying in the interval $(\tau, \tau+d\tau)$ is

$$CP(\tau)n(\tau, t)d\tau \qquad (2)$$

where C is the multiplier associated with P. Since some atom certainly passes into solution it is necessary that

$$\int_0^\infty CP(\tau)n(\tau, t)d\tau = 1 \qquad (3)$$

and hence that

$$C = C(t) = \left[\int_0^\infty P(\tau)n(\tau, t)d\tau\right]^{-1} \qquad (4)$$

Let $R(t)$ be the total rate at which atoms are passing into solution at time t. Thus during the interval $(t, t + d\tau)$, the number of atoms dissolved will be Rdt and the proportion of these having ages in $(\tau, \tau+d\tau)$ will be equal to the probability (eqn 2). Accordingly the rate of dissolution of atoms having ages in $(\tau, \tau+d\tau)$ is

$$C(t)R(t)P(\tau)n(\tau, t)d\tau \qquad (5)$$

$n(\tau+\Delta\tau, t)$ is the number of atoms having ages in $(\tau+\Delta\tau, \tau+\Delta\tau+d\tau)$ at the instant t. This must equal the number which had ages in $(\tau, \tau+d\tau)$ at the instant $(t-\Delta\tau)$ less those passing into solution during the time interval $(t-\Delta\tau, t)$. We are thus led to the equation

$$n(\tau+\Delta\tau, t)d\tau = n(\tau, t-\Delta\tau)d\tau - C(t)R(t)P(\tau)n(\tau, t)d\tau\Delta\tau \qquad (6)$$

which is correct to the second order of small quantities. Employing Taylor's theorem and proceeding to a limit, we obtain

$$\frac{\partial n}{\partial \tau} + \frac{\partial n}{\partial t} = -CRPn \qquad (7)$$

We are assuming that when an atom passes into solution it uncovers a fresh atom having age $\tau = 0$. Thus $R(t)$ is the rate of production of atoms having zero age and it follows that

$$n(0, t) = R(t) \qquad (8)$$

6.4(ii) Steady-state solution

In a steady state, R, C will be constant and n will be a function of τ only. The fundamental equation (7) then reduces to

$$\frac{dn}{d\tau} = -CRPn \tag{9}$$

and this possesses the general solution

$$n(\tau) = B \exp\left(-CR \int_0^{\tau} P(u)du\right) \tag{10}$$

Equation (8) shows that B = R and hence

$$n(\tau) = R \exp\left(-CR \int_0^{\tau} P(u)du\right) \tag{11}$$

Substituting this expression for $n(\tau)$ in equation (4) we obtain the condition

$$CR\int_0^{\infty} P(\tau) \exp\left(-CR \int_0^{\tau} P(u)du\right)d\tau = 1 \tag{12}$$

Changing the variable of integration from τ to v by the transformation

$$v = \int_0^{\tau} P(u)du \tag{13}$$

it will be found that this condition reduces to

$$CR \int_0^{V} e^{-CRv}\, dv = 1 \tag{14}$$

where $v \to V$ as $\tau \to \infty$. For this condition to be satisfied it is clearly necessary that $V = \infty$ and hence

$$\int_0^{\infty} P(u)\, du = \infty \tag{15}$$

if a steady state of this type is to be possible. Condition (1) requires that

$$R \int_0^{\infty} \exp\left(-CR\int_0^{\tau} P(u)du\right) d\tau = N \tag{16}$$

Again changing the variable of integration to v, it will be found that this condition is equivalent to

$$\int_0^\infty M(v)e^{-CRv}\,dv = \frac{N}{R} \tag{17}$$

where $M(v) = 1/P[\tau(v)]$ (18)

This condition determines C.

The function R(t) of equation (8) or R under steady-state conditions is related to the current I. Defining $S(\tau)$ (see above) to be the proportion of atoms having age (τ) which have reacted with water, it follows from (5) that the rate of dissolution of reacted atoms having ages in $(\tau, \tau+d\tau)$ is $CRSPnd\tau$ and hence that the total rate of dissolution of reacted atoms

$$R_r = CR\int_0^\infty SPnd\tau \tag{19}$$

and, hence, that the rate of dissolution of unreacted atoms is

$$R_u = R - CR\int_0^\infty SPnd\tau \tag{20}$$

In order to complete the relation of R and I it is necessary now to specify the residual charge involved in the dissolution of reacted atoms. We will treat two cases which correspond with possible mechanisms discussed in Section 7.

Case 1

Let each reacted atom carry a residual charge q and each unreacted atom a charge 3q. Then the current flowing, I, is given by

$$I = R_r q + 3R_u q$$

$$= 3qR - 2qCR\int_0^\infty SPnd\tau \qquad (21)$$

This equation relates the functions R and I.

The functions $P(\tau)$, $S(\tau)$ being given, equations (1), (4), (8), (9), (21) determine $n(\tau)$, C, and R.

For a current, I, a direct application of Faraday's laws would lead us to expect that the rate of dissolution of atoms should be

$$\frac{I}{3q} = R - \frac{2}{3} CR\int_0^\infty SPnd\tau \qquad (22)$$

The excess rate of dissolution is accordingly

$$\frac{2}{3} CR\int_0^\infty SPnd\tau \qquad (23)$$

Expressing this as a percentage of the rate of dissolution predicted by Faraday's laws, we obtain

$$E = \frac{Q}{3-Q} \times 100\% \qquad (24)$$

where $Q = 2C\int_0^\infty SPnd\tau$ (25)

E will be termed the percentage rate of excess dissolution.

Equation (21) relating R and I can be put into the form

$$I = qR\left[3-2CR\int_0^\infty Se^{-CRv}\,dv\right] \qquad (26)$$

where it is understood that $S = S[\tau(v)]$. Finally Q as given by equation (25) may be expressed in the form

$$Q = 2CR\int_0^\infty Se^{-CRv}\,dv \qquad (27)$$

Introducing Laplace transforms of the function v, these results can be expressed in simple forms. Thus if $\bar{F}(p)$ is the Laplace transform of a function F(v) putting

$$p = CR \qquad (28)$$

Equations (17), (26), (27) can be written

$$R = N/\bar{M}(p) \qquad (29)$$

$$I = qR\left[3-2p\bar{S}(p)\right]$$

$$= Nq\left[3-2p\bar{S}(p)\right]/\bar{M}(p) \qquad (30)$$

$$Q = 2p\bar{S}(p) \qquad (31)$$

Equations (24) and (25) now yield

$$E = \frac{2p\bar{S}(p)}{3-2p\bar{S}(p)} \times 100\% \qquad (32)$$

Equations (29), (30), (32) express the quantities R, I, E as functions of a parameter p. The dependence of E upon I predicted by the model for Case 1 can thus be obtained.

Case 2

Suppose that a reacted atom carries no residual charge but is discharged as a "passenger" with an unreacted Al^{+++}. This is equivalent to reacted atoms having an average charge of 1½. Unreacted atoms each

contribute a charge 3q while dissolution of the combination of a reacted atom on top of an unreacted atom also contributes a charge of 3q for the pair but exposes only one new atom. Hence

$$I = 3qR \tag{33}$$

Actual rate of removal of atoms is

$$R_u + 2R_r = R + CR\int_0^\infty SPnd\tau \tag{34}$$

The excess rate of dissolution is accordingly

$$CR\int_0^\infty SPnd\tau \tag{35}$$

Thus by equation (25)

$$E = Q/2 \times 100\% \tag{36}$$

which with the change of variable (13), (27) becomes

$$E = CR\int_0^\infty Se^{-CRv}\, dv \tag{37}$$

Introducing Laplace transforms as before we get the forms

$$E = p\bar{S}(p) \times 100\% \tag{38}$$

and $$\bar{M}(p) = \frac{N}{R} \tag{39}$$

$$I = 3qR = 3qN/\bar{M}(p) \tag{40}$$

6.5 Particular Solutions

In order to test the hypothesis quantitatively for aluminium, the following steps are necessary:

1. Values for $S(\tau)$ and $P(\tau)$ must be obtained from the experimental results of Earl and Watson.
2. Analytical expressions, which are amenable to the mathematical treatment required by the above

derivation must be fitted to these data.

3. By using these expressions to represent $P(\tau)$ vs τ and $S(\tau)$ vs τ in the analysis for both Cases 1 and 2 there will emerge predicted relations between excess dissolution and applied anodic current density that can be compared with experimental results.

6.5(i) Experimental values of $P(\tau)$ and $S(\tau)$

The function $P(\tau)$ concerns the relative probability of an atom of age τ going into solution. For example, if $P(\tau_1) : P(\tau_2) = k:1$, then an atom of age τ_1 is k times more likely to pass into solution than an atom of age τ_2. Clearly these probabilities are directly connected with the kinetic parameters of anodic dissolution embodied in the Tafel equation and also in the change in these parameters as the "age" of atoms increases. Such information has been obtained for aluminium by Earl[5] and Watson[6] over the range of atom ages relevant to the present work; it is thought that such information is currently unique to aluminium and the technique used to obtain it is the only one known. Thus using the cut electrode technique, Earl has examined the no-load potential behaviour of aluminium electrodes in the period 5-1,000 microseconds after cutting, and obtained the change in anodic activity that occurs during this time

interval. Using similar techniques, the anodic behaviour of aluminium has been examined by Watson[6] in the period from 10 milliseconds to 10 seconds of electrode age, and a quantitative relation between exchange current density and time, obtained for the anodic process. The compatability of these two sets of data, and any limitations of their accuracy and pertinence to the present work, are examined in detail in the discussion, Section 6.6. The data are shown in Fig. 6.3 where relative exchange current densities have been plotted on an arbitrary scale.

The form of function $S(\tau)$ which is the probability that an atom of age τ has reacted, may also be deduced from the work of Earl[5] and Watson[6]. As described in Section 2.2, the former worker found that there was effectively a delay of 10-20 microseconds before the onset of cathodic activity on an aluminium electrode cut under solution, and that the potential behaviour of the electrode was explicable if, after the initial delay, the cathodic activity increased exponentially with a time constant of about 200 microseconds. Watson[6] established that cathodic hydrogen evolution from aluminium almost certainly occurred only from the oxide coated surface. However, since the cathodic parameters measured in the short term by Earl[5] on apparently film-free aluminium, and in the long term by Watson[6] on

definitely oxide-coated aluminium, were quite similar there was some doubt about the finding; it was not clear whether reaction to form a film could occur in the short time involved in Earl's work. The present work has eliminated this doubt and the interpretation favoured by the author is that the times found by Earl to be involved in the establishment of cathodic activity on aluminium represent also the times involved in the formation of "oxide" film by direct reaction between water and aluminium. On the basis of this interpretation, the shape of $S(\tau)$ vs τ is determined; see Fig. 6.1.

6.5(ii) Fitting analytical expressions

Because of the nature of the relations derived that connect E, R, $P(\tau)$ and $S(\tau)$, namely equations (29), (30), (32) for Case 1, and (38), (39), (40) for Case 2, the analytical expressions which are used to approximate to the experimental data of $P(\tau)$ and $S(\tau)$ (Figs 6.3 and 6.1), must be mathematically compatible with each other, and are thereby severely limited in complexity in order to allow exact analytical solutions of these equations. This limitation makes the fit between these data and analytical expressions a matter of compromise.

From attempts by the writer to fit numerous expressions it emerged that the following two provided the nearest approximations to the data for both cases considered,

while remaining amenable to the required mathematical manipulation.

$$P(\tau) = (\tau^2 + \sigma^2)^{-\frac{1}{2}} \qquad \sigma > 0 \tag{41}$$

$$S(\tau) = (1 + \tau/\sigma - \sqrt{1 + (\tau/\sigma)^2})^{\gamma} \qquad \gamma > 0 \tag{42}$$

σ and γ are arbitrary constants.

6.5(iii) Solutions for Case 1

For Case 1 these functions are treated in the following manner. In this case condition (15) is satisfied and using equation (13) with (41) shows that

$$\tau = \sigma \sinh v \tag{43}$$

Thus from equation (18) we find that

$$M(v) = \sigma \cosh v \tag{44}$$

and hence

$$\bar{M}(p) = \frac{\sigma p}{p^2 - 1} \tag{45}$$

Equation (29) now yields

$$R = \frac{N}{\sigma}(p - \frac{1}{p}) \tag{46}$$

from which it is clear that since $R \geq 0$ then $p \geq 0$. Taking now (42) (note that $S(0) = 0$, $S(\infty) = 1$)) and employing (43) gives

$$S(\tau(v)) = (1 - e^{-v})^{\gamma} \tag{47}$$

Whence

$$\bar{S}(p) = \frac{1}{p} - \gamma \frac{1}{p+1} + \frac{\gamma(\gamma-1)}{2!} \frac{1}{p+2} - \frac{\gamma(\gamma-1)(\gamma-2)}{3!} \frac{1}{p+3} + \ldots \tag{48}$$

which series terminates if γ is an integer.

I and E as functions of p now follow from equations (30) and (32) respectively. It will be observed that I = 0 when p = 1; for this value of p it follows from equation (48) that $\bar{S} = 1/(\gamma+1)$; hence

$$E_o = \frac{200}{3\gamma+1} \% \qquad (49)$$

where E_o is the percentage excess rate of dissolution for very small current densities. Since this value is experimentally well established the value of γ in equation (42) is fixed by this equation for Case 1.

The next step to completion of this solution involves selection by trial of one value for the constant σ (dimensions of time) to give a satisfactory fit of both equations (41) and (42), representing $P(\tau)$ and $S(\tau)$, to their respective sets of experimental data. Finally, the equations (30) and (32), representing I and E, are each solved for a range of values of the variable p, to obtain the predicted relation between E and I over the range of current density, 10^{-2} to 10^{2} amp/cm^2, for which experimental results have been obtained.

By this means the best values of σ and γ for solution of Case 1 for aluminium dissolving anodically in chloride solutions have been found. They are

$$\sigma = 2.5 \times 10^{-5} \text{ (sec)}$$

and $\gamma = 4.5$

giving by (48) an excess of 13.8% at low current density. The resultant predicted curve of E vs I is drawn in

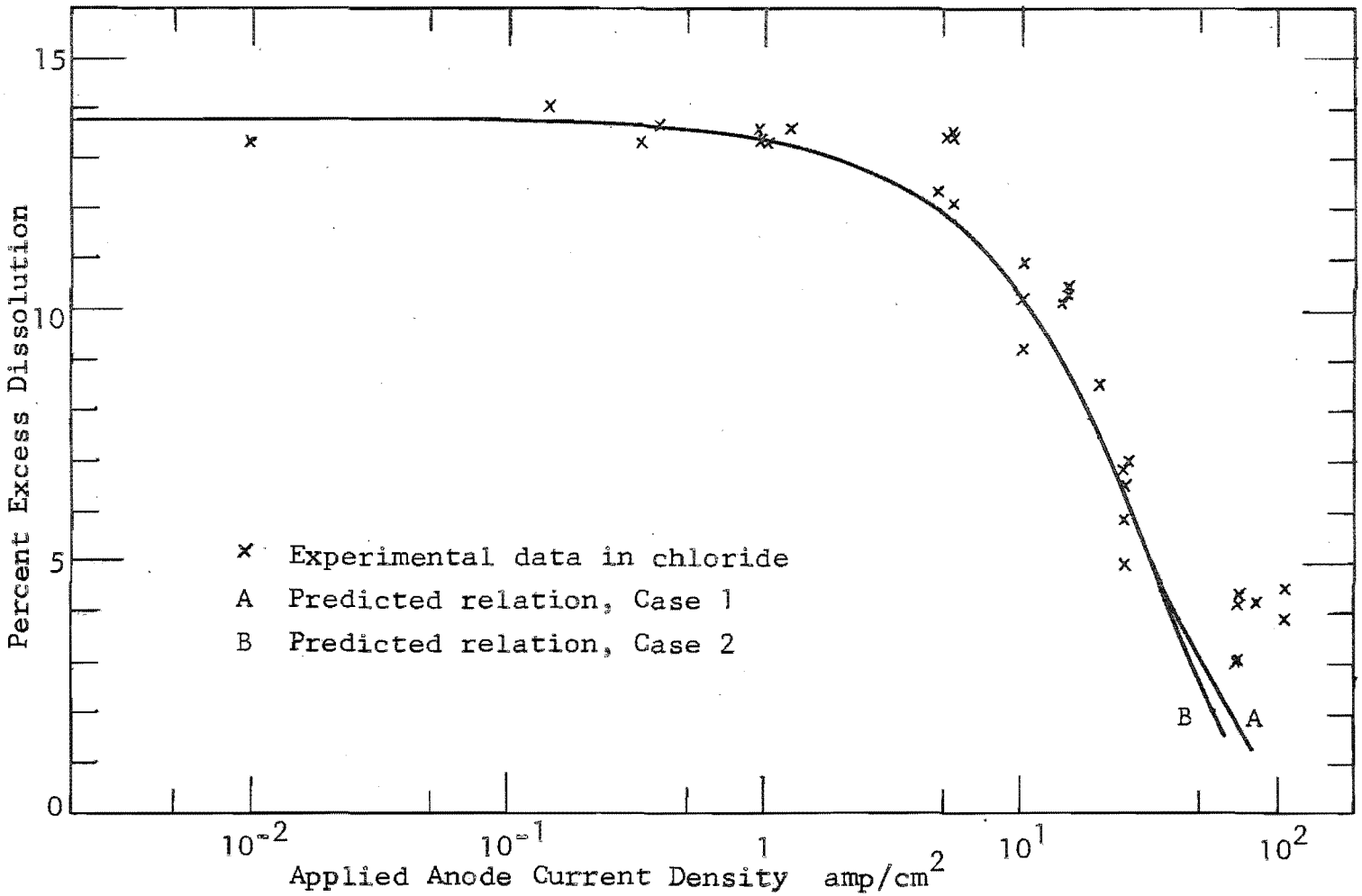

Fig. 6.4 Excess Dissolution - Current Density Relations

Fig. 6.4, together with experimental data from Sections 4 and 5. A complete solution following the above process is given for illustrative purposes in Appendix C.

Solution for Case 2

As with Case 1, condition (15) is satisfied, equations (43), (44), (45), (46), (47), (48) are again obtained and from equation (38) we find that

$$E_o = 1/\gamma + 1 \qquad (50)$$

which fixes γ for Case 2. By trial a value for σ is then found to suit (41) and (42) using the value of γ established by equation (50) and fitting to the experimental results for $P(\tau)$ and $S(\tau)$. Equations (38) and (40) are then solved for a range of values of the variable "p" to obtain a plot of E versus I which is compared with experimental results and predicted behaviour for Case 1 in Fig. 6.4. The arbitrary constants for Case 2 of the hypothesis with aluminium dissolving in chloride solution are thus found to be

$$\sigma = 2.5 \times 10^{-5} \text{ (sec)}$$

and $\gamma = 6.25$

which by equation (50) gives $E_o = 13.8\%$.

6.5(iv) Results for bromide and iodide

Insufficient experimental data have been obtained to fix the high current density characteristic of anodic dissolution in bromide solution; only a single point has been obtained in iodide. These data are insufficient to justify the above process of predicting the relationship between E and I. Results in these media are discussed later in Section 6.6 and Section 7.

6.6 Discussion

In this discussion the fit of equations and lines to data in Figs 6.1, 6.3, and 6.4 will first be examined in some detail; subsequently a brief examination of the principal assumptions will be presented.

6.6(i) Excess dissolution - Current density relationship

The success of the model in independently predicting the excess dissolution - current density relationship, when using only data from the work of Earl[5] and Watson[6], vindicates to a considerable degree assumptions made in the derivation. Examination of Fig. 6.4 shows over a nearly four-decade range of current density, the remarkably close agreement between the predicted and the experimentally determined excess dissolution - current density relationships. Only at very high current densities is there a noticeable deviation between the two,

although in view of the proportionately lower accuracy of experimental results in this range its significance is probably less than it might appear.

No experimental results of excess dissolution at current densities lower than 10^{-2} amp/cm^2 are available from the present or from reported experimental work; however, it has been observed (Fig. 4.4) that the characteristic potential behaviour continues down to about 10^{-4} amp/cm^2, which suggests that the steady level of excess dissolution would also occur down to this current density. If so, the model could clearly cover quite satisfactorily, this extra range (10^{-2} to 10^{-4} amps) of current density.

The close similarity of excess dissolution predicted by both Case 1 and Case 2 (Sec. 6.4) makes it impossible to choose between these alternatives on grounds of excess dissolution alone. Consideration of their respective mechanisms in Section 7 bears on the relative merits of the two Cases.

6.6(ii) The function $S(\tau)$ - Probability of reaction

In Fig. 6.1 the values of function $S(\tau)$ are compared with the curve inferred by the author from experimental work presented by Earl[5], and from the outcome of his computer analysis. While the two curves are not exactly coincident, their agreement is considered quite

satisfactory since the essential characteristic of very little reaction in less than 20 microseconds is common to both. The shape at longer time is not well established; Earl[5] arbitrarily assigned to the cathodic process an exponential increase in rate with time constant 200 microseconds. He obtained results that were almost as good in his computer analysis, when 20 microseconds delay followed by instantaneous establishment of cathodic process was tried, so that any curve within this region may be considered reasonable. He stated that provided the value "is close to zero for some twenty microseconds or so after cutting and then rapidly increases to its maximum value the experimentally observed potential time traces are explained."

For the postulated chemical reaction between water and aluminium, the shape taken by the probability of reaction curve when using the analytical function (42), Sec. 6.5(ii), seems to be unduly attenuated with increasing age; if the reaction rate was such that it could be 50% complete in 100 microseconds (Fig. 6.1) then ten times as long should not be necessary for 100% completion. This shape of curve is largely dictated by the mathematical function that could be handled in analytical solution of the model; however, this would have had little effect on the excess dissolution -

current density relation since by far the greatest influence is exerted by the first parts of both $S(\tau)$ and $P(\tau)$ curves.

If more definite data about reaction rate are obtained at some later date, then different mathematical expressions might be found to represent them or a computer solution of the mathematics attempted.

6.6(iii) The function $P(\tau)$ - Dissolution Relative Probability

The function $P(\tau)$ and the rather sparse experimental data are shown in Fig. 6.3; while the agreement at small τ is reasonable, the divergence as τ increases above 10^{-2} seconds is quite large. The following considerations bear on this point.

1. Ideally, the dependence of $P(\tau)$ on τ would be determined by instantaneously creating and exposing to the electrolyte, an aluminium electrode, and then following the change, with time, in anodic activity of the metal surface from which no current would be flowing either internal or external. In the work of Earl[5] and Watson[6], electrodes were cut under solution and exposed to the electrolyte in as little as 5 microseconds, which is probably a satisfactory approximation to instantaneity, since Earl found no effect whatsoever on the value of anodic parameters

whether they were determined during or immediately after cutting of the electrode. Clearly, however, the measurement of anodic activity cannot be done without some anodic dissolution, which of course results in the exposure of new and therefore "younger" and more active atoms on the surface. Naturally this leads to an increase in the activity measured to above what it would otherwise be. In Earl's[5] work this effect was minimised, since anodic parameters were deduced from the potential behaviour of an electrode carrying no external current; the only dissolution current was that needed to charge the double layer together with any arising from spontaneous cathodic activity. Calculation shows that only 1% to 3% of a monolayer need be evolved to charge the double layer, depending on its capacity (see below), while in the early stages cathodic activity was nil rising in one millisecond to reach only 10^{-4} amp/cm^2 at the mixed potential. (Earl[5], page 40, fig. 20); an aluminium electrode exposed to this cathodic current density for one millisecond, would evolve anodically only about 0.1% of a monolayer. Further, the kinetic parameters determined by Earl are a good approximation to the ideal described above because of the low age of the atoms in his work; new atoms are only moderately

more reactive than those present from the beginning (Fig. 6.3) and, for the same reason, kinetic parameters determined within 20 microseconds would be exact in terms of the present interpretation.

However, in Watson's[6] work, a small ($< 10^{-4}$ amp/cm^2) external current was applied to the electrode in order to measure the kinetic parameters. While little material is evolved at such low current densities, the equivalent of only one monolayer in 7 seconds at 10^{-4} amp/cm^2, the real anodic activity of the surface at times of 10 milliseconds and greater has decreased by a factor of about 10^3 to 10^5 compared with that at $\tau = 0$ (Fig. 6.3). Therefore the presence of even a small proportion of atoms of lower exposed age, due to dissolution, can raise the measured average anodic activity significantly above what it would otherwise be. It is not certain exactly how much this would have affected the present use of Watson's results as a measure of dissolution probability; by making estimates of areas affected, and average atom ages, that are realistic for this current density, it seems likely that his results for i_{oa} (= dissolution probability) at 1 second age would have been not more than a factor of two or three greater than for the completely undisturbed surface considered to be ideal

in the present context. Compared with the error limits on his data, a factor of this magnitude is barely significant and at ages less than 1 second the even smaller effect would be quite insignificant. Nevertheless, the effect of this factor is in the direction of bringing his experimental values closer to the $P(\tau)$ line, Fig. 6.3. Because of the nature of the function used to represent $P(\tau)$, the slope of the line at ages $\tau > 10^{-4}$ sec is quite uninfluenced by the value assigned to the constant σ; it becomes inversely proportional to τ.

2. It has already been noted that there is a divergence between $P(\tau)$ and the relative i_{oa} data as atom age increases (Fig. 6.3); as well, there appears to be some disparity between the results of Watson[6] and those of Earl[5] at atom ages in the 10^{-3} to 10^{-2} second range, which raises the question of the compatability of their two sets of data. The values plotted in Fig. 6.3 are of relative exchange current density, calculated at the standard electrode potential of aluminium. Although electrode potentials during dissolution experiments in the present work are quite different from this potential, the basis for comparison is valid since the kinetic transfer coefficient α in both Earl's and Watson's data has the same value, and the Tafel lines are therefore parallel.

The next matter to be considered is the value for exchange current density of aluminium found by Earl[5] for atom ages less than 20 microseconds. His computer analysis of the electrode potential behaviour of an unloaded electrode gave directly the transfer coefficient α, but only the ratio of electrode double-layer capacity to exchange current density C_{dl}/i_{oa}; the separate values of C_{dl} and i_{oa} were obtained by deductions made from other work, giving $i_{oa} = 2.15 \times 10^{-2}$ amp/cm^2 and $C_{dl} = 1.4\ \mu$F/cm^2 which was an unexpectedly low value. Using these values for α and i_{oa}, a Tafel line for the process of anodic dissolution of aluminium is plotted in Fig. 6.5. At -.51 volts NHE (the "critical" potential for 1NCl^- electrolytes), the predicted current density is 2.0 amp/cm^2, although these particular parameters apply strictly only for atom ages up to about 20 microseconds.

This must be compared with the following results found by Edeleanu[58] when studying the pitting of 99.999% pure aluminium in solutions of approximately 0.5n, 0.05n and 0.005n sodium chloride. Using visual and electron microscopical techniques, he observed the rate of progress of the active front of pits in aluminium and found for all solutions a uniform rate of 0.15 $\pm$ .03 mm/min. When the current

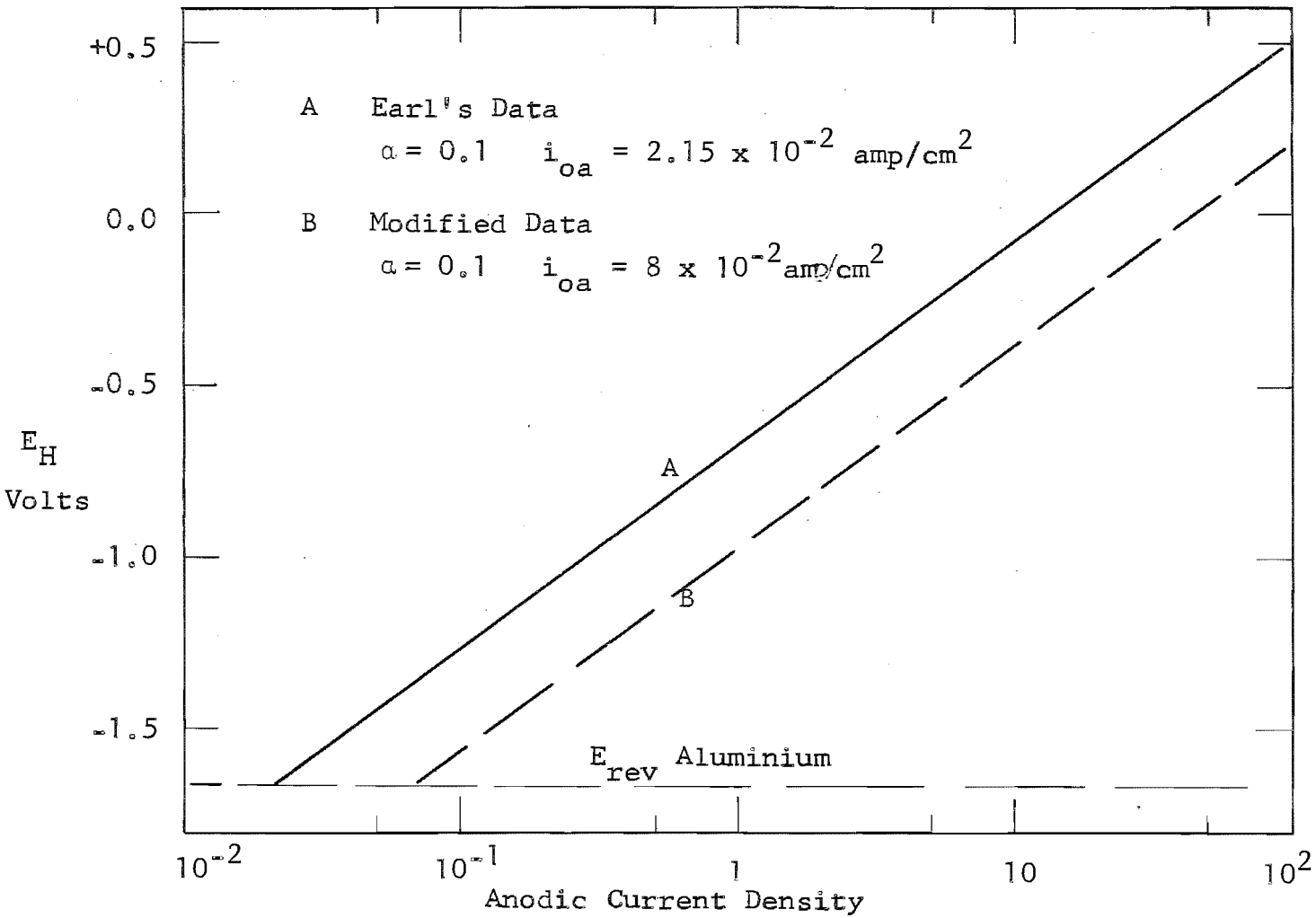

Fig. 6.5 Anodic Tafel Lines

was changed the rate of progress of individual pits did not change; presumably the active area and/or number of pits did. Transformed into terms of current density this rate of dissolution is 5.9 to 8.7 amp/cm^2 which represents by the present work an applied current density of $\frac{100}{114}$ times as much, i.e. 5.1 to 7.6 amp/cm^2. Examination of Fig. 5.5 shows that this corresponds closely with the current density where the proportion of excess dissolution dips fairly sharply from about 14% to lesser amounts with increasing current density. Edeleanu[58] noted a distinct change in the character of the dissolution when current was raised beyond a certain level. These two sets of observations are clearly consistent and indicate that the effective current density at 0.51 volts NHE is 5 to 7.6 amp/cm^2 and not 2 amp/cm^2 as was found above from Earl's[5] parameters. This suggests strongly that the value of exchange current density determined by Earl may be 2.5 to 4 times smaller than it should be. A Tafel line with this larger value of i_{oa} is plotted on Fig. 6.5. If this deduction is valid, then from the value of C_{dl}/i_{oa} found by him, a similar increase in double-layer capacity C_{dl} would have to be made, bringing it to 3.4 to 5.6 μF/cm^2 which is in agreement with the value at 1 millisecond[5], thereby eliminating the need to

explain an otherwise exceptional and unexpectedly low value of capacity and supporting the deduction. The effect of this change in i_{oa} for Earl's data is to improve the agreement at 10^{-2} to 10^{-3} seconds between Earl's[5] and Watson's[6] data (see Fig. 6.3) and also to reduce the divergence noted at greater atom ages.

6.6(iv) General precision

At this stage it becomes clear that limitations to obtaining any more accurate picture of the excess dissolution processes, say at high current density, lie principally with the inflexibility of the mathematical functions used to represent the probability of reaction $S(\tau)$ and probability of dissolution $P(\tau)$; since the data, obtained from the work of Earl and Watson to represent $S(\tau)$ and $P(\tau)$, are themselves subject to approximately 1 order of magnitude error limits, there is no point in attempting to find more elaborate functions to represent the data. Until more precise data are obtained, there is little that can be done to test the model more stringently. These points bear on consideration of the small but definite difference in amount of excess dissolution obtained in each of the chloride, bromide and iodide electrolytes. The most plausible explanation would seem to be that the

probability of dissolution of reacted species is moderately dependent on the anion in solution decreasing in the order $Cl^- > Br^- > I^-$, thereby leading to a decreased proportion of excess in the same sequence. An alternative suggestion that the rate of reaction between water and aluminium might be dependent on the anion in the electrolyte seems much less likely. In either case the matter cannot be resolved with the data at present available.

In view of these matters any reservations as to the validity of the principal assumptions made during the drawing up of the model are of secondary importance. Nevertheless, a brief discussion of the points follows.

6.6(v) Other assumptions

(a) Atom for atom parity

Because of the known close packed cubic crystal structure of aluminium the assumption that the evolution of each atom of aluminium, whether reacted or unreacted, results in the exposure of one fresh unreacted atom may appear to be unreasonable. However, the following points are offered in explanation.

1. Although it would require the evolution of perhaps three adjacent atoms from the surface of a plane to expose fully one atom on the layer underneath, on <u>average</u>, one atom is exposed by the evolution of one atom from above.

2. At small (< 100 mV) overvoltages, most atoms are evolved from the less strongly bound sites on the surface of the metal, i.e. ledges, dislocations, kinks. In these cases the evolution of one atom would render the atom immediately adjacent to it available for dissolution. At higher overvoltages atoms can be evolved from sites in the plane, and in view of the very high rate and probably large overvoltages involved at high current densities in the present work it seems highly probable that much of the evolution was occurring from such sites in the plane (Bockris[59]).

(b) 'N' the number of atoms on the surface remains constant.

While this suggests a picture of a regular plane of atoms, the realities of surface conformation do not necessarily invalidate the assumption. In the initial moment of dissolution at high current density, conditions are undoubtedly far from the ideal assumed, but in the steady state that is very rapidly established the assumption seems quite reasonable. It is not clear, however, what value N would have; since the surface is far from flat the"available area" is considerably greater than the projected geometric area but in turn the significance of the concept of area on or at which an electrode process takes place is open to conjecture. Thus Earl[5] interpreted his results in terms of

separate anodic and cathodic areas which summed to equal the total electrode area; for his results Watson[6] preferred to take it that the total electrode area was available for both electrode processes concurrently. Both of these contentions seem to be quite acceptable when note is taken both of the different times involved in their work, and of the results and hypothesis in the present work. In this connection it might be argued that the representation of probability of removal by a continuous function $P(\tau)$ is not realistic since at any instant during dissolution only relatively few atoms can actually be at active sites and therefore available for dissolution. To this it can be said that all atoms of age τ have an equal chance of being at an active site, therefore they have equal chances of being removed.

(c) The rate of reaction between water and aluminium is independent of electrode potential.

This is possibly the most sweeping assumption made, in the derivation, which seems however largely justified by the outcome of the model. Three points can be made briefly:

1. Consideration of energy level leads one to expect that a chemical reaction would be unaffected by potential except at very high field.

2. As has been pointed out in Section 2.3(i), the

driving force for reaction between aluminium and oxygen ion is already very high so that moderate increase in electrode potential would not be expected to have much effect.

3. The data from Earl's[5] work which were used as a basis for obtaining the reaction probability were measured at approximately -1.5v NHE, whereas all dissolution experiments in the present work were made at electrode potentials at least 1v more positive than this. Although the potential of the electrode when carrying 100 amp/cm^2 of applied anodic current density is not known, the higher experimental rate of excess dissolution compared with predicted suggests that there may have been some influence of electrode potential on reaction rate at this current density; the points made in Section 6.6(v) must, however, be remembered.

6.7 Conclusions

The hypothetical model has been shown to give a good quantitative account of the observed experimental data. Although the model takes a rather simplified view of electrode behaviour (partly for the want of more sophisticated information) the more obvious assumptions have been shown to be compatible with known physical facts. A foundation has been established for the examination of mechanisms contained in Section 7.

7. PROCESS MECHANISMS

7.1 Initial Behaviour of Anodes

It will be evident from what has already been written that, in the present work, the fundamental features observed in aluminium electrode behaviour arise from the interaction of anodic activity that is time dependent, through reaction with water, with the twin influences of electrode potential and type of anion in solution. A quite useful qualitative insight into the fundamentals of this interaction can be gained from the results, given below, of experiments where electrodes were cut under anodic load in various electrolytes and the first few seconds of potential behaviour monitored.

7.1(i) Experimental

These measurements were made using the cut electrode technique and equipment very much as described by Earl[4], whose work may be consulted for background details. Since these measurements were of comparatively long duration, a low-speed moving film camera was used to record electrode potentials displayed oscillographically via a 10^9 ohms input impedance cathode follower. A simple adjustable transistor circuit was used to provide a constant anodic current load from the instant of cutting the aluminium electrode. Runs were carried out with applied anode current density ranging from 10^{-3} to

10^{-1} amps/cm^2 using 4N aluminium electrodes in electrolytes of A.R. 1N KCl pH 3.2 and A.R. 1N K_2SO_4 pH 3.2. Either air or pure hydrogen was bubbled through the electrolyte for twenty minutes prior to each run.

7.1(ii) Results

Examples of potential-time traces obtained in the above work are shown in Figs 7.1 and 7.2, where traces taken at similar current densities in chloride and sulphate electrolytes are superimposed, the better to demonstrate the fundamental differences in behaviour in these two media. No effect of the presence of dissolved oxygen was evident in this work.

The traces in Figs 7.1 and 7.2 show clearly that the first few seconds of aluminium's potential response to the anodic load are quite markedly different in each electrolyte. In Fig. 7.2, because of an unsuitable time scale, any difference in the early parts of the traces is masked by the more rapid potential response at higher applied currents; however, the traces in Fig. 7.1 clearly demonstrate the more important characteristics, and the applied current was high enough (10x) to swamp any effect of local current. Referring to Fig. 7.1:

1. Even at quite low anodic current densities in

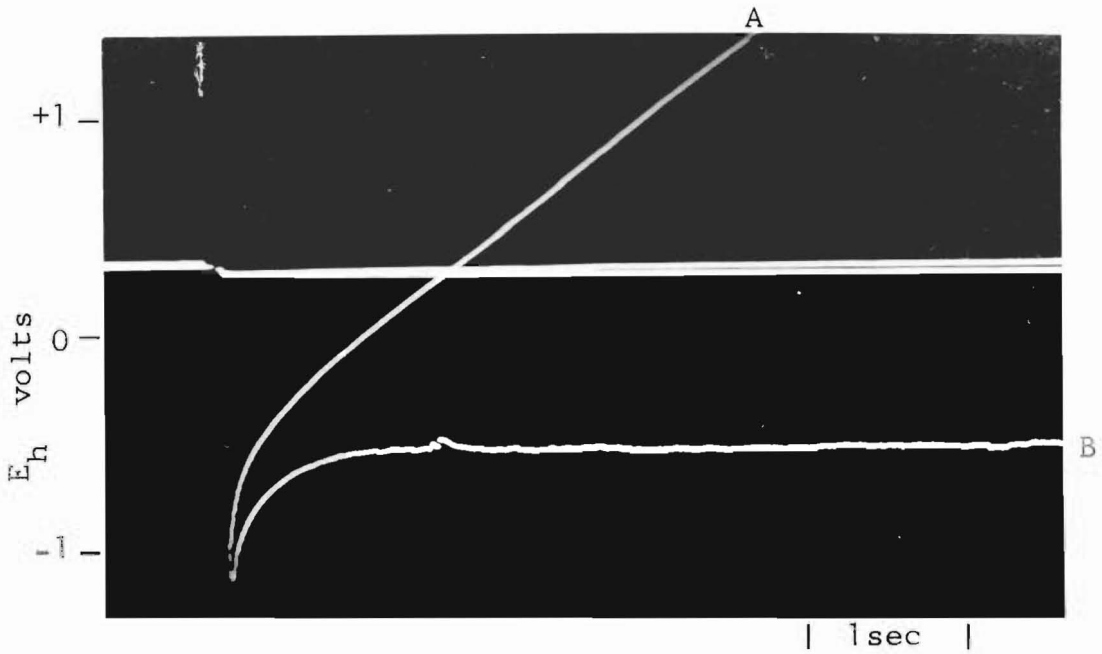

FIG. 7.1 INITIAL ANODE POTENTIAL RESPONSE
A. In K_2SO_4 at 0.8×10^{-3} amp/cm^2
B. In KCl at 2.3×10^{-3} amp/cm^2

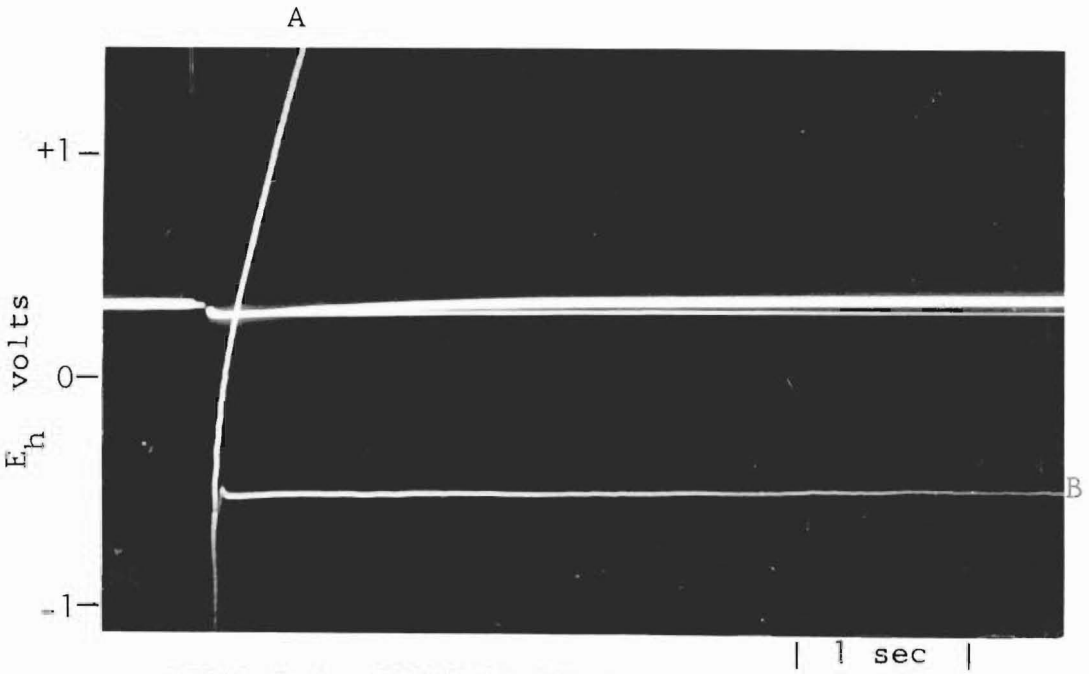

FIG. 7.2 INITIAL ANODE POTENTIAL RESPONSE
A. In K_2SO_4 at 1.2×10^{-2} amp/cm^2
B. In KCl at 1.27×10^{-2} amp/cm^2

sulphate solution the electrode is passivated readily.

2. The difference in response between electrodes in chloride and in sulphate is apparent at electrode potentials somewhat more negative than -1v NHE.

3. The characteristic dissolution potential in chloride is not instantaneously established; by comparing Figs 7.1 and 7.2, and from several similar runs, this process seems to be connected with the passage of a certain amount of current rather than being dependent solely on sufficient time for reaction with water.

7.1(iii) Discussion

It is assumed that these results of work in sulphate and chloride may be considered typical of the two types of anodic behaviour, oxidation and dissolution respectively (see Section 2.4(i)). The fall to the minimum potential studied by Earl[5], is not visible here largely because of low film speed; furthermore, in these traces the rate of the subsequent one or two milliseconds of potential rise may not be reliable, because of the possibility of the cathode follower being momentarily paralysed before the cut by the 6v bias applied by the current impressor across the insulated electrode. However, other experimental observations bear on the very early behaviour:

1. In times up to 50 microseconds after the cut,

Earl[5] detected no difference in anodic kinetic parameters whether they were determined in chloride or in sulphate solutions. Unfortunately not much significance can be attached to this finding because of the very wide error limits applicable to these particular results.

2. The differing rates of the subsequent millisecond open circuit rise to the mixed potential (e.g. B-C of Fig.2.1) in sulphate and chloride solutions, sulphate being twice as fast, were shown by Earl[5] to result from differences in cathodic process kinetics in the presence of these anions.

It has been implied, perhaps without sufficient explicit support, that the active dissolution potential is critically dependent on the anion and its concentration in the electrolyte. Numerous references establishing this behaviour and supporting the present work are available.

1. Bond et al[60] when studying pitting of aluminium in 0.5n chloride solution found no pitting of zone refined aluminium after 90 min. at -.5v NHE, but definite pitting at -.48v NHE and stated that"the potential at which pitting first occurred was quite reproducible".
2. Anodic polarisation of aluminium in 0.5MNaCl at pH11 showed very clearly a critical activation potential

of -.46v NHE.[61]

3. Kolotyrkin[43] has reviewed the electrochemical behaviour of numerous metals in the presence and absence of "activating" anions and has established clearly for aluminium and other active metals the occurrence of a critical potential for pitting, which is precisely dependent on the particular activating anion and its concentration in solution.

Together with all evidence earlier presented, the above considerations clearly establish that the Phenomena do not occur on aluminium unless:

1. There are suitable activating anions present in the electrolyte.
2. A sufficiently positive (depending on anion and concentration) electrode potential is reached.
3. Sufficient time/current has passed.

On the basis of these three facts and also in accord with the analysis of the model Section 6, some views on possible mechanisms for the excess dissolution are now developed.

7.2 The Hypothesis-Postulated Mechanism

It is postulated that the excess dissolution results from the activating anion directly interfering with the process of protective film formation. The sections of Watson's[6] work that demonstrate conclusively that film

formation in aqueous solution is the result of chemical reaction between water and aluminium have been reviewed in Section 2.3(ii). In order to illustrate the basic ideas, a hypothetical reaction scheme is drawn out below; it is much more explicit than the available experimental evidence can justify, but the ground work for further experimental work may thus be laid.

It seems reasonable that the first stage of this process would be between one molecule of water and one atom or ion of aluminium in the surface of the electrode. Thus we may obtain, for example, the following hypothetical reaction scheme which is consistent with Case 1 of the model in Sections 6.4 and 6.5.

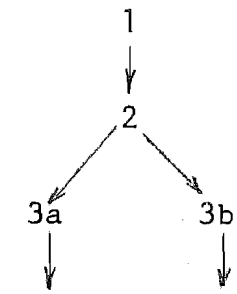

$Al + H_2O$	adsorption $\rightarrow$	$AlO\langle^{H}_{H}$	(1)
$AlO\langle^{H}_{H}$	reaction $\rightarrow$	$AlO^{(+)} + 2H$	(2)
$AlO^{(+)} + Cl^-$	evolution $\rightarrow$	$AlO{\cdot}Cl + e$	(3b)
$AlOCl + H_2O$	hydration hydrolysis $\rightarrow$	$Al(OH)_2Cl$	(4)

In reaction (1), Al is an atom on the surface of the metal, and the water molecule is perhaps just adsorbed before the evolution of hydrogen (as the atomic species) in reaction (2) and the formation of the hypothetical dischargeable

species AlO or AlO^+, which may be evolved (3b) as AlOCl, the electron going to the anode, and the AlOCl being hydrolysed (4) or hydrated to some final stable form which would depend on pH. Alternatively, if reaction (3b) does not occur quite rapidly, the adjacent aluminium atoms may also have proceeded to reaction (2), allowing formation of the first layer of oxide film. It seems improbable that reaction would stop at a monolayer of this material but would proceed to use the residual valence, after reaction (2), in further reaction with water; adjacent atoms of aluminium might have to adjust position/diffuse in order to satisfy requirements of bond angle, bond energy and interatomic distance of the resulting "oxide" film. The observed[11] non-stoichiometry of aluminium oxide films with their temporary metal richness could well arise from reactions of this general type.

In equation (1), it is suggested, lies the slow step in the overall process of excess dissolution. Earl[5] has examined and discussed the possibility that necessary orientation of water molecules and their adsorption on the metal surface may be relatively slow processes for aluminium. In equation (2) the further step to chemical reaction produces the postulated intermediate "ion" on the surface of the metal, plus atomic hydrogen which would normally recombine to form molecular hydrogen.

It is suggested that the species "AlO^+" cannot be discharged without a suitable acceptor/catalyst anion, e.g. Cl^-, and this stage represented by equation (3a) is likely to be potential dependent. Whether or not an exact species such as AlOCl would be formed cannot be decided without further investigation; the molecule is, however, known[62]. The last equation (4) represents the transformation of the evolved species to a stable hydrated form in aqueous solution. It is more difficult to draw up a reaction path consistent with the charge relationships assumed for Case 2 of the model (Sec. 6.4), namely average charge transfer of 1½ per reacted atom, but it is possible that it might be one of the following:

(a) Equal numbers of aluminium atoms react to, say, AlO^+ and to, say, $AlOH^{++}$ so that the discharge of these reacted species results in an average charge transfer to the anode of 1½.

(b) Some aluminium atoms react with water to satisfy fully their valence of three, e.g. (Al O OH) and are discharged electrochemically in conjunction with an unreacted atom.

Each of these schemes is rather implausible, but some more complex sequence of discharge steps could possibly give the effective charge transfer of 1½ for each reacted species. Similarly, although no mathematical analysis

has been undertaken for the case of an average charge transfer to the electrode of two, for each reacted species, the necessary relations could readily be developed, and a reaction scheme drawn up. These elaborations would not add materially to present knowledge of the fundamental processes involved in the Phenomena, but merely provide alternative mechanisms from amongst which the most plausible could be selected for further investigation.

7.3 Discussion

This discussion deals first with matters closely concerning the proposed mechanism, before presenting a brief consideration of more general features of the model, and practical implications of the findings.

7.3(i) The reaction scheme

In effect, the proposed process of excess dissolution and in particular Step 2 of the hypothetical reaction scheme involves reduction of water at the anode. Stated thus it is at least startling and indeed the process sounds to be impossible; there can be no doubt, however, of the great reactivity of the bare metal surface that is continuously "created" and exposed at a high rate by the forced dissolution. Considerable support for the general concept is afforded by work,

reported in Appendix A, that involved high current density dissolution of aluminium in aqueous 1N perchloric acid solution. As reported earlier (Sec. 4.4(ii)) the perchlorate anion is notably stable and difficult to reduce in a dilute aqueous solution such as this, yet it was found in these experiments that reduction of perchlorate ion to chloride ion was occurring on the anode surface to such effect that an excess dissolution of about 40% was observed at 80 amp/cm^2 applied current density. This confirms both the high reactivity of the bare metal surface and the fact that for some reason reaction of the metal with water is comparatively slow. Since the "available area" for reaction, created by the dissolution, is directly proportional to the applied current, but its exposed "life" inversely proportional to the current, only a fast reaction can capitalise on the momentarily (7 microsecond lifetime at 100 amp/cm^2) available reactive surface. In the reaction of water with aluminium, it has already been shown that although the absolute rate of excess dissolution increases with increasing current density the proportion of excess decreases; in aqueous perchlorate both the rate and the proportion of excess increase with current density (Appendix A).

It is interesting to note that when Earl[5] carried out high-speed, no-load, cut electrode, experiments in an

electrolyte of 98% methanol saturated with KCl the shift in potential from peak to mixed potential was very much slower than in aqueous chloride; there is a clear inference that the reduced "concentration" of water in the methanol, compared with full aqueous solution, allowed only a much slower rate of the inhibiting chemical reaction of the metal with water.

7.3(ii) Critical dissolution potential

It is tempting to identify the critical potential, observed in the lower current density dissolution experiments, with the change transfer step 3 of the above hypothetical reaction scheme. For the following reasons this seems unjustified.

1. In all of the runs during which electrode potential was observed, the electrode carried an air-formed oxide film, and very clearly attack was confined to limited areas of the electrode, much of the surface remaining unattacked. The critical potential would therefore seem to be concerned more with disruptive penetration[72] of the oxide film by the activating anion than simply with the actual process of excess dissolution. This is examined again in 7.3(v).
2. Were the critical dissolution potential a kind of reversible potential for the excess dissolution

process, then it would clearly prohibit evolution of the postulated reacted species at any potential that was more negative. If correct this would invalidate the use of Earl's[5] and Watson's[6] i_{oa} data to represent the dissolution probability function (Sec.6) since their data were all measured at more negative potentials than the "critical"; the success of the model when based on their data discounts the notion. Further, the traces in Fig. 7.1 show clearly that the difference between anodic behaviour in chloride and sulphate is evident at much more negative potentials than the "critical" value, which may be taken to indicate interference with the passivation process at these more negative potentials.

The delay in reaching the critical potential noted in Fig. 7.1 may well be associated with establishment of a concentration of the activating anion at the electrode surface.

7.3(iii) Formation of particles

Although the mass of aluminium particles formed during anodic dissolution of the metal has, in the present work, been quite a small proportion of the total anode excess weight loss it is interesting to speculate about their origin and the reasons for their formation. Fig. 7.3 is a microphotograph of some particles collected

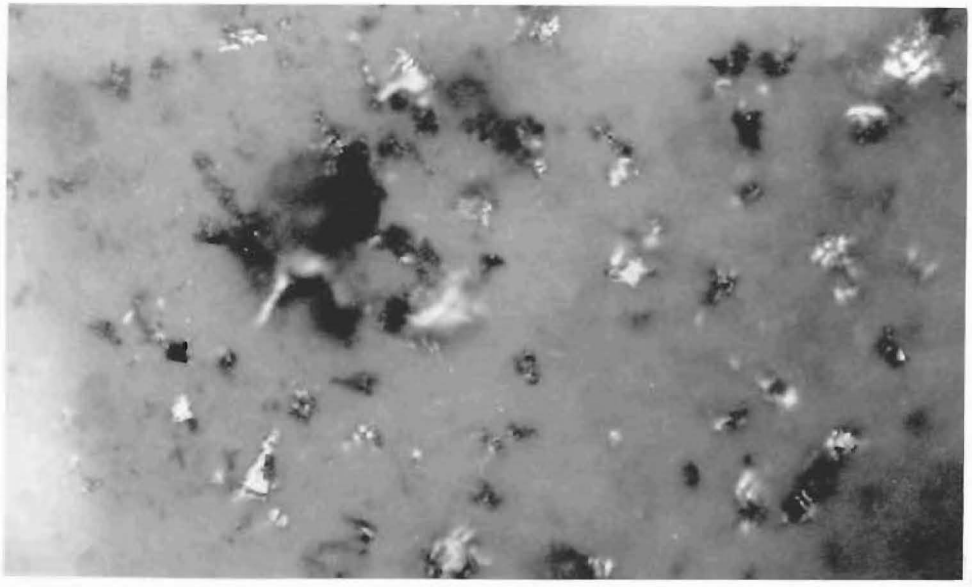

|30 micron|

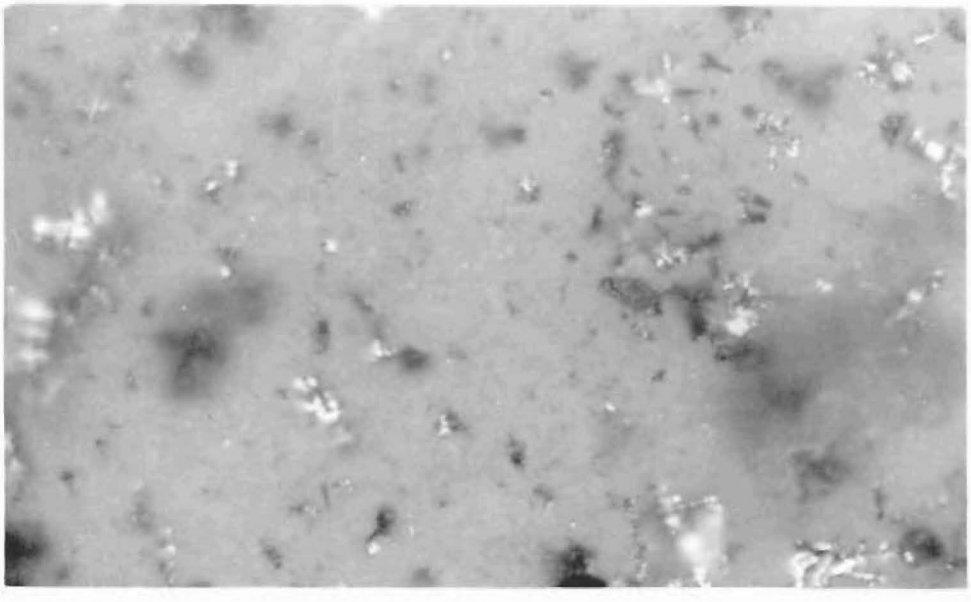

FIG. 7.3 MICROGRAPHS OF PARTICLES ON FILTER

on a Millipore membrane (Section 5) from high current density dissolution. As has already been noted (Section 5) the particles formed during high current density dissolution range in size up to about thirty microns and appear to have the form of flakes a few microns thick. Straumanis[24] has attributed the formation of particles of metal to disruption of the oxide film and consequent removal of small flakes of metal strongly bonded to the detached oxide.

In the present work, at high current densities the entire electrode surface became active from the moment of switching on the current; under such conditions, particles equivalent to a layer of metal beneath the oxide might be expected to detach with the air formed, hours old, and presumably strong, oxide film; these conditions should be the most favourable possible for the Straumanis[24] mechanism of particle formation. By this reasoning there should have been the same quantity of particles formed for each run in the present work, since the electrode area was the same (0.1 cm^2). This was not found to be so, and although the total quantity of particles collected could sometimes be equated with a layer 0.1 cm^2 by a few microns thick, in many runs very little particulate aluminium was collected at all.

Although the distinction between particles formed, and particles collected, has generally been maintained until

now, it is probable that efficiency of collection of particles formed at high current density was near to 100% on the millipore membrane. The assumptions involved are that:

1. No significant quantity of particles was formed smaller than the 0.8 microns diameter of pores in the membranes.
2. No significant disappearance of particles by dissolution before they could be collected. Calculations have been made to obtain the rate of disappearance of particles by spontaneous dissolution assuming a current density of 10^{-4} amp/cm^2 for the cathodic process; this figure makes considerable allowance for possible effects of small size on increasing the specific activity of such material. On this basis, for a one order of magnitude decrease in diameter of spherical particles of aluminium, the following times would be needed.

	ΔD	ΔT
Decrease from	100 μ to 10 μ	30 days
" "	10 μ to 1 μ	72.4 hours
" "	1 μ to .1 μ	435 minutes

TABLE 7.1 CALCULATED PARTICLE DISAPPEARANCE RATE

The agency postulated to be causing the formation of the flake-like particles of aluminium in the present work, is atomic hydrogen. From the reaction scheme (Section 7.2) it is clear how atomic hydrogen might be formed in solution by the reaction of aluminium and water; the presence of atomic hydrogen with a concentration half-life of about five minutes has been experimentally determined in electrolytes from the anodic dissolution of magnesium[53]. In the normal course of events the pairs of hydrogen atoms combine to form molecules leading in turn to bubbles of gas. Clearly, however, the atomic form of hydrogen can exist in solution for significant periods, which suggests that combination of pairs of atoms to form molecules may take place only on suitably active surfaces. Because of their extremely high mobility, diffusion of the atoms under a concentration gradient would take place in both directions normal to the surface of the electrode; that is, away from the electrode, and, it is suggested, towards and into the metal of the electrode. If two atoms met at a suitable site during its lifetime on the surface, they would form a molecule of gas; many atoms must do this, but diffusion of atomic hydrogen into the body of the electrode metal is a well established phenomenon[65] for several metals. Recombination of atoms to form molecules and pockets of gas could then occur at a

distance under the surface and result in a flake of metal becoming detached by the pressure of gas formed.

Various points relevant to this proposition can be briefly mentioned.

1. The role of impurity distribution and especially of micro-segregation of impurities which is common in high purity aluminium[60] could be important in this connection, especially in providing paths for diffusion, sites for recombination and possibly in determining the size of flakes.
2. Different amounts of particles formed in different runs could result from the effect of electrolyte flowrate on the boundary (diffusion) layer thickness adjacent to the electrode.
3. Although aluminium normally has an apparently low permeability for molecular hydrogen[66] this is almost certainly an effect of the oxide film. In the present case there is no film as such and hydrogen atoms are the diffusing species.
4. Reported experimental observations and discussion of similar effects has been presented by Draley and Ruther[67].

7.3(iv) The hypothesis and other metals

Because excess dissolution and the other related phenomena have been observed on metals other than

aluminium, for example, magnesium and beryllium[38,64], it is desirable that any explanation proposed for aluminium should be able to account for similar behaviour of other metals. Since more work has been done with magnesium, this brief examination of other metals will be confined to consideration of its reported behaviour in relation to the hypothesis. The following points emerge from references (40), (38), (41), (39):

1. Percentage excess dissolution, based on anode gas evolution, is generally much higher on magnesium than aluminium, being approximately 60% excess in chloride; this is consistent with the more reactive nature of this metal.
2. Excess anode weight loss is considerably more than equivalent to the anode gas evolution. The further weight loss not accounted for by 'normal' excess dissolution was associated with the production of what has been variously described as "grey active oxide" and as an oxide mass containing small metal particles. This behaviour is probably connected with the lesser protectiveness compared with aluminium of the film formed on magnesium in these circumstances; attack occurs in the presence of several anions other than halide, such as formate and acetate. To this may be added the observation, that activation takes place at much more negative potentials for magnesium

than for aluminium, viz. -1.5volts NHE for 1N Cl^-, even having regard for the lower reversible magnesium potential. There is also the finding discussed earlier (Section 4) that for magnesium excess dissolution was proportional to the anion transport number which is a clear differentiation from aluminium behaviour.

3. It is significant that Earl[5] obtained a no-load potential transient for magnesium that exactly parallelled that for aluminium viz. a fall to a minimum potential with a subsequent rise to a mixed potential.

Although each metal has some unique features in its behaviour, it is judged on the basis of this brief comparison that there may well be for magnesium, a mechanism for excess dissolution similar to that proposed for aluminium in the present work.

Mention must be made of Kolotyrkin's[42] exposition on pitting corrosion where a generalised mechanism is proposed. He makes the statement that "the critical potential of pitting is the minimum potential at which the aggressive anion becomes capable of the reversible displacement of the passivating oxygen from the metal surface. As a result of this, the reaction of the direct formation of metal compounds with the aggressive

anion begins to surpass the rate of interaction with the oxygen of the water." While this may be a quite reasonable hypothesis for pitting of such metals as stainless steel, zirconium, and copper, it is evident from the present work that it is not a satisfactory explanation of the behaviour of more reactive metals such as aluminium and magnesium.

7.3(v) The model and practical aspects

(a) In order to relate the present work to practical corrosion situations, it is necessary to consider principally, behaviour during comparatively low current density dissolution. It has been noted already (Sections 4 and 7.3(ii)) that at current densities less than, say, 1 amp/cm^2 in chloride, attack was very non-uniform, being confined largely to a small proportion of the surface of the electrode. The fact that the electrodes carried initially an oxide film formed during some hours in the atmosphere, means that conditions during dissolution did not conform exactly to the ideal implicit in the model, viz. that the activity of the electrode surface at any current density was dependent solely on a steady-state distribution of ages of atoms on the surface, arising from reaction of water and steady dissolution.

Watson[6] found that upon immersion of an electrode

carrying an oxide film formed in air, its anodic exchange current density was initially about two orders of magnitude less than for an electrode that had been cut under and exposed to the aqueous electrolyte for about 1 second, although the values for the two types of electrode converged with time to become the same after a few minutes in solution. These matters do not, however, seriously affect the applicability of the model to these low current density runs.

If we were to start with a completely film-free electrode, immersed in aqueous electrolyte and passing a moderate anodic current, it is clear that in a short while the condition and behaviour would be quite closely similar to that for an electrode initially carrying an air-formed oxide film. In the former case because of the tendencies inherent in the model, the longer lived atoms would have such reduced probabilities of dissolution that the dissolution would rapidly become non-uniform, being then confined largely to the most recently attacked areas where the atoms with greatest probability lie. Starting under either condition, there would therefore soon be only a small proportion of the electrode active, and the bulk of it largely passive, at low current density.

By taking note of the earlier discussed (Sec.6.6 (iii)) work of Edeleanu[58] concerning rates of progress

active pit fronts in aluminium, it is possible to make several useful observations. His results were used in Section 6.6(iii) to show that inside an active pit at -.5v NHE the real current density is 5-7 amp/cm^2. It becomes clear why, as successfully predicted by the model, there is a substantially constant proportion of excess dissolution at current densities ranging down from 5 amp/cm^2; in these circumstances the real current density on the areas to which the current is largely confined, is constant and independent of the apparent current density. At any applied current density the "active" area may therefore be calculated; this active area must not be confused with the much larger area that has been attacked during the course of a run.

(b) We turn now to experiments conducted in bromide and iodide solutions; from Table 4.4 it may be seen that the dissolution potentials were -.34v and -.22v NHE respectively. On Fig. 6.5, using the anodic Tafel line corresponding with Edeleanu's[58] and with Earl's[5] data, we find that the current densities corresponding with these potentials are approximately 9 amp/cm^2 and 15 amp/cm^2 respectively; when the experimentally determined relation between current density and excess dissolution (Fig. 5.5) in chloride is examined we find that these current densities correspond with percentage

excess dissolutions of about 11.5% and 10% respectively. These two figures are in fact the same as the experimentally observed steady low current density excess dissolution of aluminium in these two electrolytes (Table 4.4). This suggests clearly that the inability of the bromide and iodide to activate the electrode until more positive electrode potentials are reached than chloride, results in even higher local current densities on the active areas in these two media. These considerations are generally consistent with the already recorded visual observations regarding localisation of attack (Sections 2 and 4).

(c) The bearing of these considerations on pitting corrosion of the metal may be seen; particularly some light is shed on the known autocatalytic nature of pitting; it seems likely also that there are two distinct roles for the activating anion in pitting corrosion of aluminium: firstly, initiation by disruption of the oxide, and then continuation of the attack by interfering with film repair process.

(d) These matters are relevant also to the characteristic potential excursions observed by Hagyard et al[46] to occur on micro-electrodes of aluminium exposed to aerated chloride solution. It is suggested that the observed behaviour may be associated with relative

current densities of the anodic and cathodic processes, (the currents must be equal in the steady state). The local anode current density in pits and presumably also at breaks in the oxide film is about 6-7 amp/cm^2 in chloride solution at -.5v NHE. The sizes of the spontaneous breaks that occur in aluminium oxide films are not known but there is presumably a range of sizes. The smallest electrodes used in these experiments were almost 10^{-5} cm^2; in aerated chloride the cathodic process is reduction of dissolved molecular oxygen, the maximum rate being fixed by diffusion of that species; it is about 10^{-4} amp/cm^2 under these conditions[6].

In this case a break in the film with an area of about 10^{-10} cm^2 carrying a current 5 amp/cm^2 would give a current approximately the same as that for the cathodic process; under these conditions continued dissolution might be expected. If, however, the break were appreciably larger or appreciably smaller an unstable condition would result in rapid potential excursions; at some intermediate size of break oscillatory diffusion phenomena might arise leading to the occasionally observed oscillatory potential. It appears that this suggestion is capable of being developed into a more generally accurate explanation of these phenomena than has yet been obtained.

7.4 Conclusion

When the suggested mechanism and the companion quantitative model are considered together, there is a very reasonable accounting for a wide variety of experimentally observed behaviour; the validity of the model is not dependent on the correctness of the particular mechanism proposed.

8. NOTATION

8.1 Symbols

All symbols used in the mathematical derivation of the model (Section 6) are therein defined. Other symbols used in the text are:

α	kinetic transfer coefficient
μ	micron, (10^{-6})
$\mathring{A}$	Angstrom unit (10^{-10} metre)
C_{dl}	electrode double layer capacity, $\mu F/cm^2$
F	Faraday, coloumbs/gm equivalent
ΔG	free energy, cal/mole
I	current density, current, amp/cm^2, amp
i_{oa}	anode exchange current density, amp/cm^2
m	milli 10^{-3}
R	resistance, ohms
t_{Cl^-}	transport number (chloride)
V	voltage, volts

8.2 Abbreviations

A.R.	analytical reagent grade chemical
C.P.	commercially pure grade chemical
E.D.T.A.	ethylene diammine tetra-acetate
I.R.	resistive voltage drop
m.eq.	milli-equivalents
mm Hg	millimeters of mercury manometric head

N.H.E.	normal hydrogen electrode reference potential
N.T.P.	normal temperature and pressure
p.p.m.	parts per million
P.T.F.E.	polytetrafluorethylene

9. BIBLIOGRAPHY

1. Jecks P.M., B.E. Project Report, University of Canterbury (1958)
2. Hagyard T. and Williams J.R., Trans. Faraday Soc., 57, 2288 (1961)
3. Hagyard T. and Earl W.B., J. Electrochem. Soc., 114, 694 (1967)
4. Earl W.B., B.E. Honours Thesis, University of Canterbury (1961)
5. Earl W.B., Ph.D. Thesis, University of Canterbury (1965)
6. Watson I.G., Ph.D. Thesis, University of Canterbury (1965)
7. Hagyard T., Earl W.B., Kirkpatrick K.J., and Watson I.G., J. Electrochem. Soc., 113, 962 (1966)
8. Lanyon M.A.H. and Trapnell B.M.W., Proc. Roy. Soc., A227, 385 (1954-5)
9. Hart R.K., Proc. Roy. Soc., A236, 68-88 (1956)
10. Latimer W.M., Oxidation Potentials, 2nd edn, Prentice-Hall, N.Y. (1955)
11. Grunberg L. and Wright K.H.R., Proc. Roy. Soc., A232, 403 (1955) and Brit. J. App. Physics, 9, 85 (1958)
12. Hunter M.S. and Fowle P., J. Electrochem. Soc., 103, 483-5 (1956)

13. Andreeva V.V., Proc. Inst. Phys. Chem., A.N. U.S.S.R., 2, 79-98 (1957); C.A. 53, 8754a

14. Andreeva V.V. and Shishakov N.A., Zhur. Fiz. Khim., 32, 1671-2 (1958); C A52 19799d

15. Kirk-Othmer, Encyclopedia of Chemical Technology, 2nd edn, Standen A., Ed., Interscience (1963) vol. II, p.4

16. Evans U.R., The Corrosion and Oxidation of Metals, Arnold, London (1960)

17. Deltombe E. and Pourbaix M., Corrosion, 14, 496t-500t (1958)

18. Porter F.C. and Haddon S.E., J. App. Chem., 3, 385 (1953)

19. Lorking K.F. and Mayne J.E.O., Brit. Corros. J., 1, 181 (1966)

20. Lepin L. and Kadek V., Corrosion Science, 6, 177-81 (1960)

21. Hagyard T. and Santhiapillai J.R., J. App. Chem., 9, 323-30 (1959)

22. Hoar T.P., Chapter 4 in "Modern Aspects of Electrochemistry", vol. II, ed. J.O'M. Bockris, Butterworth, London (1959)

23. Young L., "Anodic Oxide Films", Academic Press, London (1961)

24. Straumanis M.E. and Wang Y.N., J. Electrochem. Soc., 102, 304 (1955)

25. Straumanis M.E. and Poush K., J. Electrochem. Soc., 112, 1185 (1965)

26. Davidson A.W. and Raijola E., J. Am. Chem. Soc., 78, 556-59 (1956)

27. Davidson A.W., et al., J. Am. Chem. Soc., 74, 732 (1952)

28. Davidson A.W., et al., J. Am. Chem. Soc., 72, 1700 (1950)

29. Hampel C., ed., "Encyclopedia of Electrochemistry", Rheinhold, N.Y. (1964)

30. Tomashov N.D. and Modestova V.N., Trudy Inst. Fiz. Khim. A.N. SSSR No.5, Issledovan KorroziiMetd No.4, 75-98 (1955), C.A. 50: 11138f

31. Masing G., et al., Z. Electrochem., 55, 160-5 (1951)

32. Masing G., et al., Z. Metallkunde, 40, 311-17 (1949)

33. Masing G., et al., Z. Electrochem., 56, 8-16 (1952)

34. Yokota Y., J. Electrochem. Soc., Japan O/E, 28, E204 (1960)

35. Hisamatsu Y., J. Electrochem. Soc., Japan O/E, 27, E73 (1959)

36. Okomoto G., et al., J. Electrochem. Soc., Japan O/E 27, E173 (1959)

37. Hoehy G.R. and Cohen M., J. Electrochem. Soc., 105, 245 (1958)

38. King P.F., J. Electrochem. Soc., 113, 536-9 (1960)

39. Glicksman R., J. Electrochem. Soc., 106, 83 (1959)

40. Greenblatt J.H., Corrosion, 18, 125t (1962)

41. Straumanis M.E., et al., J. Electrochem. Soc., 110, 1117-1120 (1963)

42. Kolotyrkin Ja. M., J. Electrochem. Soc., 108, 209 (1961)

43. Kolotyrkin Ja. M., Proc. Second Internat. Congress on Metallic Corrosion, p.23, N.Y. (1964)

44. Wyatt G., B.E. Chem. Project Report, University of Canterbury (1961)

45. Kirk I.G. and Johnson R.K., B.E. Chem. Project Reports, University of Canterbury (1962)

46. Hagyard T. and Prior M.J., Trans. Far. Soc., 57, 2295 (1961)

47. Vogel A.T., "Quantitative Inorganic Analysis," 3rd edn, Longmans, London (1961)

48. Furman N.H., ed., "Scotts Standard Methods of Chemical Analysis, 6th edn, D. Van Nostrand, N.Y. (1962)

49. McGeer J., J. Chem. Education, 29, 534-8 (1952)

50. Lohanyai N. and Redey L., Period Polytech. Chem. Eng. Hong 6, 121 (1962)

51. Epelboin I. and Froment M., J. Chim. Phys., 60, 1301-9 (1963)

52. Sidgwick N.V., "The Chemical Elements and their Compounds", Clarendon Press, Oxford (1952)

53. Uhlig H.H., et al., Electrochimica Acta, 11, 469-82 (1966)

54. Straumanis M.E., In ref. 29.

55. Miller J.M., B.E. Chem. Project Report, University of Canterbury (1964)

56. Plumb R.C., J. Electrochem. Soc. 105, 502 (1958)

57. Bass L., Proc. Roy. Soc., 151, 125 (1964)

58. Edeleanu C., J. Inst. Metals., 89, 90 (1960-1)

59. Bockris J. O'M. and Conway B.E., Edrs, "Modern Aspects of Electrochemistry", No.3, Butterworths, London (1964) Chapter 4

60. Bond A.P., et al., J. Electrochem. Soc., 113, 773-7 (1966)

61. Kaesche H., Z. Physik Chem. N.F. 26, 138 (1960)
34, 87 (1962)

62. Moeller T., "Inorganic Chemistry", p.751, Wiley, N.Y. (1952)

63. Pearson E.C., et al., Can. J. Technol., 30-31, 511 (1952-3)

64. Straumanis M.E., J. Electrochem. Soc., 108, 1087 (1961)

65. Wach S., et al., Corrosion Sci., 6, 271 (1966)

66. Smithells C.J., ed., "Metals Reference Book", vol. II, p.569-74, Butterworths, London (1962)

67. Drayley J.E. and Ruther W.E., J. Electrochem. Soc., 104, 329 (1957)

68. Edeleanu C. and Evans U.R., Trans. Far. Soc., 47, 1121 (1951)

69. Mears R.B. and Brown R.H., Ind. Eng. Chem., 29, 1087 (1937)

70. Aziz P.M. and Godard H.P., J. Electrochem. Soc., 102, 577 (1955)

71. Straumanis M.E. and Bhatia B.K., J. Electrochem. Soc., 111, 357 (1963)

72. Pryor M.J., Z. Electrochem., 62, 783 (1958)

10. APPENDIX A - DISSOLUTION IN PERCHLORATE SOLUTIONS

Consideration of anodic dissolution of aluminium in aqueous perchlorate solutions has been postponed until the foregoing has been presented, to avoid confusion of the issues. Although this work gave results of considerable interest, only very few runs were made and results of some are rather contradictory and of low accuracy. Later runs at high current densities in flowing electrolyte gave more reliable results, but being incidental to the main experimental programme the work was not pursued. In the light of the hypothesis expounded in the earlier part of the thesis, an interpretation of the results can be made, but some reservations must be held until additional experimental work confirms the results and further investigations are made.

10.1 Experimental

These runs were carried out using the apparatus and techniques described fully in Sections 4 and 5; for runs in static electrolyte 4N aluminium was used and 5N aluminium for the flowing electrolyte runs.

10.2 Results

TABLE 10.1

Run No.	Appd Current Density amp/cm^2	Anode Gas % Excess	Gross % Excess Wt loss	Dissolution Potential v. NHE
103	.085	14.7	42	-.23 to .25
104	.93	15.8	29.8	-.12 to -.23
114	.46	14.6	14.9	-.18
117	4.58	13.9		-.02
214	84.8		approx. 34.5	
215	67.6		38.9	
221	64.5		38.6	
222	22.4		17.2	
223	9.87		15.4	
224	79.9		46.7	
225	98.2		34.2	

Examination of significance of results presented in Table 10.1:

Electrolytes Runs 103 and 104 were carried out in electrolyte made from C.P. $BaClO_4$, which contained approximately 0.04% chloride. Electrolyte for runs 114-225 was prepared from AR $HClO_4$ (chloride-free) to one normal concentration for 114-221 inclusive, and inadvertently to 0.75N for runs 222-225.

Current densities Figures for current density have accuracies consistent with the method which was used; in runs 103-117 inclusive in static electrolyte, current density was based on evolved cathodic gas volume; for runs 214-225 in flowing electrolyte, the integrated coulombs divided by time gave the mean current (see Section 3).

Anode gas evolution These figures were obtained only for the static electrolyte runs and accuracy is consistent with the results in Section 4. Expressed as an average percentage excess the figure takes the value 15 ± 3%. Gas evolution from the anode was observed during high current dissolution in flowing electrolyte runs.

Gross excess weight loss These figures are the difference between actual and expected weight loss expressed as a percentage of the expected weight loss. In the static electrolyte runs there was an indefinite contribution to weight loss by the formation of particles; quantities of particles were observed in the electrolyte during and after the runs. Results obtained in flowing electrolyte, apart from run 214, are essentially net excess since insignificant amounts of particulate aluminium were collected on the Millipore filter membranes. In run 214, the first at high current density in perchlorate, the unexpectedly large excess dissolution caused the electrode surface to retreat

well below the P.T.F.E. seal (Fig. 5.1) so that electrolyte flow conditions for most of the run were uncharacteristic; dissolution proceeded smoothly nevertheless, although a very large number of particles was formed.

Electrode potential Dissolution potential was obtained only in static electrolyte runs and would have been most accurate at the lower current densities in runs 103-104. Generally, the potential became more negative as the run progressed.

The following assumptions have been made in processing the excess dissolution data which are plotted in Fig. 10.1.

1. During the dissolution of aluminium in perchlorate electrolytes, several simultaneous processes are assumed to occur at the electrode. They are:

(a) Normal faradaic dissolution effectively as trivalent cations.

(b) Excess dissolution exactly as has been observed in chloride electrolytes, i.e. of the water reacted species.

(c) Excess dissolution connected with the perchlorate anion.

2. On this basis the net excess dissolution due to 1(c) at any current density, is obtained by subtracting from the observed gross excess value in perchlorate

(Table 10.1), the amount of excess found at the same applied current density in chloride (Fig. 5.5).

3. For runs in static electrolyte the lack of information means that as well as assumptions 1 and 2, an allowance for particle formation should be made; the only available indication is from runs in .1N HCl solution where weight loss of solid aluminium from the electrode sometimes equalled or exceeded the dissolution. On this basis for runs 103 and 104 any figure between about 0 and 10% excess due to "perchlorate" dissolution seems possible; for reasons presented in the discussion a figure of 5% will be arbitrarily chosen.

10.3 Discussion

It is suggested that the electrode potential observed during dissolution of aluminium in 1N perchlorate solution in run 103 for example, is determined in fact by the chloride ion concentration. Tomashov et al[30] have plotted critical dissolution potential versus chloride ion concentration for levels of 2.5 to .01N. By extrapolation, a potential of -.23 to -.25v NHE corresponds with a concentration of 3 or 4 x 10^{-4}N chloride ion; since the impurity level in the barium perchlorate used was < 0.04% which corresponds with a concentration in the bulk electrolyte

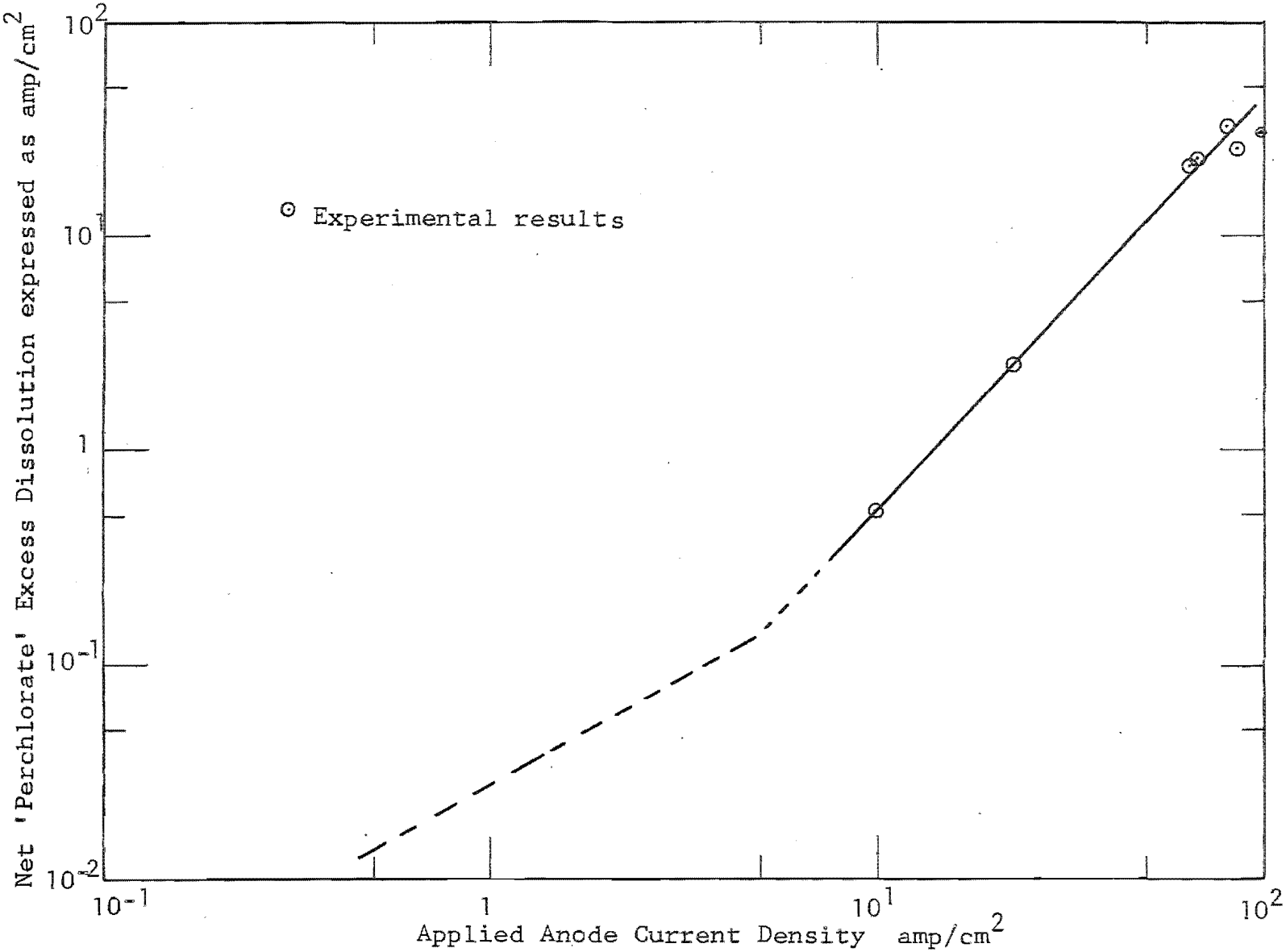

Fig. 10.1 Excess Dissolution in Perchlorate Solution

of $< 4 \times 10^{-4}$N the connection is established.

Further to this, the following points are added.

1. The small discrepancy would readily be accounted for by inexact potential measurements (IR drop).
2. Quantitative analysis for chloride in perchlorate electrolytes that were free from chloride before dissolution showed that significant concentrations of chloride were present after dissolution, indicating that in spite of its extreme stability (see Sec. 4.4(ii)) ClO_4^- is reduced under these circumstances.
3. Shift to more negative potentials as dissolution progressed would be the result of increase in chloride concentration from reduction of ClO_4^- to Cl^- at the anode.
4. The similarity of observed low current density excess dissolution (15 $\pm$ 3%, Table 10.1) in perchlorate to that in chloride (13.8 $\pm$ 3%, Table 4.4) is then readily explained; if instead perchlorate had a pitting activation roughly the same as iodide (-.22v) then by the argument of 7.3(v)(b) an excess dissolution of only 10% would be expected. By implication, the gas evolution from the anode during dissolution in perchlorate has been taken to result solely from "chloride" type excess dissolution; the perchlorate type excess dissolution

is assumed not to result in any hydrogen evolution from the anode. It seems improbable that ClO_4^- and halide ions would be interchangeable in the role envisaged for the anion in the mechanism, Section 7.2.

5. The even more positive potential observed in 1N A.R. $HClO_4$ (run 114 -.18v NHE) corresponds with a concentration of about 5×10^{-5}N chloride; initially the chloride concentration from $ARHClO_4$ would have been extremely low, but granted that ClO_4^- ion can cause breakdown of the protective film on aluminium, and initiation of attack, reduction of ClO_4^- at the metal surface would take place and rapidly build up this small concentration of chloride.

Two queries that may arise are:

1. Why then is there apparently so much particle formation at low current densities?
2. Could a sufficient concentration of chloride have been maintained adjacent to the anode at very high current densities since such runs were carried out under high flow rates?

(i) In answer to this it seems from examination of all the results, the lower the concentration of halide, in sequence $Cl^- < Br^- < I^-$, or other activating anion, the more the non-dissolution weight loss increases. It is conjectured that this may be associated with the

differing pitting geometries noted elsewhere (Sec. 2); possibly there is a greater tendency to undermining in the cases of more area restricted, high intensity attack. It may be noted from Table 4.2 that steady conditions are attained apparently quite quickly during dissolution in perchlorate.

(ii) Quantitative analysis of bulk electrolyte after run 224 gave a value for chloride concentration of approximately 1.25 ± 10^{-4}N. While this value is low it is clear that in the diffusion layer adjacent to the electrode seat of chloride production, during dissolution, it could have been high enough to enable electrochemical dissolution of the intermediate water-aluminium species.

These observations generally are the basis for the contention that the part of excess dissolution associated with perchlorate specifically is obtained by subtracting the amount due to the "chloride". Because the number of water molecules present in the electrolyte is overwhelmingly greater than any other solute species, it is contended that perchlorate or other anions would not affect the rate or extent of reaction between water and aluminium significantly. At this anode, however, perchlorate species can react with highly reducing aluminium atoms/ions on the metal surface, themselves being reduced possibly by stages to chloride; ClO_3^-, ClO_2^-, are possible intermediate stages, although they

are much more readily reduced than perchlorate. There is a rather wide range of possibilities and it seems unwise to speculate about exact mechanisms that could be involved. Since ClO_4^- is a charged species (compared with water), the rate of reaction could well be potential dependent; inspection of Fig. 8.1 shows that the rate of "perchlorate reaction" increases more rapidly than the increase in applied current density, which strongly suggests potential dependence for the reaction. It may be reasoned thus:

1. The reaction must be very rapid compared with even the 7.36 microsecond average lifetime of atoms of aluminium on the electrode dissolving at 100 amp/cm^2.
2. For such a rapid reaction the available area becomes current density dependent since usable new surface is "created" at a rate directly dependent upon the current.
3. As the anode current density increases, the anode potential becomes more positive. A solely area-dependent process would increase in step with the current density while a potential and area-dependent process would change and, in this case, increase in rate even more rapidly as is observed in the present case. By extension of this reasoning to the region of applied current densities, less than about 5 amp/cm^2 where, as before, potential is

presumably constant and active area is directly proportional to the applied current, the assertion made earlier about the level of excess due to perchlorate, being proportional only to applied current follows directly. The figure of 5% was chosen so that the lower branch of the curve below 5 amp/cm^2 would link with the established upper part at about 5 amp/cm^2.

4. If, as has already been suggested by Earl[5] and repeated in the present work, the reaction of water and aluminium is slow because of relatively slow orientation of that molecule, then the more rapid reaction of perchlorate could be associated with the symmetrical tetrahedral configuration of the species.

Unfortunately, there appears now to be an inconsistency since the steps (Section 10.2) leading to Fig. 10.1 clearly imply that no charge transfer is involved in "perchlorate" dissolution, but we now find that the rate is potential dependent. If the "perchlorate" dissolution does involve charge transfer, then it is clearly at the expense of some normal trivalent dissolution since there is only so much applied current; in this case the actual proportion of aluminium ions being dissolved by each process is unknown and dependent on the charge transfer per ion dissolved. These quantities could apparently be established by quantitative analysis of the electrolyte

for all reduction products of perchlorate after a run.

For run 224 a titration for chloride in perchlorate electrolyte, gave a value of .000474 equivalents of chloride in the total electrolyte. Since the chloride has come from reduction of perchlorate the equivalents of that ion reduced is equal eight times the chloride equivalent (valence +7 to -1); therefore the figure 0.00379 = 3.79 meq is obtained. Before this figure is examined in conjunction with the observed aluminium weight loss for that run it is well to note that in determining the chloride:

1. No allowance for chloride present before dissolution has been made.
2. The titration is probably subject to ± 10% error.
3. No analysis for other possible reduction products has been made.

In run 224 the excess weight loss from the anode was 0.04872 gm, and with negligible weight loss as particles the net excess associated with perchlorate (after subtraction of the "chloride" excess) is accordingly .0446 gm. This weight can be converted to equivalents, the figures obtained depending on the valence assumed for the reaction; for example, one case would involve no charge transfer to electrode, another, one charge to the electrode and two to the perchlorate reduction, and yet a third two charges to the electrode and one to

perchlorate reduction. On this basis the figures of 4.99 meq, 3.3 meq, and 1.65 meq of perchlorate reduction are obtained for this weight of aluminium. Except in the first case, that is, dissolution associated with perchlorate involving no charge transfer to the anode, these figures are not the correct basis for comparison with the equivalents of perchlorate reduced. If the dissolution of aluminium that is associated with the perchlorate reduction involves as well some charge transfer to the electrode, then although in terms of its definition the amount of excess dissolution is not changed, the proportion of ions involved is different from the nominal, by a factor dependent on the charge involved, and determined by simple proportion. For the case of one charge going to the electrode the factor is 1.5 and for the case of two charges per ion of aluminium the factor is 3. We find, as before, (Section 4) therefore that since 4.99 meq and 1.5 x 3.3 meq and 3 x 1.65 meq are in fact the same figure, it is not possible to distinguish between process mechanisms by simple stoichiometry.

It can be deduced that the maximum possible excess dissolution, when that process involves charge transfer, is 50%, in which case all aluminium cations would be evolved by the excess dissolution process. Further, the same limit does not apply to the possible excess

dissolution if the perchlorate reaction with aluminium involves no charge transfer to the electrode; the implication for experimentation diagnostic with regard to reaction mechanism is obvious. It appears that reduction products other than chloride alone, must be formed since the amount of reduction of perchlorate to chloride is insufficient to account for the excess whatever the mechanism. (Al excess meq = 4.99, Cl^- meq = 3.79

It is appropriate to consider results obtained by Epelboin et al[51] during electropolishing of aluminium, and numerous other metals, in anhydrous solutions of perchloric acid or perchlorates, in acetic acid or ethyl alcohol. Under these conditions, for many metals the apparent valence of the metal is notably less than the conventional figure. There was no gas evolution from the anode under these conditions, and it was claimed as well that there was neither chemical attack nor simultaneous electrochemical reactions. To account for the much greater dissolution of aluminium than predicted by the valence of three, they postulated formation of Al^+ ions which reduced ClO_4^- ions that were adsorbed on the electrode. Amounts of chloride equivalent to the excess dissolution were found in the electrolyte after the run; it is pertinent to reiterate the inability of stoichiometric measurements to determine mechanism in such cases.

10.4 Conclusions

Under the conditions of the present experiments in perchlorate, a quite remarkable behaviour has been observed with measured dissolution greatly in excess of the expected. While experimentation under the conditions of high current density dissolution is not easy, the direction to go is clear and the dividends from continued work may be considerable. It is evident that the transient existence of bare aluminium, postulated in the present work, allows and promotes reduction of perchlorate at the anode in spite of the stability of that anion.

11. APPENDIX B

The Electrode Potential of Evaporated Aluminum Films in Chloride Solution

T. Hagyard, W. B. Earl,[1] K. J. Kirkpatrick, and I. G. Watson[2]

Department of Chemical Engineering, University of Canterbury, Christchurch, New Zealand

Potential measurements as negative as -1.67 E_{H_2} volts in 1*N* KCl solution pH 3.2, have been measured on a freshly cut aluminum surface by a technique devised by Hagyard and co-workers (1, 2). A polythene-coated aluminum rod immersed in 1*N* KCl solution was cut by a ruby travelling at 1000 cm/sec. Potential measurements were made using a high-impedance cathode follower coupled to an oscilloscope. From the instant the cut was made into the aluminum, its potential was recorded by photographing a single traverse of the oscilloscope trace. A typical potential measurement is shown in Fig. 1.

The initial rapid potential rise to the peak was attributed to the dissolution of aluminum charging the double layer. After reaching the peak potential, only a small fraction of the electrode surface was thought to remain actively anodic while the slower hydrogen discharge process took place over most of the metal surface. The exponential fall in potential was attributed to the polarization of the anodic and cathodic processes. The information gained using this technique enabled the kinetics for aluminum dissolution and hydrogen discharge on aluminum to be studied.

The object of the present work was to confirm the validity of the measurements made by the above technique. The possible alternative explanations of the potential behavior of freshly cut aluminum that were considered by the authors were (*a*) that instantaneous high temperatures were generated at the cut surface by the shearing action of the ruby cutter; the high temperatures would be rapidly reduced by heat dissipation into the bulk of the metal, (*b*) severe stressing and dislocation of the aluminum electrode surface followed by relaxation of the surface structure; the peak in this case would be a stress potential.

Vacuum evaporated aluminum films were used in this work to obtain an uncontaminated oxide-free aluminum surface comparable with that exposed by the previous technique. The aluminum film was formed in an evacuated, degassed, Pyrex glass bulb by evaporating 99.99% aluminum from a stranded tungsten wire that was supported on tungsten leads. The target area was a smoothly ground glass button. Electrical contact with the aluminum film was made by a tungsten wire sealed through the center of the button. Figure 2 is a sectional drawing of the bulbs used. To limit the area on which the measurements were made, the shape of the button was designed so that with straight line evaporation only the front surface of the button was coated with aluminum.

The glass bulbs were evacuated to a vacuum better than 0.1μ by a two-stage G.E.C. mercury diffusion vacuum pump with liquid nitrogen trap. The bulbs were baked under vacuum for more than 2 hr at 400°C. After baking, the aluminum was evaporated rapidly (3-5 sec) to give a thick (2-10μ) nontransparent coating of aluminum over the interior of the bulb. Holland (3) recommends rapid evaporation for high quality films. At the start of evaporation aluminum vapor was relied on to act as a getter of any residual gases. Subsequent deposits of aluminum were assumed to be uncontaminated and oxide free. At the completion of the evaporation process, the bulb was sealed off from the vacuum pump.

[1] Present address: Shawinigan Chemicals Ltd., Montreal East, Quebec, Canada.

[2] Present address: Monsanto Chemicals Ltd., Acrefair, Denbighshire, North Wales.

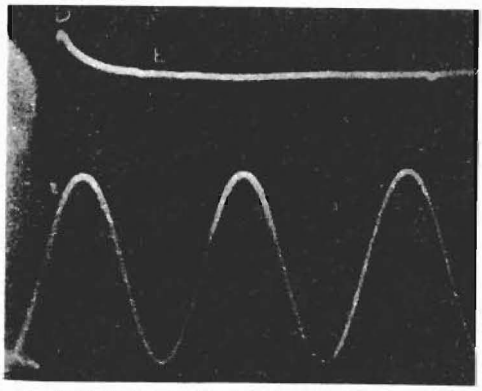

Fig. 1. Electrode potential of freshly cut aluminum vs. time. [From ref (1)]. IN KCl + HCl to pH 3.2, 300 cps sine wave has base at zero volts N calomel scale and is 1 S. Weston in amplitude, D peak potential, E mixed potential.

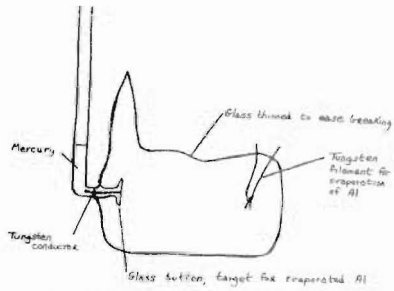

Fig. 2. Diagrammatic section of glass bulb

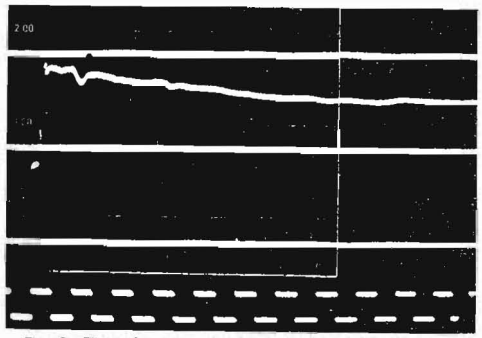

Fig. 3. Electrode potential of evaporated aluminum vs. time. Solution IN KCl + HCl to pH 3.2. Square wave 1000 cps.

Potential measurements were made in a 1*N* Analar KCl solution contained in a polythene beaker. The reference electrode was a normal calomel electrode. The electrical measuring circuit was a fast response (0.1 μsec) cathode follower, input impedance 10^7 ohms, coupled to a Cossor 1065 pulse oscilloscope. The potential of the evaporated aluminum film was measured by breaking the evacuated bulb under solution with a polythene-coated steel cutter. The cutter was driven through the bulb by a spring-loaded hammer device. A continuous photographic record of the potential change was obtained for the 10 msec following contact between the aluminum film and the KCl solution.

Figure 3 is an example of the potential-time trace obtained from evaporated films. Each trace reached a peak potential of -1.67 E_H volts then decayed in a similar but not entirely reproducible manner to the trace shown. The potential could be measured to better than ±0.05v. The authors believe that the difference in the potential decay characteristics between the two techniques is associated with the different mode of wetting the electrode surface. With the previous technique the electrode was a small v notch that was driven past the solution. The total time to cut and wet the electrode surface in this case was of the order of 10 μsec. The electrode area for the evaporated film method was approximately 1 cm^2. In this case the electrode was wet by the solution rushing into the evacuated glass bulb. It seems probable that the relatively large electrode area is wet progressively over possibly a millisecond or more. A peak potential was to be expected the instant the solution made electrical contact with the solution. Thereafter until the total electrode surface was wetted a mixed potential would result between that part of the electrode surface being wetted and that part already wet. The two jumps in potential at A and B, (shown in Fig. 3) were quite reproducible and could be associated with shock waves. A vigorous discharge of gas bubbles from the aluminum surface was observed immediately after the bulb was broken. It was strongly suspected that the gas discharged was hydrogen.

The conditions for the alternative explanation of the peak potentials obtained by the previous technique were absent from the evaporated aluminum films. When exposed to solution the films were neither at a high temperature nor in a severely stressed condition. The fact that the same peak potential has been obtained by two independent techniques is strong evidence that potential measurements by the earlier technique are valid.

Manuscript received May 4, 1966.

Any discussion of this paper will appear in a Discussion Section to be published in the June 1967 JOURNAL.

REFERENCES

1. T. Hagyard and J. R. Williams, *Trans. Faraday Soc.*, 57, 2288 (1961).
2. W. B. Earl, B. E. Thesis, University of Canterbury (1961).
3. Holland, "Vacuum Deposition of Thin Films," John Wiley & Sons, Inc., New York, N. Y. (1956).

12. APPENDIX C - SAMPLE CALCULATION OF A PARTICULAR SOLUTION OF THE MODEL

The following figures apply to Case 1 of the model (Section 6.5(iii)) and to excess dissolution results measured in chloride electrolyte. All equation numbers refer to the same equations in Section 6.

1. Fitting functions to $P(\tau)$ and $S(\tau)$ data

We have $$P(\tau) = (\tau^2 + \sigma^2)^{-\frac{1}{2}} \qquad (41)$$

$$S(\tau) = (1 + \tau/\sigma - \sqrt{1+(\tau/\sigma)^2})^{\gamma} \qquad (42)$$

and also that $$E_o = \frac{200}{3\gamma + 1}\ \% \qquad (49)$$

As before, E_o is the percent excess dissolution at low current density, τ is the age of atoms on the surface, $P(\tau)$ is the relative probability of removal of an atom of age τ, $S(\tau)$ is the probability that an atom of age τ has reacted, and σ and γ are arbitrary constants.

For dissolution in chloride, experiment has established that E_o lies between 13.5% and 14%. Taking a value of E_o = 13.8%, equation (49) gives a value for γ = 4.5. With γ = 4.5, the next step is to find a value for σ such that equations (41) and (42) will represent as closely as possible the experimentally established values of these two functions (Figs 6.3 and 6.1). Trial values for σ were substituted in (41) and

(42), the resulting curves plotted and compared. A value of $\sigma = 2.5 \times 10^{-5}$ sec. has been found to give the optimum fit for both functions. Tables of the values of $S(\tau)$ and $P(\tau)$ have been drawn up below using $\sigma = 2.5 \times 10^{-5}$ sec. and $\gamma = 4.5$. These figures are plotted in Figs 6.1 and 6.3.

$P(\tau) = (\tau^2 + \sigma^2)^{-\frac{1}{2}}$ $\qquad \sigma^2 = 6.25 \times 10^{-10}$

τ sec	τ^2	$\tau^2 + \sigma^2$	$P(\tau)$
10^{-6}	10^{-12}	6.26×10^{-10}	4×10^{4}
10^{-5}	10^{-10}	7.25×10^{-10}	3.72×10^{4}
2×10^{-5}	4×10^{-10}	11.25×10^{-10}	2.98×10^{4}
5×10^{-5}	25×10^{-10}	31.25×10^{-10}	1.79×10^{4}
10^{-4}	10^{-8}	1.063×10^{-8}	9.7×10^{3}
10^{-3}	10^{-6}	10^{-6}	10^{3}
10^{-2}	10^{-4}	10^{-4}	10^{2}

$$S(\tau) = (1 + \tau/\sigma - \sqrt{1 + (\tau/\sigma)^2})^{\gamma}$$

τ sec	τ/σ	$(\tau/\sigma)^2$	$1+\frac{\tau}{\sigma}$	$[1+(\frac{\tau}{\sigma})^2]^{\frac{1}{2}}$	$S(\tau)^{\frac{1}{\gamma}}$	$S(\tau)$
10^{-6}	.04	1.6×10^{-3}	1.04	1.008	.0392	4.7×10^{-7}
10^{-5}	.4	.16	1.4	1.077	.323	6.2×10^{-3}
2×10^{-5}	.8	.64	1.8	1.281	.519	5.2×10^{-2}
2.5×10^{-5}	1	1	2	1.414	.586	.09
5×10^{-5}	2	4	3	2.236	.764	.298
10^{-4}	4	16	5	4.1231	.877	.554
5×10^{-4}	20	400	21	20.024	.976	.896
10^{-3}	40	1600	41	40.01	.99	.956

2. Solution of equations to give E vs I

We have from Section 6.5(iii) when equations (41) and (42) above are transformed, that

$$\bar{M}(p) = \frac{\sigma p}{p^2 - 1} \qquad (45)$$

$$M(v) = 1/P\,[\tau(v)] \qquad (18)$$

and $$\bar{S}(p) = \frac{1}{p} - \frac{\gamma}{p+1} + \frac{\gamma(\gamma-1)}{2!}\cdot\frac{1}{p+2} - \frac{\gamma(\gamma-1)(\gamma-2)}{3!}\frac{1}{p+3} + \ldots \qquad (48)$$

The equation for current density I is

$$I = Nq\,[\,3 - 2p\bar{S}(p)\,]\,/\bar{M}(p) \qquad (30)$$

Substituting for $\bar{M}(p)$ from (45) gives

$$I = \frac{Nq}{\sigma}\,(3 - 2p\bar{S}(p))\cdot\left(\frac{p^2 - 1}{p}\right) \qquad (30a)$$

where $N = 1.537 \times 10^{15}$ atoms Al/cm^2 and

$q = 1.601 \times 10^{-19}$ coulombs/electron.

The equation for excess dissolution is

$$E = \frac{2p\bar{S}(p)}{3-2p\bar{S}(p)} \times \frac{100}{1} \qquad (32)$$

Equations (45) and (48) are solved to give $\bar{M}(p)$ and $\bar{S}(p)$ respectively for a range of values of p; these are then substituted into (30a) and (32) to give corresponding values of E and I. Values are tabulated below.

$$\bar{S}(p) = \frac{1}{p} - \frac{4.5}{p+1} + \frac{4.5x3.5}{2.1} \cdot \frac{1}{p+2} - \frac{4.5x3.5x2.5}{3.2x1} \cdot \frac{1}{p+3} \text{ ...etc}$$

p	$\bar{S}(p)$	$2p\bar{S}(p)$	$3-2p\bar{S}(p)$	E
1.0001	.18185	.3637	2.6363	13.8
1.01	.17762	.3588	2.6412	13.6
1.1	.14452	.3179	2.6821	11.9
1.2	.11630	.2791	2.7209	10.3
1.4	.07777	.2178	2.7822	7.8
1.6	.05118	.1638	2.8362	5.8
2.0	.02802	.1121	2.8879	3.9
2.5	.01386	.0693	2.9307	2.4
3.0	.00750	.0450	2.9550	1.5

p	1/p	$p - \frac{1}{p}$	$(3-2p\bar{S}(p))(\frac{p^2-1}{p})$	I
1.0001	.9999	.0002	5.25×10^{-4}	$5.17x10^{-3}$
1.01	.990	.02	5.23×10^{-2}	$5.15x10^{-1}$
1.1	.910	.19	5.12×10^{-1}	5.04
1.2	.833	.367	.996	9.81
1.4	.704	.696	1.91	18.7
1.6	.625	.975	2.77	27.3
2.0	.5	1.5	4.33	42.6
2.5	.4	2.1	6.15	60.6
3.0	.333	2.67	7.89	77.6

The values of E and I from these two tables are plotted against each other in Fig. 6.4 to compare the relation obtained from the present dissolution experiments with the independent prediction of the model.